CHALMERS
UNIVERSITY OF TECHNOLOGY

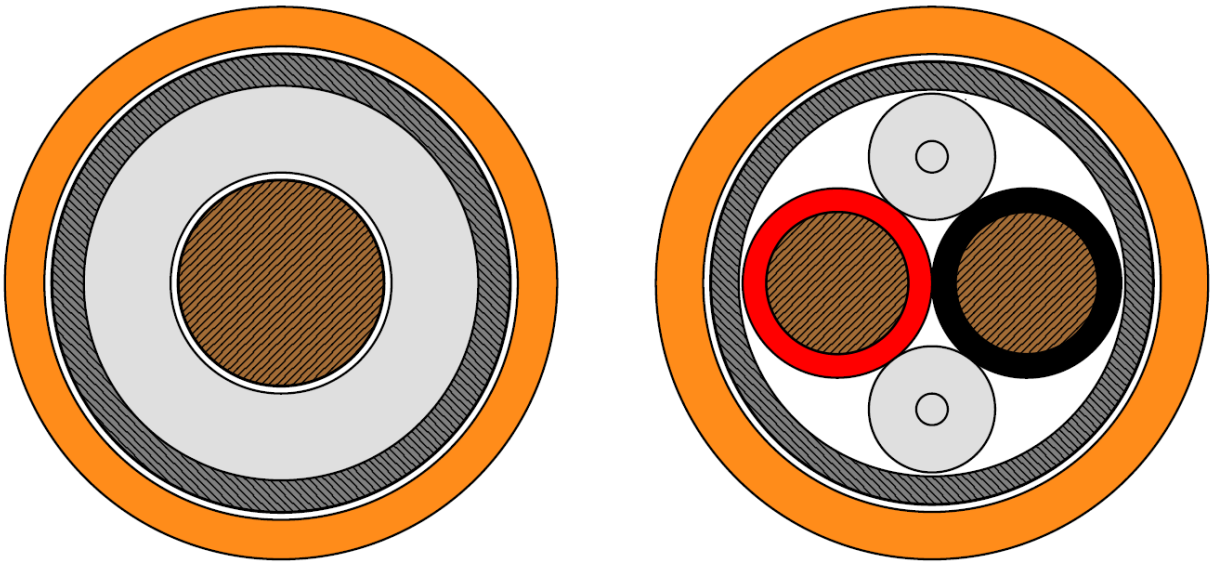

Cable modelling for electric vehicle drivetrains

In collaboration with Volvo GTT

Master's thesis in Electric Power Engineering

Alan Cordic

Azka Wanitwijan

DEPARTMENT OF ELECTRICAL ENGINEERING

CHALMERS UNIVERSITY OF TECHNOLOGY
Gothenburg, Sweden 2021
www.chalmers.se

Master's thesis 2021

Cable modelling for electric vehicle drivetrains

In collaboration with Volvo GTT

Alan Cordic
Azka Wanitwijan

CHALMERS
UNIVERSITY OF TECHNOLOGY

Department of Electrical Engineering
Division of Electric Power Engineering
Chalmers University of Technology
Gothenburg, Sweden 2021

Cable modelling for electric vehicle drivetrains
In collaboration with Volvo GTT
ALAN CORDIC
AZKA WANITWIJAN

Supervisor: Per Widek, Volvo GTT
Examiner: Torbjörn Thiringer, Electric Power Engineering

Master's Thesis 2021
Department of Electrical Engineering
Division of Electric Power Engineering
Chalmers University of Technology
SE-412 96 Gothenburg
Telephone +46 31 772 1000

Cover: The cross-section of the coaxial cable and the twin-axial cable used in the electrical vehicle.

Typeset in LaTeX
Printed by Chalmers Reproservice
Gothenburg, Sweden 2021

Cable modelling for electric vehicle drivetrains
ALAN CORDIC & AZKA WANITWIJAN
Department of Electrical Engineering
Chalmers University of Technology

Abstract

The ongoing electrification of electric vehicles is one of todays very hot topics. The electric vehicle is composed of many parts, machine, converters and batteries just to name a few. But it also contains things which are not thought about too much. Even though the electric machine is very important, the cable modelling may be as much important or even more important. The cable modelling, and the understanding of todays both co-axial and twin-axial cable models are a must. The cables are what connects and joins very important parts of the electric vehicle. It is thus a very crucial part of getting the different parts of the electric vehicle to work together in a coherent and functional way. Many times when talking about cables, the conductor is the main talking point, and many may forget the shielding. In this report the shield as well as DM and CM currents has been given importance. The shield is modelled as a separate conductor in this work, and the impedance of ground plane is also investigated, just to name a few.

This work has also investigated the importance as well as problematics of determining and simulating functional cable models as a part of electrical vehicles. The work has put its main focus in measurement techniques of electrical parameters as well as cable modelling in the simulation software COMSOL. A comparison of theoretical and measured quantities for shielded coaxial cables as 1x50mm^2, 1x70mm^2 and 1x95mm^2 as well as 2x4mm^2 has been done. This work gives an insight in how to obtain a cable model, and what physical factors that are determining each electrical parameter. The most important electrical parameters in this report are studied carefully and cable parameters are compared with each other.

The final outcome of this work can ensure for correct measurement techniques on coaxial cables, as well as final cable models. The final result also includes most of the values obtained of the measured parameters. This work takes into account possible errors, and discussions regarding them as well as the outcome and method of the report.

Keywords: Coaxial cable, Twin-axial cable, Electrical vehicle, Electrical parameters, COMSOL simulation, Measurement, Techniques, LCR, EMI, EMC, Shielded, Cables.

Acknowledgements

Firstly, we would like to express our sincerest gratitude to the Electromobility department at Volvo GTT for the opportunity to let us do the Master's thesis and letting us use the eqiupment for this project. We would also thank our supervisor Per Widek for his expertise and experience for always guiding and supporting us to move forward with the project. Secondly, we would to thank our examiner Torbjörn Thiringer, professor at Chalmers University of Technology, for continuously providing encouragement and guidance throughout the project. Furthermore, we would like to acknowledge Urban Lundgren at RISE and Tarik Abdulahovic at ABB for their kindness and time for supporting us with the theoretical discussions of the project. Finally, we would also like to thank Yuriy Serdyuk, professor at Chalmers, for the very informative technological discussions we had, as well as the support.

Alan Cordic & Azka Wanitwijan, Gothenburg, August 2021

Contents

1
Introduction

1.1 Background

In a traditional electric vehicle, the main important components are converters, batteries and the cable system as well as the electrical machine. The cables could be of different type or size depending on where they are used in the vehicle and what purpose they serve. However, one aspect when working with cables in electric vehicles is that there is always a chance of the conductors interfering with each other for higher frequencies. The cable modelling may not be as simple as one thinks it is. It might not be a resistance in series with an inductance that is the solution, the problem could be more complex than that. As the vehicle electrification keeps on increasing, the demand for a working cable simulation model is a must. By having so many parts working together in the electric vehicle, the switching of converters for example, may affect other equipment as well. It is thus very important to make a cable model that will account for these things. A cable model that can withstand these requirements is a must in today's industry. How does one minimize errors when measuring electrical parameters, and in what way can the cable parameters be determined and analyzed, in a secure and correct way? These are some of the important topics of today's electrical system (or in the topic of EMC in general), and also some of the points that will be covered in this work. A working cable model is very important for the rest of the functionality of the electric vehicle.

1.2 Problem description

The points below are tasks to be solved during the project:

- Create usable circuit equivalent models of the cables that will be used in the electric vehicles and tune the models to make them correspond to the behavior of the real cable in frequency domain.
- The impedance behavior should match as good as possible in both simulated and measurements in up to 30 MHz in frequency.
- Study how to measure using an LCR meter for each specific parameter in the models.
- Compare the values from the LCR measurement with simulation and theoretical calculation.
- Explain for the reason for a certain behavior in the measured impedance model, and account for the parasitic elements.

- Investigate the CM and DM currents behavior in the cable at frequency domain.
- Explain for any inaccuracies between the measured impedance model and the simulated model at a certain frequency range.

1.3 Aim and purpose

The main goal of this project is to model two different types of cables used in an electric vehicle which are coaxial and twin-axial cables where different dimensions and lengths will be taken in consideration. The aim is to build a practical model in three-phase that would be as close as possible to the real simulated and theoretical case at high frequency up to 30 MHz. But also to implement the + and - battery cables in a model. Therefore a 2 parallel coaxial cable set-up will also be studied. Various methods of measuring each LCR parameters in the equivalent pi-model will be studied by using both LCR and DC meters. The behavior of common mode and differential mode currents in the cable in the frequency domain will be investigated as well. This is to understand how the return path of each types of currents will choose to flow in a cable system of an electric vehicle drivetrain.

1.4 Delimitations

This project puts its focus on the impedance modelling of the cables, and any tests to improve already existing equipment will not be done. The equipment that exists will be used in the analysis, and the main focus is to model the existing system as good as possible. The criteria is to have a simulated model from COMSOL and PLECS that does not deviate from the measured tests more than 5%.

2

Theory of transmission line

In order to properly simulate the cable and obtain its parameters, it is necessary to know about the theoretical background of computing these parameters. In the following sections the necessary knowledge needed to compute and analyze the cable parameters will be explained.

2.1 Types of testing cable

In this project there will be two different types of cables that will be tested and simulated. Both of them are manufactured by HUBER+SUHNER.

2.1.1 Coaxial Cable

The first type of testing cables is a coaxial cable which consists of six layers which can be seen in Figure 2.1. This coaxial cable is the cable model of FHLR91XC13X, a single-core, shielded cable that is used in road vehicle applications.

The innermost layer of this cable is a conductor which consists of bunches of bare copper strands. The conductor is designed to transmit electricity or signals through the cable and it is important that this layer is well protected by the outer layers. Without a decent protection, aging, degradation and eventually breakdown can occur. The next layer is tape that covers the conductor. The following layer is dielectric insulation, an insulator that is made by RADOX where the dielectric properties are exceptional [1]. The insulation layer is designed to keep the transmitted signal flowing strongly with low interference from the outside i.e. from the outermost layer of the coaxial cable as much as possible and also minimize the leakage from the conductor. It acts as a secondary protection if something is leaking through the outermost layer. The outer layer of the dielectric insulation is the shield also known as EMC-screen which is a tin plated copper braid. The shield is used to prevent the electromagnetic radiation of the conductor from emitting outside and not letting a signal from outside interfere with the transmitted signal in the cable. The outside of the shield is coated with a tape layer, the same as outside the conductor. The final layer is a sheath that is made of RADOX Elastomer. The sheath (it can also be called jacket) acts as the primary protection of the cable, where it protects the inner layer of the coaxial cable from possible vulnerabilities that can damage the cable such as humidity, surrounding contaminants, moisture and erosion.

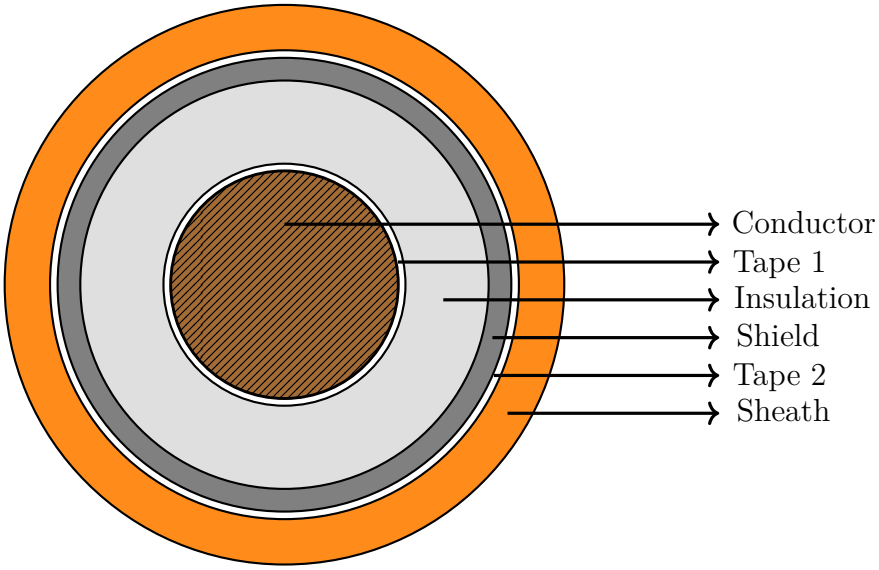

Figure 2.1: Cross section of a coaxial cable

In this project, the layers of tape will neglected since they are extremely thin. Because of this, it will later simplify the cable model in terms of simulation and calculation. In the tables below, the necessary variables of the cables that will be used for obtaining the desired parameters are presented.

Table 2.1: Diameter for each layer of coaxial cable with different thickness.

Diameter (D)	1x50mm^2	1x70mm^2	1x95mm^2
Conductor	9.3mm	11.5mm	13.4mm
Tape 1	9.4mm	11.6mm	13.5mm
Insulation	11.5mm	13.7mm	16.2mm
Shield	12.6mm	14.6mm	17.4mm
Tape 2	12.7mm	14.7mm	17.4mm
Sheath	14.9mm	17.0mm	19.9mm

Table 2.2: Different materials and values of relative permittivity (ϵ_r) that are used in the coaxial cable.

Layer	Material	ϵ_r
Conductor	Bare copper	1.0
Insulation	RADOX 155S	2.8
Shield	Tinned copper	1.0
Sheath	REMS	4.8

2.1.2 Twin-axial Cable

The next type of testing cable is the twin-axial cable where the conductor's cross-sectional area is $4mm^2$ with different lengths of 1m, 5m and 10m. The twin-axial consists of four layers [1]. The innermost layer is the core where it is comprised of two conductors where each conductor is made of bare copper strands and two RADOX insulators. One of the conductors (red) is designed to transmit the input signal while the other (black) is made to receive the returning signal. The following layer is the shield which is made of braided tin-plated copper. Both conductors and insulators are enclosed by a common shield. The outer layer of the shield is called tape and the outermost layer is called the sheath. Each layer has the same properties and behavior as a coaxial cable. The geometry of the twin-axial cable can be illustrated in Figure 2.2.

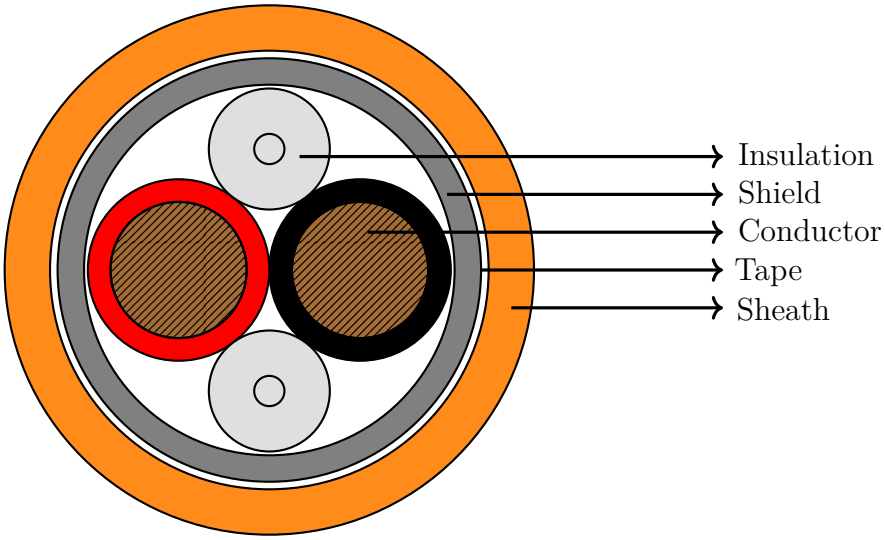

Figure 2.2: Cross section of a twin-axial cable.

In the same way as for the coaxial cable case, the tape layer will be neglected because of its extremely thin thickness which will not affect the results even if it is included in the model or not. In the following tables shown, the necessary dimensions of a 2x4mm^2 twin-axial cable is presented.

Table 2.3: Diameter for each layer of 2x4mm^2 twin-axial cable.

Diameter (D)	2x4mm^2
Each conductor	2.46mm
Core	3.55mm
Shield	7.81mm
Tape	7.92mm
Sheath	10.20mm

Table 2.4: Different materials and values of relative permittivity that are used in the twin-axial cable.

Layer	Material	ϵ_r
Conductor	Bare copper	1
Insulation	RADOX 155S	2.6
Shield	Tinned copper	1
Sheath	REMS	4.8

2.2 Shielded cable in electrical system

In an electrical system, electromagnetic interference (EMI) plays an important role since it can be harmful and it can degrade nearby operation or other components of the system [2]. By shielding the cables as an alternative, one can avoid and protect the equipment from this undesirable effect. The shield which is surrounding the conductor will reduce the interference from outside of the cable to reach the conductor that is transmitting the signal. However, in reality there is still some energy that go through the shield but it is extremely low. There will be no disturbances in the transmitted signal at all because most of the EMI have in advance been mitigated by the shield. In industrial applications, there are two types of shielding used for protecting the cables which are foil and braided shielding [3]. In this project, the braided shield will be used for testing.

Figure 2.3: Test cable with braided shield.

2.3 Ground reference plane for testing

In a test set-up when placing one or two shielded cables above a ground plane, the ground plane will act as a reference point when measuring the voltages between the points of interest. The voltage of the ground plane is defined as zero reference point [4]. Afterwards, when the models are simulated in different simulation platforms such as COMSOL multiphysics and PLECS, the ground reference plane will be required in the model. The ground plane can as well be used as a return path.

Therefore, in this system, the ground plane will also be considered as a conductor as well as the already existing inner conductor and the shield of the cable [5][6].

Figure 2.4: Ground reference plane for the test set-up made of a long aluminum sheet.

2.4 Common mode and differential mode current

At the connection between the power inverter and the motor drive in an electric vehicle system, there will occur some particular parasitic effects where the current flows through the parasitic capacitors which exists between different parts of the system. This undesired effect of current is called common mode (CM) current, it will flow via the parasitic capacitor down to the ground reference or the vehicle chassis and return via the AC power supply through the connection to ground. This can cause electromagnetic interference (EMI) which will damage the electrical components in the system or even the vehicle [7]. By protecting such interference, a shielded cable can be one of the solution. Because 90% and 10% of the CM current will flow via the parasitic capacitor through the shield of the three-phase cable and metallic vehicle chassis, respectively. Which means that the shield will be used as the main path of the current flow. The differential mode (DM) current will simply flow from the power supply into the load and return from the load to the power supply [8]. Both paths of CM and DM current can be illustrated in the figure below.

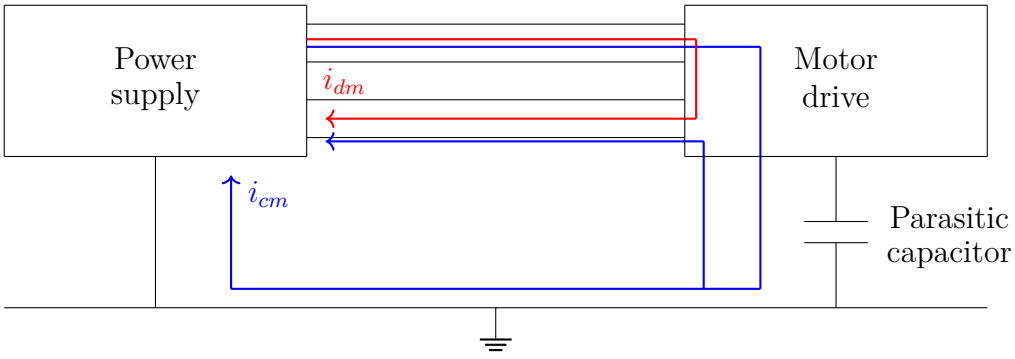

Figure 2.5: Common mode (blue) and differential mode (red) currents paths in an electric vehicle system.

2.5 Pi-model in transmission line

The pi-section equivalent circuit of a transmission line is typically comprised of a series-impedance and half the capacitance at each end of the circuit [9] which can be shown as in the figure below.

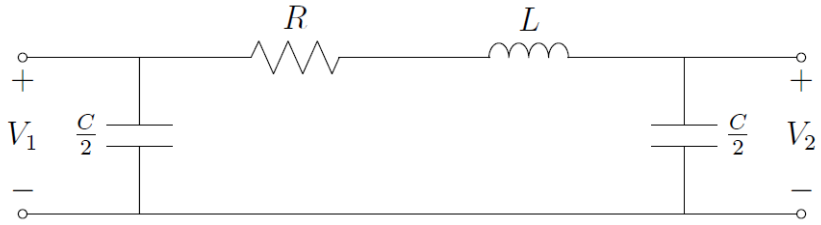

Figure 2.6: A nominal pi-model of transmission line.

2.5.1 Pi-model of single shielded coaxial cable laying on ground plane.

When it comes to a shielded coaxial cable, the shield will also act as a conductor since it is made out of tinned copper braid. Both of conductor and shield of the cable will then contain series-impedance such as self-resistance (R_c & R_s) and self-inductance (L_c & L_s) and coupling capacitance (C_{cs}) between each other. There will as well be mutual inductance between the conductor and the shield (M_{cs}). Since the shielded cable is placed on a ground reference plane where the plane is made of aluminium. Thus, there will be inductance (L_g) in it and a coupling capacitance between the shield (C_{sg}). But the capacitance between the conductor and ground plane will not be taken in consideration because it is already composed of C_{cs} and C_{sg}. The whole model can be represented as in Figure 2.7.

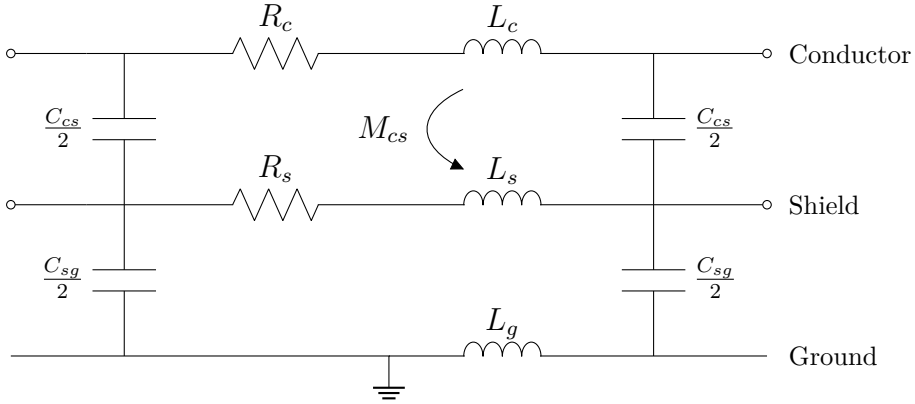

Figure 2.7: Equivalent circuit of single shielded coaxial cable

2.5.2 Pi-model of two parallel coaxial cables

A model for two shielded cables placed next to each other will be represented exactly in the same way as an equivalent circuit of a single shielded cable but in addition this model will have more parameters between each layer of both cables. The most obvious one is the mutual inductance between each shield of the cable (M_{ss}). While the mutual inductance such as between the conductor in the first cable and the shield in the second cable will be neglected for simplicity reason in the model, due to the small value. The two shielded cables model can be shown as in Figure 2.8.

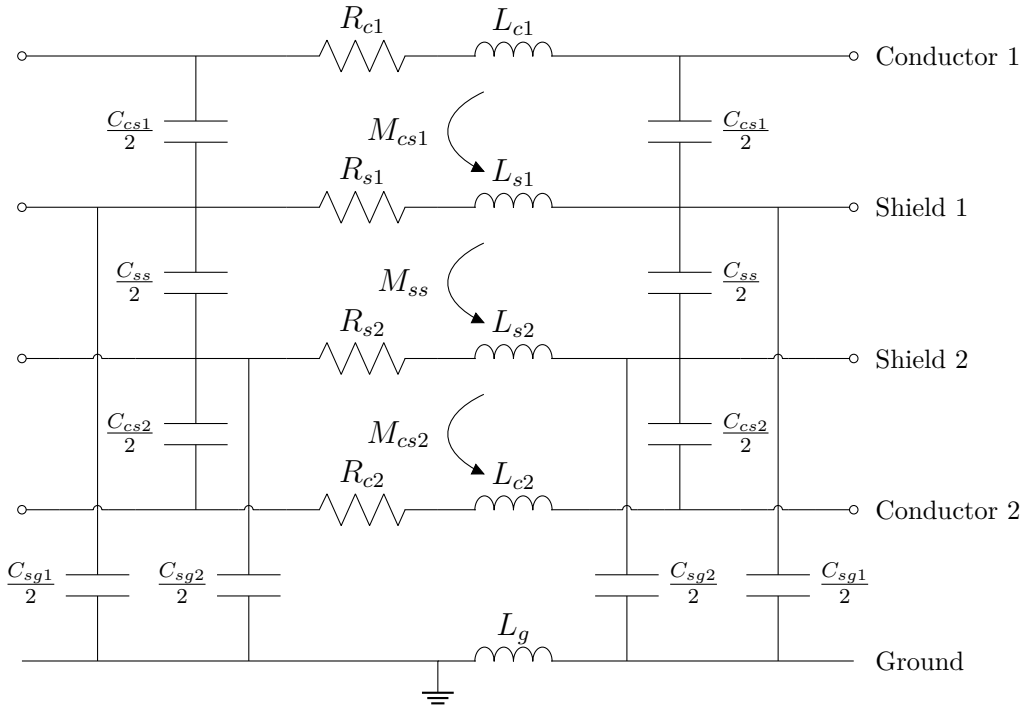

Figure 2.8: Total circuit representation of two shielded coaxial cables on an aluminium sheet.

2.5.3 Pi-model of three parallel coaxial cables

Lastly, a model of three shielded coaxial cables placed parallel to each other can be presented below as Figure 2.9. All parameters will remain the same as in the model of two parallel coaxial cables and apart from that the mutual inductance between each shield (M_{ss12}, M_{ss13} and M_{ss23}) will also be included in the three phase model.

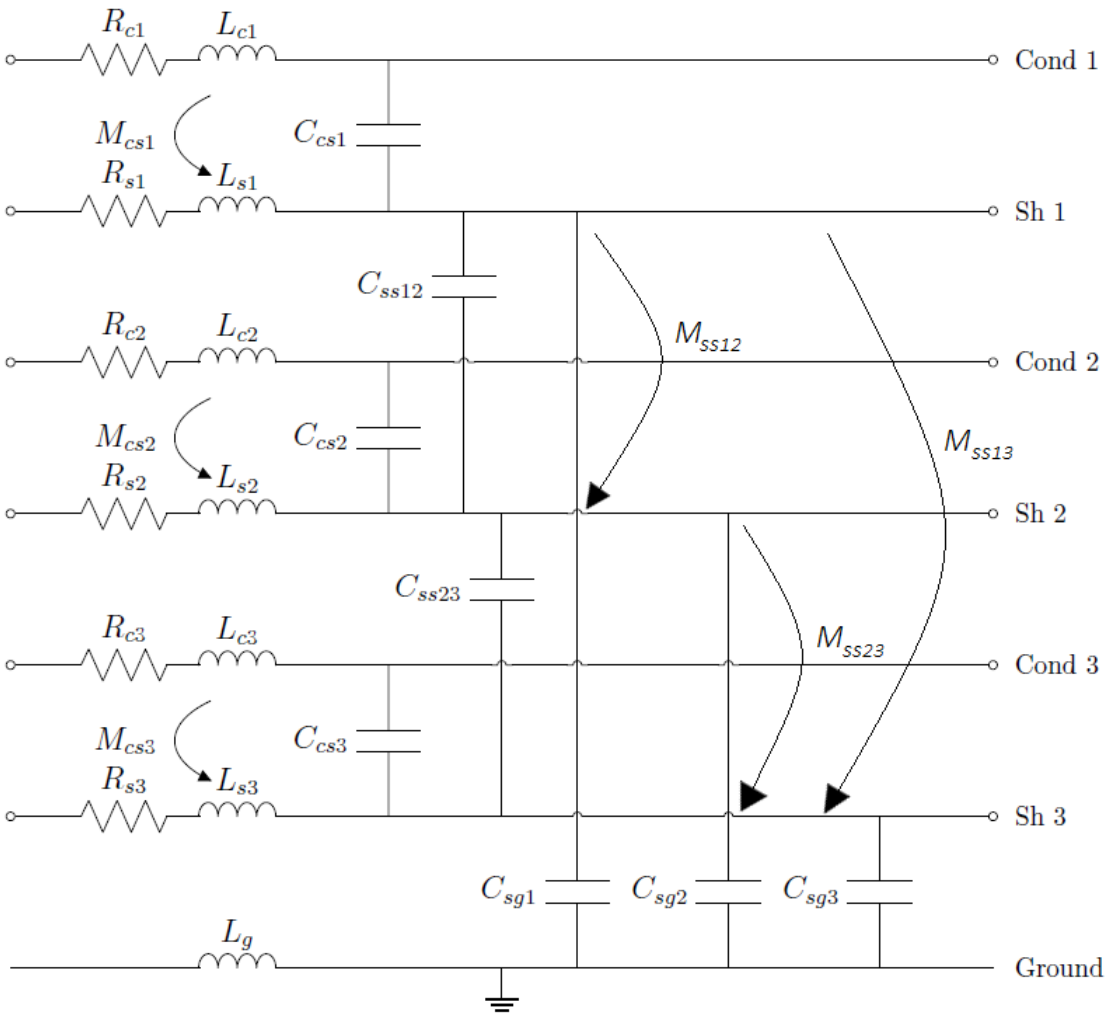

Figure 2.9: Total circuit representation of three shielded coaxial cables on an aluminium sheet.

2.5.4 Pi-model of single shielded twin-axial cable

This type of cable will have two conductors which means that the model will remain the same as in Figure 2.7 but an extra equivalent circuit of a conductor will be placed between the first conductor and shield. As well as the coupling capacitance between those two conductors (C_{cc}). The following figure shows the twin-axial equivalent pi-model.

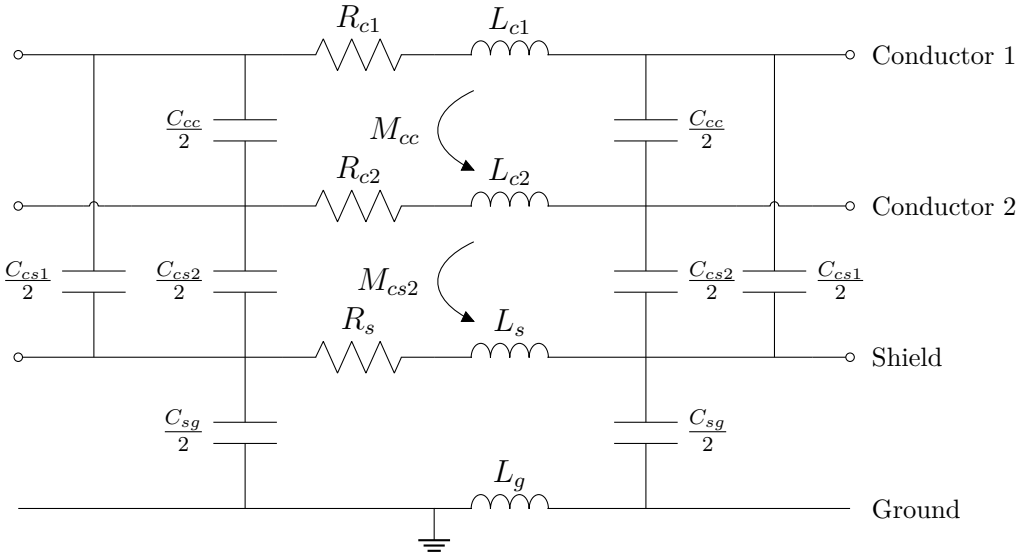

Figure 2.10: Equivalent circuit of single shielded twin-axial cable

2.6 Impedance characteristic

2.6.1 Resistance

The resistance of the conductor in a cable when applying DC current into it can be defined as

$$R = \frac{\rho l}{A} \tag{2.1}$$

where ρ is represented as the conductor resistivity, l is the conductor length and A as the conductor cross-sectional area. By applying AC current into the conductor, it will occur a phenomenon called skin effect where the current distribution at the cross-section of the conductor will no longer be homogeneous. The result is that the current density becomes largest at the surface of the conductor [10]. This means the current will mostly flow on the 'skin' of conductor where the distance between the outer surface of the conductor and the level of current flow is called skin depth (δ). The skin depth can be calculated from

$$\delta = \sqrt{\frac{2\rho}{\omega\mu}} \tag{2.2}$$

where ω is the angle velocity of the flowing current and μ is the permeability. When δ is known the resistance for AC current can be calculated from (2.1) as

$$R = \frac{\rho l}{A - x} = \frac{\rho l}{A - (\pi(r - \delta)^2)} \tag{2.3}$$

this equation is valid when $r >= \delta$. Where x is the area limited by δ and r is the conductor radius [11].

2.6.2 Capacitance

Between two voltage potentials, with different values, lies an electric field, according to following equation

$$E = -\nabla V \tag{2.4}$$

according to (2.4), there will exist an electric field as long as there is a potential gradient between for example two bodies. This means, that if there exists between two conducting objects or between a conducting object and ground a voltage gradient then there exists and electric field. A capacitance can easily be formed between two conducting medias with different voltage potentials. Capacitance is defined as the charge divided by the voltage difference between two points

$$C = \frac{Q}{V}[F] \tag{2.5}$$

according to Gauss's law the electric flux that passes through an closed loop surface is equal to the charge that is enclosed by this surface. This is very important because the charge is needed in order to calculate the capacitance. The charge enclosed by a surface is simply obtained if one integrates the surface integral of the electric field intensity vector, D.

$$Q = \oint_S D \cdot dS \tag{2.6}$$

where the electric field intensity, D, is defined as the permittivity, ϵ, multiplied with the electric field vector, E. D is given in $\frac{C}{m^2}$, integrated over an surface area gives simply the charge given in Coulomb. S in dS is the surface of the integration. Now that the charge is known, the voltage potential needs to be defined. This can be derived from (2.4). The voltage of an object in space can be obtained by integrating the electric field over a line as follows

$$V = -\int_l E \cdot dl \tag{2.7}$$

the capacitance can now be fully defined as

$$C = \frac{Q}{V} = \frac{\oint_S D \cdot dS}{-\int_l E \cdot dl} \tag{2.8}$$

or if one perhaps wants to write it in terms of the electric field then it becomes [12]

$$C = \frac{Q}{V} = \frac{\epsilon \cdot \oint_S E \cdot dS}{-\int_l E \cdot dl} \tag{2.9}$$

however, there is perhaps an easier way of calculating the capacitance and that is by taking use of the electric energy stored in the electric field. This relation is simply derived from the stored energy in a capacitor

$$W_e = \frac{CV^2}{2} \tag{2.10}$$

this relation will be used in COMSOL for calculating the capacitance in different locations, because of its simplicity and because COMSOL has a function calculating the energy. Solving for the capacitance, results in

$$C = \frac{2W_e}{V^2} \tag{2.11}$$

where V, is the voltage difference between the formed capacitor.

2.6.3 Inductance

2.6.3.1 Self-inductance

When a current is flowing through a piece of wire, a magnetic field is formed around the wire [13]. The magnetic flux can be defined as:

$$\Phi_1 = \int_{S_1} B_1 \cdot dS_1 \tag{2.12}$$

where B_1 is the magnetic flux density created by a current flowing through a wire, B_1 given in $\frac{Wb}{m^2}$. Φ_1 is the magnetic flux that passes through the area. The relation can also be described in simple terms by

$$B_1 = \frac{\Phi_1}{A_1} \tag{2.13}$$

where A_1 is the area that the flux lines passes through.

The term self inductance is referred to as the inductance that is due to one conductor. The self inductance can be defined as

$$L_1 = \frac{\Phi_1}{I_1} \tag{2.14}$$

where, Φ_1 is the flux created by the current flowing through L_1, which is the self inductance term. I_1 is the current that passes through the conductor. The inductance can also be specified taking use of the magnetic energy stored in the magnetic field. The magnetic energy is defined as

$$W_m = \frac{1}{2}LI^2 \tag{2.15}$$

solving for L gives

$$L = 2\frac{W_m}{I^2} \tag{2.16}$$

where W_m is obtained by surface integration of the whole domain (including cable and air around it), including all magnetic flux lines that is due to one conductor. Then this value is divided by I^2, which is the squared value of the applied current in the conductor.

2.6.3.2 Mutual inductance

If there is a conductor that is not energized and placed close to a current carrying conductor, then there will exist a mutual term between the two conductors, that is called the mutual inductance.

The magnetic flux lines tend to spread around the conductor that is energized in the air and covers parts of the other conductor. When this happens, there will be a voltage induced in the other coil which was not conducting any currrent initially. The induced voltage in the other conductor will allow for a current to flow in the conductor. The inductance that is "created" due to the flux lines of the other conductor can be simply defined as

$$L_{21} = \frac{\Phi_{21}}{I_1} \tag{2.17}$$

where Φ_{12} is the magnetic flux observed by the second conductor, where the '2' in Φ_{21} stands for the flux observed by conductor 2, and '1' that it is created by conductor 1. I_1 is the current flowing in conductor 1. In the same way, one can calculate the mutual inductance term if current flows in conductor 2 and measure over conductor 1. But if the conductors are equal, the mutual inductance turns out to be the same in both cases. That is, $L_{21} = L_{12} = M$ [14].

The mutual inductance, as defined earlier, can be derived from the voltage induced. Therefore, there is also another way of defining the mutual inductance term. If V_2 is the voltage induced in the second conductor due to the current in the first conductor, then one can use ohm's law in order to also calculate the mutual inductance as well. The scenario of mutual inductance can be illustrated in figure 2.11, the magnetic field due to conductor 1 is covering second conductor as can be seen.

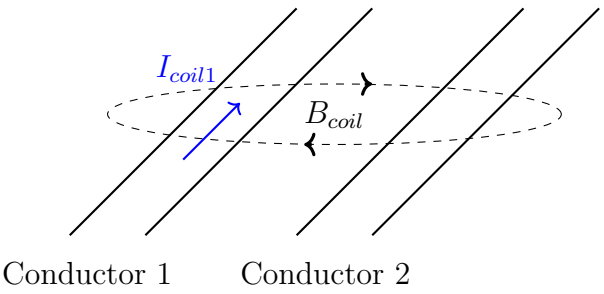

Figure 2.11: Two parallel conductors surrounded by a magnetic field

2.7 Frequency response

The impedance measurements that have been conducted will be done in frequency domain. In order to give a good background understanding of this topic, this section will provide with information about frequency response of a simple R-C circuit. The frequency response of a circuit is usually plotted in a Bode plot, including two plots,

one amplitude plot and a phase plot. The amplitude plot will be analyzed and used mostly in the Results section.

2.7.1 RC-circuit

Assume a simple RC circuit, where a voltage source is feeding the circuit at one end and the voltage output is measured in the other end.

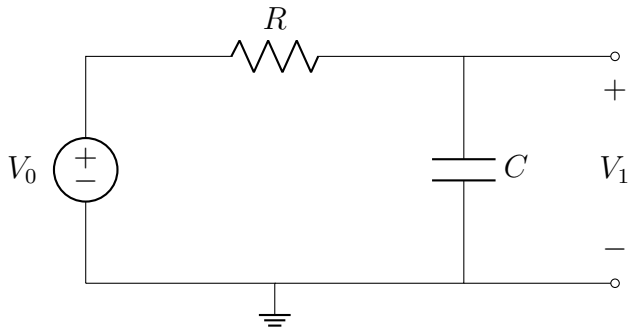

Figure 2.12: RC circuit with voltage source

The transfer function is defined as the ratio between output voltage and input voltage.

$$H(j\omega) = \frac{V_1}{V_0} \tag{2.18}$$

as the components are in series, voltage division can be applied. The voltage V_1 is then equal to

$$V_1 = V_0 \frac{\frac{1}{j\omega C}}{\frac{1}{j\omega C} + R} = V_0 \cdot \frac{1}{1 + j\omega RC} \tag{2.19}$$

solving for $H(j\omega)$ gives

$$H(j\omega) = \frac{V_1}{V_0} = \frac{V_0 \frac{1}{1+j\omega RC}}{V_0} = \frac{1}{1 + j\omega RC} \tag{2.20}$$

the amplitude function is equal to

$$|H(j\omega)| = \frac{1}{\sqrt{1^2 + (\omega RC)^2}} \tag{2.21}$$

the phase function of a fraction is equal to the phase of numerator subtracted with the phase of the denominator, as follows

$$\angle H(j\omega) = 0 - \tan^{-1}(\frac{\omega RC}{1}) = -\tan^{-1}(\omega RC) \tag{2.22}$$

having in mind that the amplitude of a bode plot is in dB, the value for the amplitude is converted into $A = 20 \log |H(j\omega)|$ [dB].

Plotting this, with some standard values of R and C gives the frequency response in figure 2.13.

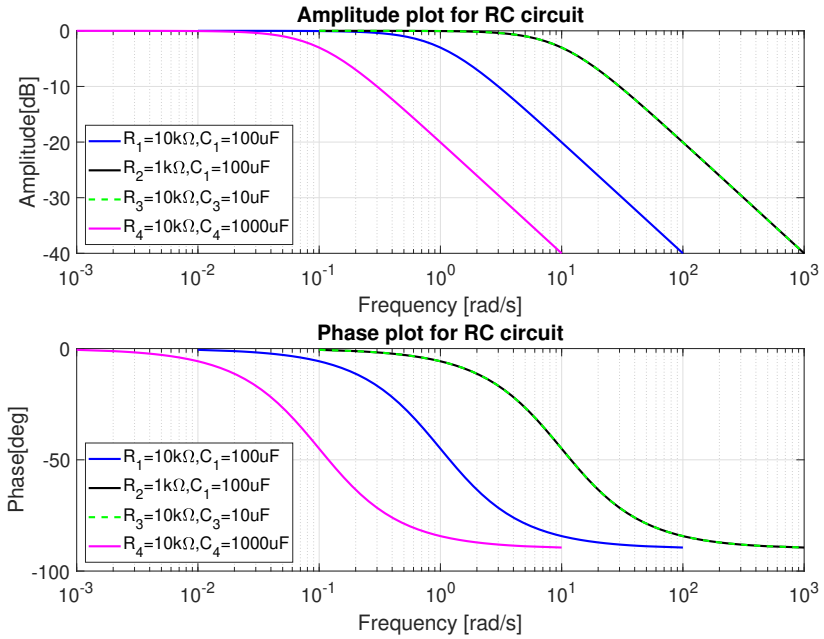

Figure 2.13: RC circuit frequency response with different values for R and C

As can be seen in figure 2.13, the plots change with the values of R and C. The displacement either to the right or the left depends on if the resistance or capacitance is increased or decreased. As can be found in the figure, the cut-off frequency will vary according to values of R and C. However, there is no change if R is decreased or if C is decreased the result is the same, as can be seen by the black and green plots. On the other hand, if values of R or C are increased then the cut off frequency decreases. The cut-off frequency is defined as the frequency when the amplitude reaches -3dB. After this value the decay is linear in the amplitude graphs as can be noticed. This is a so called low-pass filter, it blocks high frequencies. The cut off frequency is the frequency at which the resistive impedance is equal to the capacitive reactance, $R = X_C$

$$R = \frac{1}{\omega_c C} \tag{2.23}$$

Solving for the cut-off frequency, f_c, gives

$$f_c = \frac{1}{2\pi RC} \tag{2.24}$$

This relation can be a good tool in analyzing results connected to bode plots [15].

3

Electrostatic and Electromagnetic Field Theory

3.1 Electrostatics and Electric Currents

In this section the calculation of electrical parameters for a coaxial cable will be explained and formulated. A cross section of the coaxial cable structure can be seen in Figure 3.1, where each layer radius is given as a, b, c and d. With a being the inner conductor radius, b being the inner radius of screen, c being the outer radius of the screen and d being the radius of the whole cable, or the so called sheath.

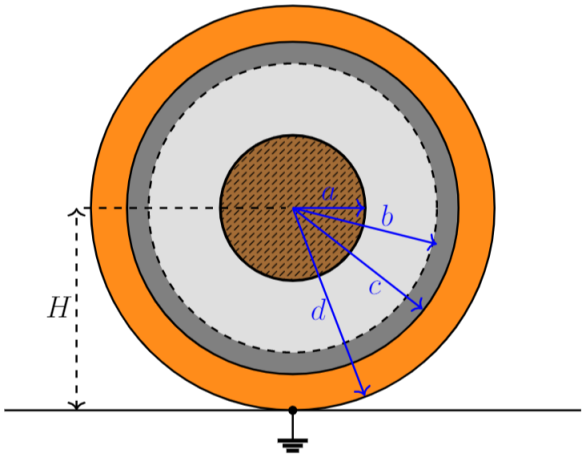

Figure 3.1: One coaxial cable placed over ground plane

3.1.1 Capacitance between conductor and shield

By using Gauss's law for a cylindrical geometry one can obtain the capacitance inside the insulation, that is between conductor and screen. By integrating the closed loop electric flux one will obtain the electric charge as stated by

$$Q = \oint D \cdot dS \tag{3.1}$$

where $d\mathbf{S} = 2\pi rl$, and D is equal to $\epsilon_0 \epsilon_r E$ and can then be rewritten in terms of the electric field as

$$Q = \oint \epsilon_0 \epsilon_r E \cdot dS = \epsilon_0 \epsilon_r E(r) \cdot 2\pi rl \tag{3.2}$$

solving for the electric field that is dependent on the radius r

$$E(r) = \frac{Q}{\epsilon_0 \epsilon_r \cdot 2\pi r l} \tag{3.3}$$

now what is left is to obtain the voltage from the electric field, and then use charge-voltage relationship to obtain the capacitance. Taking use of (2.7) one can integrate the electric field over the insulation area, that is limited by the outer conductor radius and inner screen radius. Doing so gives a voltage between a-b as in Figure 3.1.

$$V = \int_a^b E(r) \cdot dr \tag{3.4}$$

now, replacing $E(r)$ with (3.3) and solving gives

$$V = \int_a^b \frac{Q}{\epsilon_0 \epsilon_r \cdot 2\pi r l} \cdot d\mathbf{r} = \frac{Q}{\epsilon_0 \epsilon_r \cdot 2\pi l} \cdot \ln \frac{b}{a} \tag{3.5}$$

taking now use of (2.5) in the formulation of capacitance the result becomes [16]

$$C = \frac{Q}{V} = \frac{Q}{\frac{Q \cdot \ln \frac{b}{a}}{\epsilon_0 \epsilon_r \cdot 2\pi l}} = \frac{2\pi l \epsilon_0 \epsilon_r}{\ln \frac{b}{a}} \tag{3.6}$$

which is then used when computing the capacitance inside the cable between conductor and shield.

3.1.2 Capacitance between two parallel shielded cables

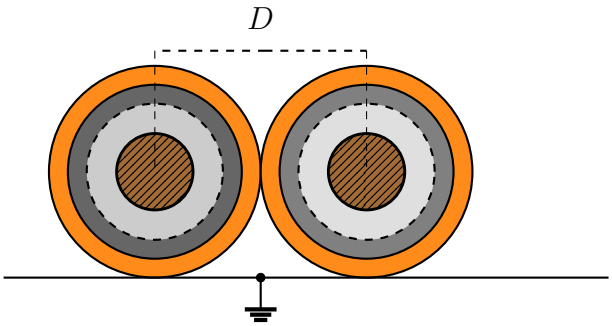

Figure 3.2: Two coaxial cables placed over ground plane

For two coaxial cables placed next to each other the capacitance is dependent on the length of the radius of the screen (c) and the distance between the cables (D), seen in Figure 3.2.

$$C = \frac{\pi \epsilon_0 \epsilon_r}{cosh^{-1} \frac{D}{c}} \tag{3.7}$$

which is basically derived from the formula for two conductors separated by a distance D in air, with a radius c [17]. However, here ϵ_r is accounted for which is the

relative permittivity of the sheath material in this case. However for this to properly work, it is required that the distance is kept as close as possible between the two cables, which is of course very hard in practice. Just becuase of the reason of permittivity. Because the permittivity in air is 1, and in the insulation it is higher. In fact, it would mean to divide the capacitance into two parts. One being in the air and one inside the sheath material. Which will of course make it more complicated. For those reasons, we plan for possible inaccuracies between the measured capacitance and the theoretical capacitance between the two shields.

3.1.3 Capacitance between shielded cable and ground plane

Looking at the geometry of the cable, if the cables are placed exactly next to each other as in Figure 3.2, then the distance from shield to shield between the cables should be twice as from one cable-shield to ground. That means that the capacitance theoretically should be twice as much for shield-ground case than shield-shield case. As a reference for hand calculation of shield to ground capacitance this statement will be used.

$$C = 2\frac{\pi\epsilon_0\epsilon_r}{cosh^{-1}\frac{D}{c}} \tag{3.8}$$

3.2 Electromagnetic Field

3.2.1 Self-inductance of conductor

The self inductance of the conductor in a coaxial cable consists of two parts. One is the common external inductance, the other is the internal inductance. The internal inductance is due to the internal magnetic fields inside the conductor, and the external inductance is due to the external magnetic fields outside the conductor. Recalling from (2.12) and (2.14), it is known that the inductance is defined as the magnetic flux divided with current. Which means that if the magnetic flux is known, and the current applied to the circuit then the inductance is easy to compute. To solve for L, first the magnetic flux is defined

$$\Phi = \int B \cdot dA \tag{3.9}$$

replacing B with $\frac{\mu_0 I}{2\pi r}l$ and solving gives

$$\Phi = \int_a^c \frac{\mu_0 I}{2\pi r} l \cdot dr = \frac{\mu_0 I l}{2\pi} \ln\frac{b}{a} \tag{3.10}$$

finally solving for the inductance, gives

$$L = \frac{\Phi}{I} = \frac{\mu_0 l}{2\pi} \ln\frac{b}{a} \tag{3.11}$$

worth to notice, is that b is the inner radius of shield and a is the radius of the conductor and l is the length of the cable. Which, means that this formula is explaining for the magnetic flux linkage between conductor and shield. The internal

inductance of the conductor is equal to $\frac{\mu_0}{8\pi}$. Total inductance for the conductor would then equal [18]

$$L = L_{ext} + L_{int} = \frac{\mu_0}{2\pi} \ln \frac{b}{a} + \frac{\mu_0}{8\pi} \tag{3.12}$$

3.2.2 Self-inductance of shield

Self-inductance can be calculated and derived by a conductor placed in the air domain, where the inductance is only dependent on the height over ground plane H, and c the radius of the conductor [19].

$$L = \frac{\mu_0 \mu_r}{2\pi} \ln \frac{2H}{c} \tag{3.13}$$

3.2.3 Mutual inductance between cables

The mutual inductance between two cables can be calculated as follows [20]

$$L = \frac{\mu_0 \mu_r}{4\pi} \ln(1 + \frac{H^2}{D^2}) \tag{3.14}$$

It is dependent only on the height over ground H, and the separation D between the cables. It can be better illustrated in Figure 3.2. This is however assumed that the distance from one cable to ground is the same for both, in other words the cables are parallel. Otherwise the expression would be different for different placements of cables, that are not parallel with each other.

3.2.4 Inductance of two-wire transmission line

If a distance D separates two conductors, both current carrying, in opposite directions then the total inductance can be calculated as follows,

$$L = 4 \cdot 10^{-7} \cdot ln(\frac{D}{r'}) \tag{3.15}$$

note that r' is the geometric mean radius of each conductor, defined as $r' = re^{-\frac{1}{4}} = 0.7788r$. However, in the twin-axial case it would be of interest to obtain the self inductance of each conductor's inductance, in that case, assuming the two wires are the same, it is enough to divide the value obtained in (3.15) with 2 [21].

4

Cable modelling in simulation

In this section the modelling of coaxial cables will be explained. The modelling is done in COMSOL in order to mainly obtain the electrical parameters from the cable.

4.1 Coaxial cable modelling in COMSOL

The modelling in COMSOL is done in both the stationary and frequency domain. The reason is to first see the values as stationary but then also see how they change during a frequency sweep. The dimensions of the cable are given by the manufacturer HUBER+SUHNER, and used in the COMSOL simulation. Worth to mention is that all simulations are done with the cable being put on the ground plane in COMSOL. The simulation is done in 2D domain, instead of 3D because 3D produced the same result as 2D. Due to symmetry it is enough to multiply the values obtained in 2D by the length of the cable. 2D simulation gives electrical parameter values per meter length of the cable.

4.1.1 Single coaxial cable placed on the ground plane

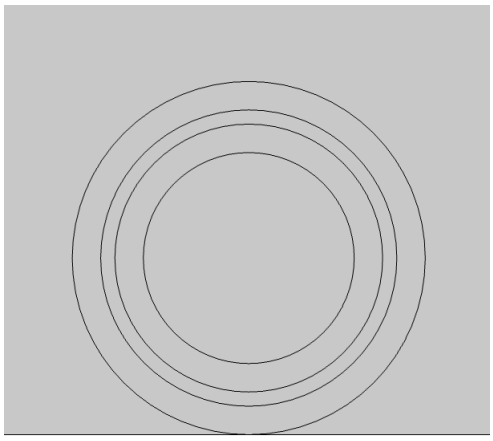

Figure 4.1: Geometry of coaxial cable in COMSOL

In Figure 4.1 the coaxial cable setup is shown in COMSOL. The outer part of the cable is set as air domain while the cable domains are taken from the manufacturer.

The conductor is made out of copper as well as the shield. The two insulation domains are made of RADOX material. The two physics that are used are electrostatics and magnetic fields in COMSOL. Electrostatics to compute the capacitance, and magnetic fields in order to compute resistance and inductance.

4.1.1.1 Capacitance calculation of single coaxial cable

The capacitance calculation is done in steps, so that each capacitance is solved one by one. By assigning terminals to each boundary the capacitance can be computed with an in-built COMSOL function.

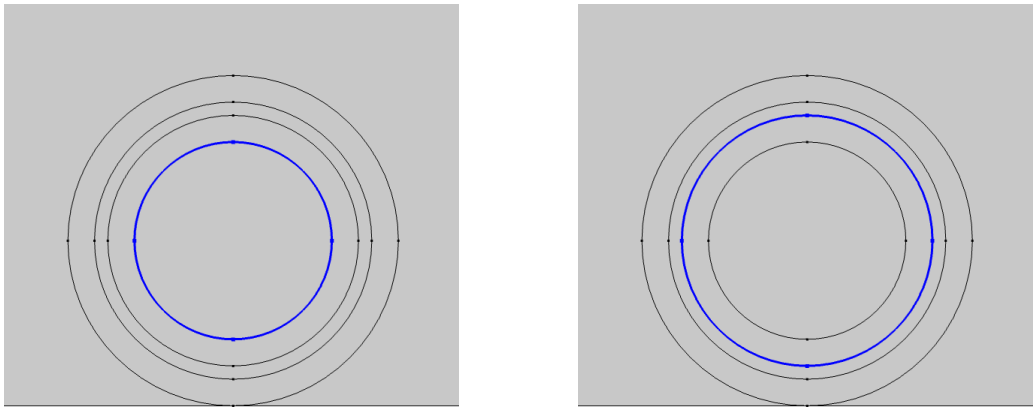

(a) Terminal of 1V applied on the outer Conductor

(b) Terminal of 0V applied on the inner of Shield

Figure 4.2: Set-up for calculating capacitance between conductor and shield

The method for obtaining the capacitance is done by assigning 1 V terminal to the conductor boundary, and 0 V terminal to the shield inner boundary. In this way there will exist a field inside the insulation part and thus the capacitance can be calculated. It is of no importance to assign a certain amount of voltage, because the capacitance will still be the same. Thus, it is fine to only use 1 V.

As for the calculation of capacitance between shield and ground, same procedure is used. Just that now the terminals are moved to shield and ground.

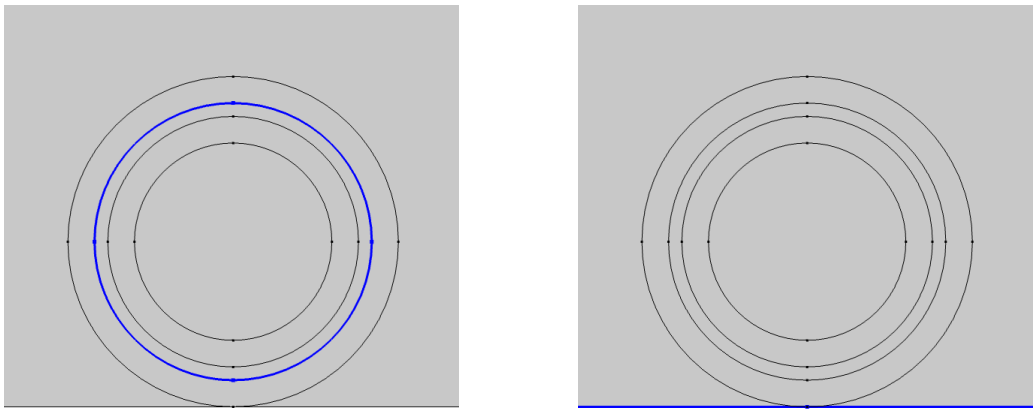

(a) Terminal of 1V applied on the Shield (b) Ground domain

Figure 4.3: Set-up for calculating capacitance between shield and ground

4.1.2 Two coaxial cables placed parallel to each other on a ground plane

To make two identical objects in COMSOL, the array function is used so that the next cable is placed exactly next to the first cable, on the ground plane.

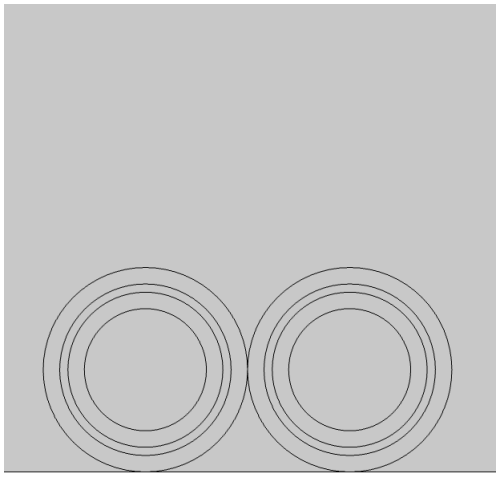

Figure 4.4: Geometry of two coaxial cables in COMSOL

4.1.2.1 Capacitance simulation of two coaxial cables

Here, the capacitance between the two cables is of special interest. When one of the shields are energized, it is interesting to see the other shields capacitive coupling.

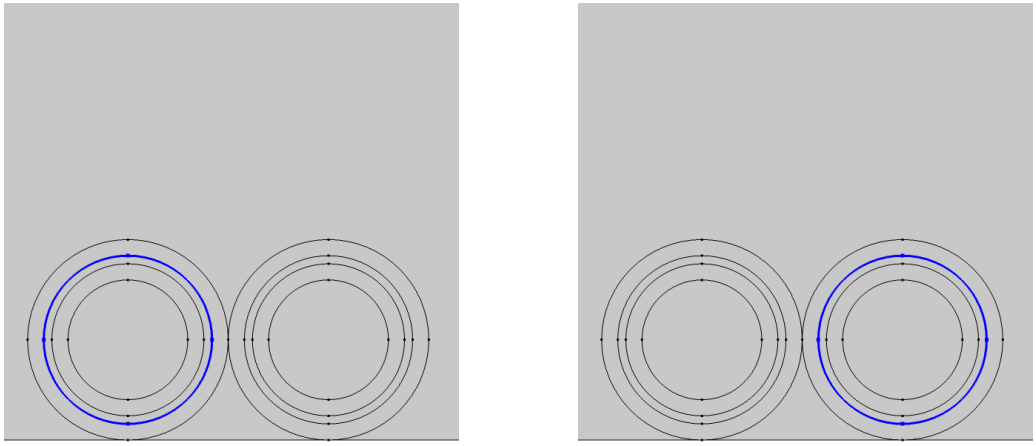

(a) Terminal of 1 V on shield (b) Terminal of 0 V on shield

Figure 4.5: Set-up for calculating capacitance between shield and shield

4.1.2.2 Inductance simulation of two coaxial cables

The inductance simulation is done by taking use of magnetic fields in COMSOL. The first thing is to assign a coil domain for the current to flow in a conductor. Then one applies a current of for example 1 A. The magnetic field that is created is then studied in order to obtain the inductance. It is the chosen domain of integration that will determine which inductance that is obtained.

4.1.2.3 Self inductance of inner conductor

The self-inductance of the inner conductor is defined earlier as the inductance of the inner conductor added with its external inductance out to the shield. When solving for inductance in COMSOL, there is a feature that can be used when taking use of coils. That feature is that COMSOL can automatically calculate the inductance desired. However, COMSOL likes to include all magnetic fields that is due to one conductor when calculating for the coil inductance. This can be problematic because the definition is that the self-inductance of the conductor is defined as the magnetic fields out to the shield and not beyond that. If one would apply 1 A of current in the middle conductor and evaluate the coil inductance, one would obtain the total inductance of the whole domain. To do it correctly, the chosen domain as in Figure 4.6 will be integrated over in order to obtain the self-inductance of the conductor.

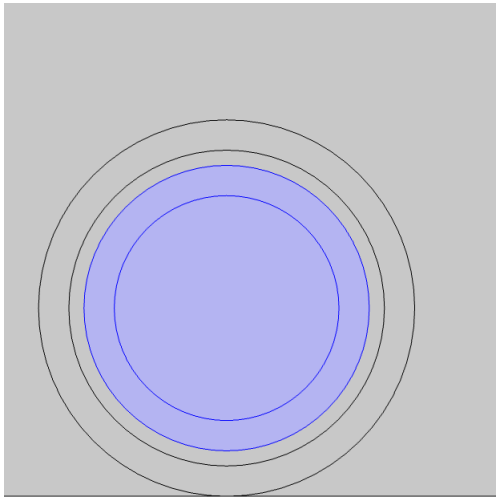

Figure 4.6: Area of integration to obtain L_c

4.1.2.4 Self-inductance of shield

For the self-inductance of the shield 1 A of current will now be applied to the shield only. By taking use of the in-built feature in calculating inductance the self-inductance of the shield can be obtained. The same value would be obtained if one would integrate over the whole domain.

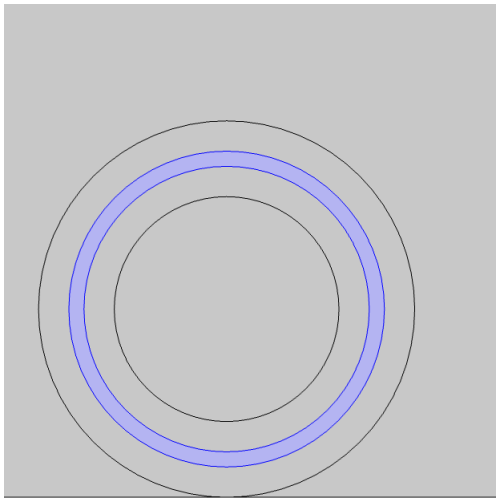

Figure 4.7: 1 A of current applied on the shield

4.1.2.5 Mutual inductance between conductor and shield

As for the mutual inductance between conductor and shield the same procedure is used. 1 A of current is applied on to the conductor and 0 A on the shield. And then evaluating the mutual inductance, using COMSOL's coil feature. The other way around is done by applying 1 A on the shield and 0 A on the conductor to obtain the mutual inductance. It is possible to show that these two values are the same which is as expected.

4.1.2.6 Mutual inductance between two cables

The same procedure is done when calculating the mutual inductance between cables. Theoretically there would exist mutual inductances between 4 conductors (having two conductors and two shields into account), when having two cables next to each other. However it can be shown show in simulation that each of the individual mutual inductance is the same. For example the mutual inductance between conductor 1 and shield 2, has the same value as the mutual inductance between conductor 1 and conductor 2. This can be explained by the fact that if a current is applied in conductor 1 (inner conductor) then the field that shield 2 would "feel" is the same field conductor 2 would feel. This is because conductor 2 is enclosed by shield 2. Which basically means that if a field is generated in one cable, then the field that is covered by the shield in the next cable is the same field that is covered by the conductor in the next cable, hence same the inductance.

4.1.3 Single twin-axial cable placed on a ground plane

The twin-axial cable as seen in Figure 4.8 is modelled using two conductors instead of one in the coaxial case. The two conductors have a separate insulation as can be seen in the figure, but a common shield and sheath.

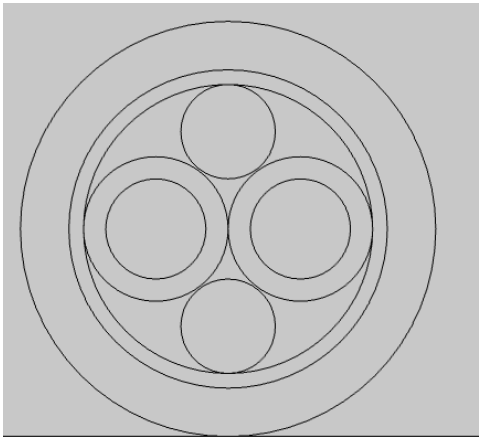

Figure 4.8: Geometry of twinaxial cable in COMSOL

4.1.3.1 Capacitance simulation of a twin-axial cable

In order to obtain the capacitance between conductor and shield, one terminal is set on the conductor's boundaries and the other terminal on the shield's inner boundary, as seen in Figure 4.9a and 4.9b. It is the same procedure as for the coaxial cable.

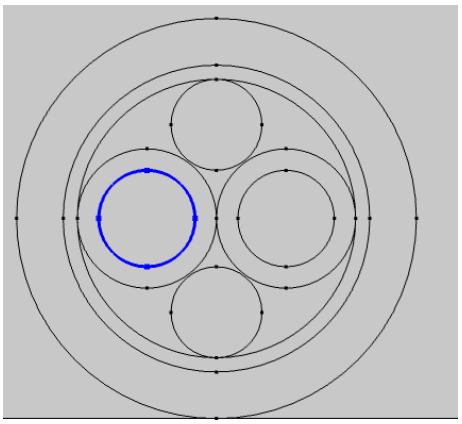

(a) Terminal of 1V applied on Conductor

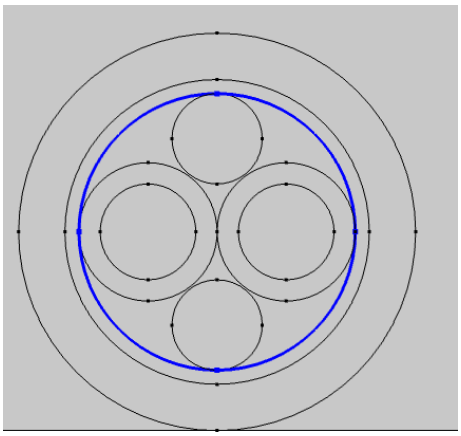

(b) Terminal of 0V applied on the Shield

Figure 4.9: Set-up for calculating capacitance between conductor and shield

And as for the conductor-conductor capacitance same procedure is done and shown in Figures 4.10a and 4.10b.

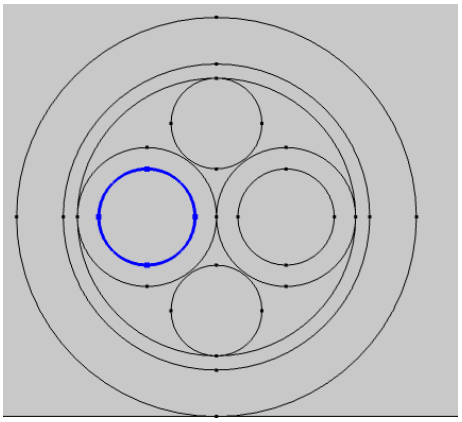

(a) Terminal of 1V applied on first Conductor

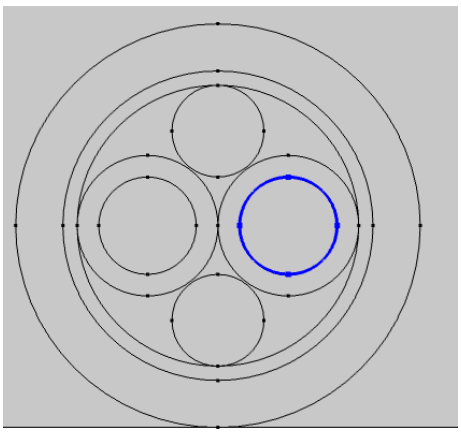

(b) Terminal of 0V applied on second conductor

Figure 4.10: Set-up for calculating capacitance between the two conductors

4.1.3.2 Inductance simulation of a twin-axial cable

To obtain the inductance, currents are applied at different locations in order to generate magnetic fields. To obtain the self inductance of the conductor 1 A of current is applied as in Figure 4.11a, and the return current is sent through the other conductor in the same cable in Figure 4.11a, but in opposite direction. To further obtain inductance in the shield, similarly 1 A of current is applied in the shield region, as can be seen in Figure 4.11b.

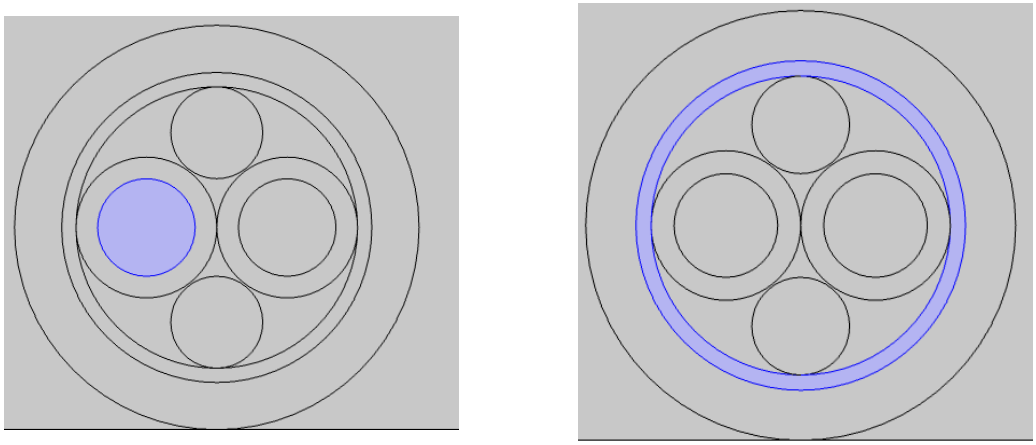

(a) Coil of 1 A applied on conductor

(b) Coil of 1 A applied on shield

Figure 4.11: Set-up for calculating inductance by feeding current in the conductor and shield separately

5

Cable measurement

5.1 Measurement method

5.1.1 LCR instrument

The LCR meter measures the current through the test cable and the voltage across it at various frequencies which in this case are between 1Hz-30MHz. Hence, the phase angle between the current and voltage will be obtained. By using these measured parameters the impedance of the test cable can be computed. When the values of desired impedance and frequency are known, they can be used to calculate the inductance, capacitance and resistance at different locations of the test cable. In this project, a PSM3750 frequency response analyzer and an IAI2 impedance analyzer from Newton4th Ltd. were used for the measurements. There are two types of methods for performing the measurement.

5.1.1.1 4-Wire Kelwin connection (4WK) PSM3750 and IAI2

The first method is called 4-Wire Kelwin (4WK) where both PSM3750 and IAI2 will be connected with each other. The principle of this method is that there will be two test probes, the first probe is the current measurement and the second probe is the voltage measurement across the test cable. While the purpose of IAI2 is to measure a higher current to the device under test, compared to PSM3750. It has also higher input impedance and is able to provide an auto shunt in the setting of the instrument where the shunt value will change depending on the test impedance [22].

This method only performs well under a frequency of 5MHz and over that value it will perform poorly. As mentioned above, this project will study the frequency range up to 30MHz. Therefore, the 4-Wire Kelwin method will not be used as a primary method for this project.

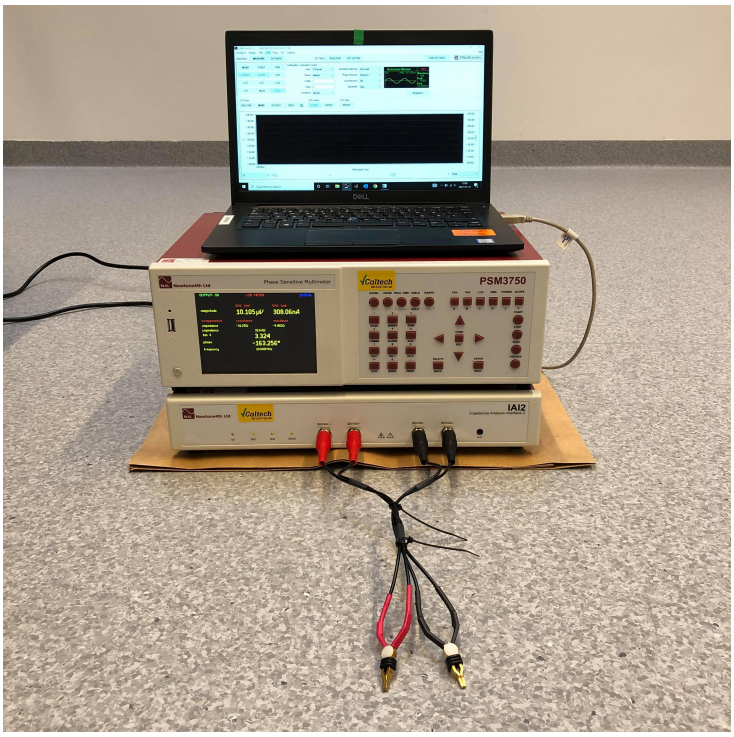

Figure 5.1: PSM3750 (above) and IAI2 (below) instrument used for 4-Wire Kelvin method.

5.1.1.2 Pearson current sensor with PSM3750

For this method, a PSM3750 instrument is the only instrument that will be used for the measurement setup. But instead it will have two separate coaxial cables for measuring current and voltage, respectively. Each coaxial cable will have two probes, see Figure 5.2. The frequency range for this method is 100Hz-50MHz. The frequency range is chosen from 100Hz and above, because the measurement method is inaccurate below this frequency. This method will be mainly used in this project and also at the Volvo Electromobilty department.

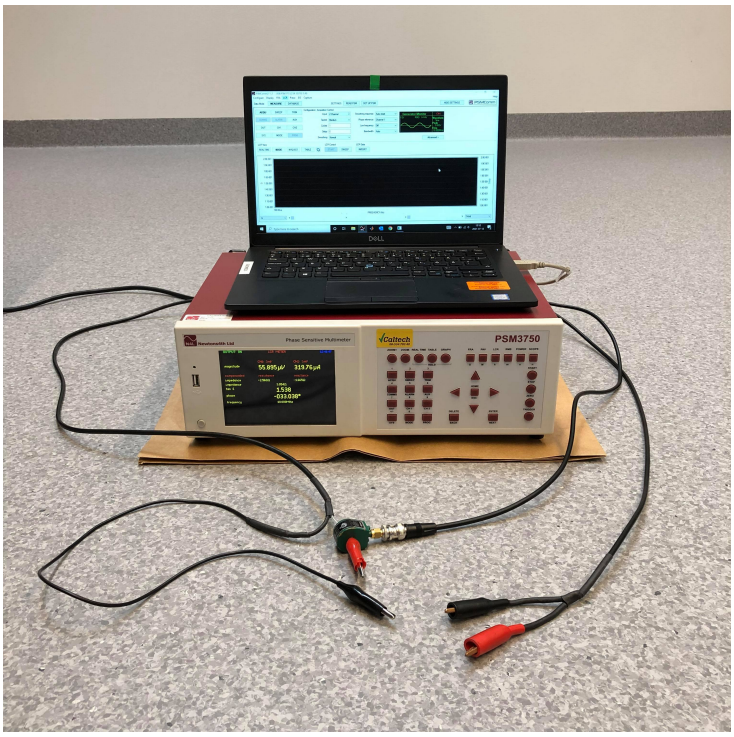

Figure 5.2: PSM3750 instrument used for Pearson current sensor method.

5.2 DC measurement

5.2.1 Resistance measurement of cable and connector

To measure the resistance in cable and connector, one of the easiest ways to obtain the resistance is by using a DC meter. The DC meter for this test setup is an EA-ELR 10080-1000 DC electronic load. This instrument works by sending in different values of the current (I_{DC}) and measure the voltage drop (U_{DC}) depending on the current value with a Fluke multimeter. The values of the resistance (R_{DC}) will then be obtained by substituting the measured values of the current and the voltage in the Ohm's law below

$$U_{DC} = I_{DC} R_{DC} \tag{5.1}$$

$$R_{DC} = \frac{U_{DC}}{I_{DC}} \tag{5.2}$$

5.3 Cable stripping

For measuring the test cable, it needs to be stripped so that the conductor and the shield can be measured easier because the test probes are made of crocodile clips.

(a) Preparing test cable and cable socket.

(b) Cut off the sheath until the shield.

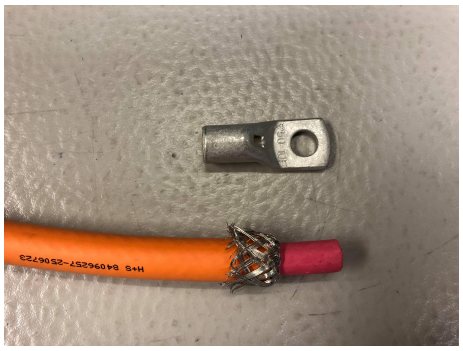

(c) Unreel the braided shield and pull it back.

(d) Cut off the insulator that surrounds the conductor.

(e) Insert the conductor into the cable socket and press it.

(f) Tape around the cutting area to separate conductor and shield.

Figure 5.3: Cable stripping procedures.

This procedure begins with preparing a test cable and a cable socket, see Figure 5.5.a. Then cut off the sheath of the cable until it reaches the shield which can be shown in Figure 5.5.b. The next step is to push back the braided shield, see Figure 5.5.c so it does not touch with the conductor when the insulator is cut off as in Figure 5.5.d. Now the conductor can be inserted into the cable socket as Figure 5.5.e and press it so the cable socket holds. Lastly, twist the braided shield to a long stick and tape around the cable as Figure 5.5.f. It is important to make sure that the conductor and shield of the cable is actually separated from each other to avoid the short circuit.

Table 5.1: Measured lengths of different dimensions of coaxial cables

Dimension	1 meter	5 meter	10 meter
1x50mm^2	0.99m	4.95m	9.99m
1x70mm^2	0.98m	4.97m	9.97m
1x95mm^2	1.00m	4.97m	9.94m
2x4mm^2	0.99m	4.99m	9.99m

The lengths of different dimensions of test cables will be later used to calculate the LCR values in per meter in Chapter 6.

5.4 Impedance measurement of coaxial cable

In this section, the methods of measuring each inductance and capacitance in a shielded coaxial cable based on Figure 2.8 using Pearson current sensor with PSM3750 will be presented.

5.4.1 Measurement of self-inductance

The test cable that will be used in this case will be bent as a U-shape which can be seen in Figure 5.4, so the current and voltage probes can be reached to both ends of the cable.

Figure 5.4: A 50mm^2 test cable that is bend as U-shape placed on ground reference plane.

According to Figure 5.5 the equivalent circuit of a single shielded coaxial cable can also be represented as in the following figure.

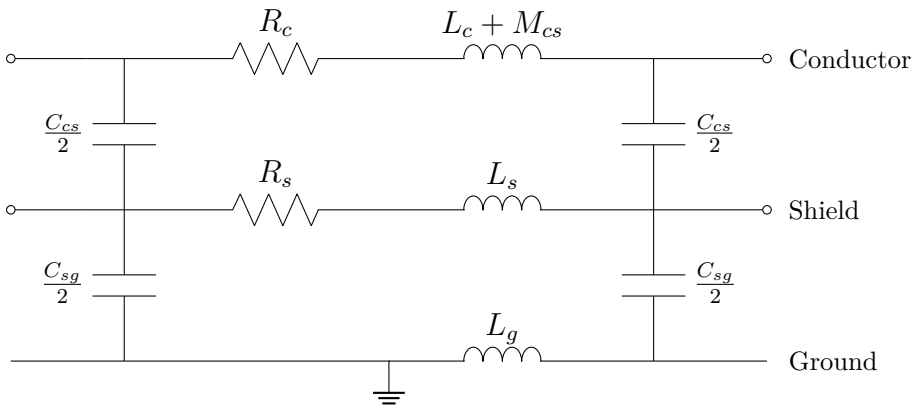

Figure 5.5: Equivalent pi-model of single shielded coaxial cable.

The total inductance when one measures the conductor is equal to $L_c + M_{cs}$, while the total inductance in the shield will remain as L_s, where it is theoretically equal to M_{cs} [23]. But in reality it will slightly differ because of the inaccurate placement of the test probes at the arbitrary points of the test cable. By this it can be concluded that they are not completely equal to each other when it comes to the LCR measurement but instead approximately equal each other ($L_s \approx M_{cs}$). So both values require to be measured separately.

To obtain the total inductance in the conductor ($L_c + M_{cs}$), the current and voltage probes will be clamped at each side of the conductors, while the shields of the test cable will be open-circuited. These connections can be shown in Figure 5.6.

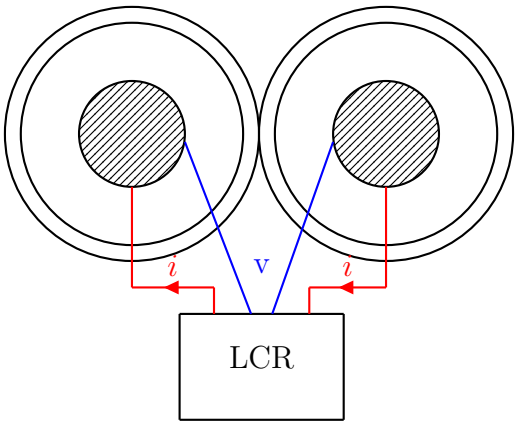

Figure 5.6: Connection of measuring the total inductance in conductor.

The obtained value for the total inductance in the conductor will then be equal as $L_c + M_{cs}$ which can be clearly seen in the equivalent pi-model below.

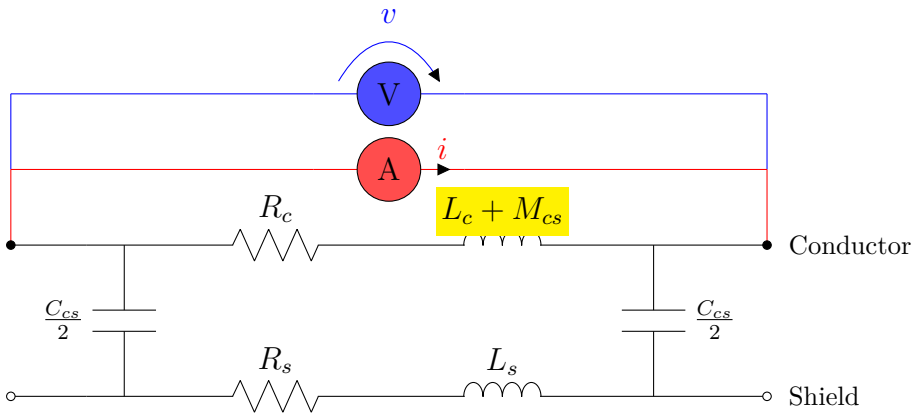

Figure 5.7: Measurement of total inductance in conductor ($L_c + M_{cs}$) as equivalent pi-model.

In order to find L_c individually, the shield needs to be short-circuited. This is due to the fact it takes some time to induce the current in the shield which will lead to a reduction of inductance. Therefore the value at the beginning will be $L_c + M_{cs}$ and when the current has been induced in the shield, the electromagnetic fields between the outer surface of the shield and external sheath will cancel out each other, or in other words the mutual inductance (M_{cs}) in these specific locations will be cancelled out. Therefore the only value left is L_c at higher frequencies. The measurement method can be illustrated in Figure 5.8.

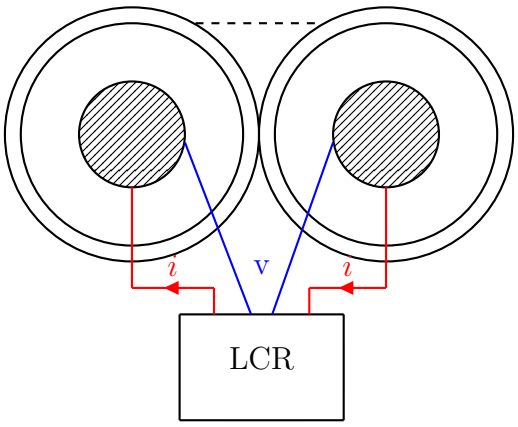

Figure 5.8: Connection of measuring mutual inductance between conductor and shield.

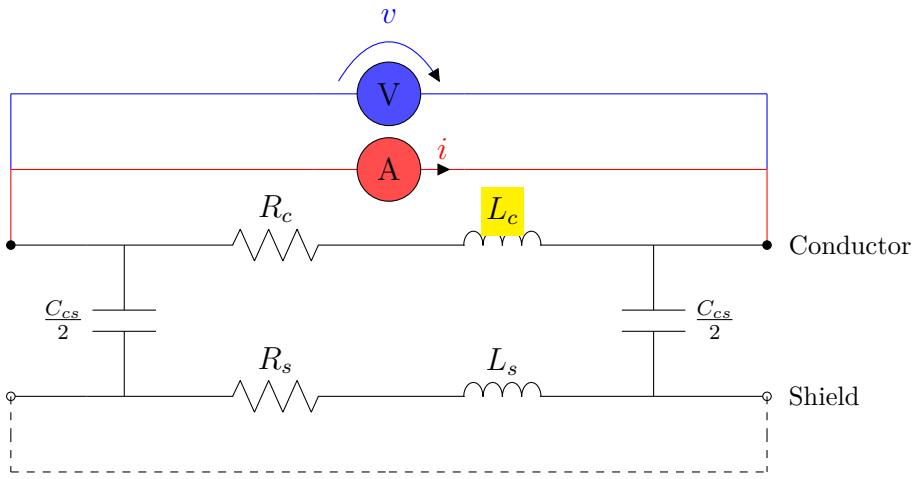

Figure 5.9: Measurement of self-inductance in conductor (L_c) as equivalent pi-model.

The self-inductance(L_s) of the shield can measured directly from the LCR instrument by connecting both current and voltage probes at the shield while the conductors are open-circuited which can be illustrated as in following figure.

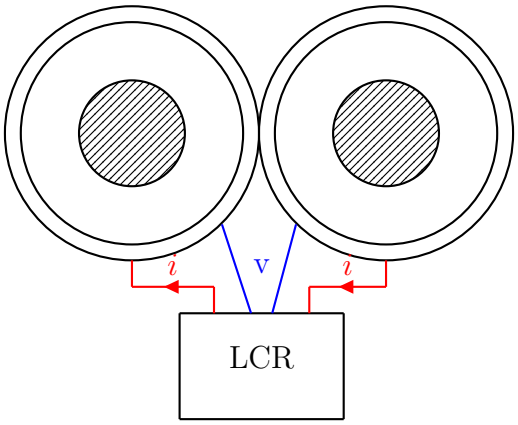

Figure 5.10: Connection of measuring the total inductance in shield.

According to the equivalent pi-model in Figure 5.11, the value of self-inductance in shield will be L_s.

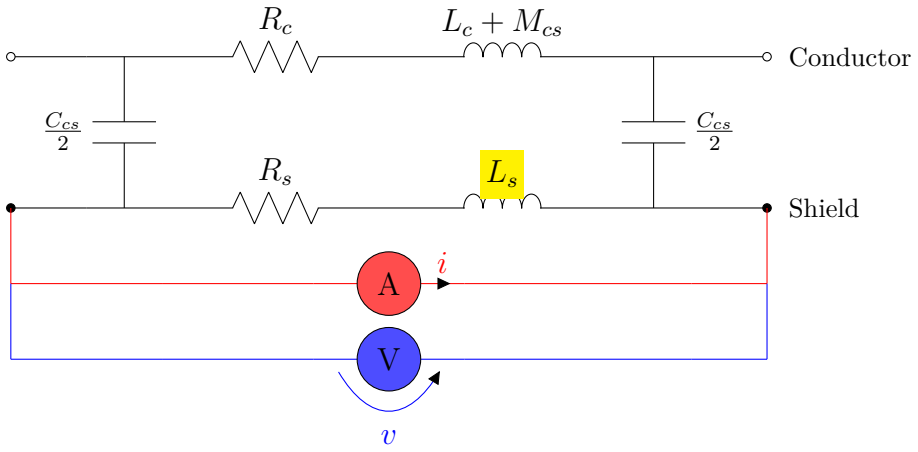

Figure 5.11: Measurement of self-inductance in shield (L_s) as equivalent pi-model.

To study the behavior of DM and CM current, the ground plane plays an important role in this investigation. The test cable will no longer be bent as an U-shape but instead placed in a straight line since it is sufficient to measure only one end of the cable. In order to find the ground plane inductance (L_g), one can apply the current through the conductor at the front side of the cable while the back side of the conductor is connected (short-circuited) to the ground plane. The current and voltage probes will be clamped to the conductor and the ground plane, respectively as shown in Figure 5.12.

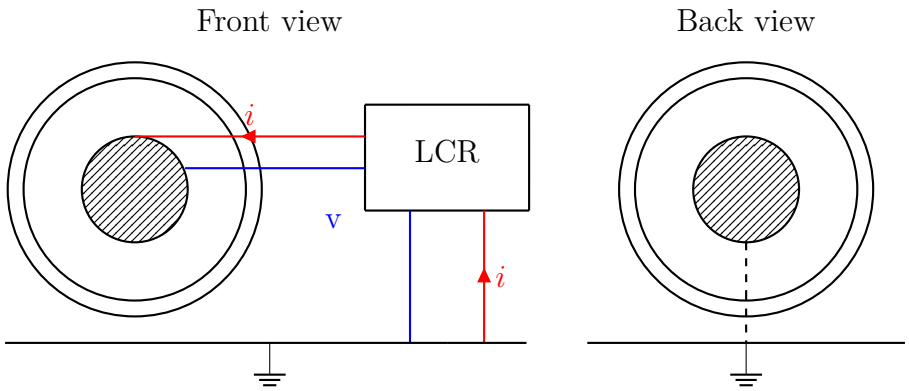

Figure 5.12: Connection of measuring the capacitance between shield and ground plane.

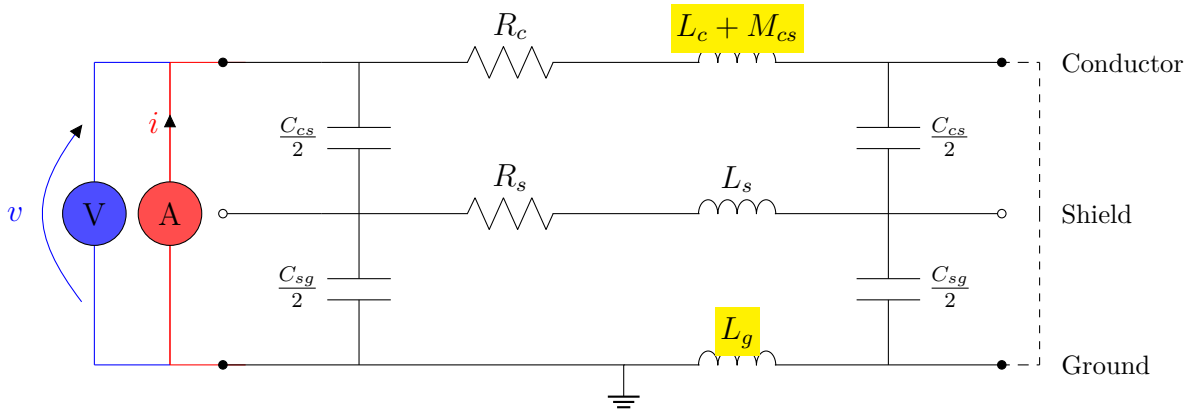

Figure 5.13: Measurement of total inductance in conductor and ground plane ($L_c + M_{cs} + L_g$) as equivalent pi-model.

This will give the sum of inductance in the conductor and the ground plane. Where L_g can be calculated since the total inductance in the conductor is known.

It is also interesting to investigate which path the return current will choose to flow if the conductor is applied with current. If it goes between the ground plane or the shield. It is known that one of the shield's purposes in the coaxial cable is to provide a return path of the current [24]. In other words, the transmitted signal will flow through the conductor and the received signal will flow back through the shield. The test cable in this case will also be placed as a straight line on the ground plane. The flowing current of this case setup can be studied by applying the current into the conductor and let the return from the shield at the front side of the cable be where the ends of both parts are connected (short-circuit). This will result in the difference between the inductance in the conductor and the shield which can be expressed as $(L_c + M_{cs}) - L_s$. This can be illustrated below.

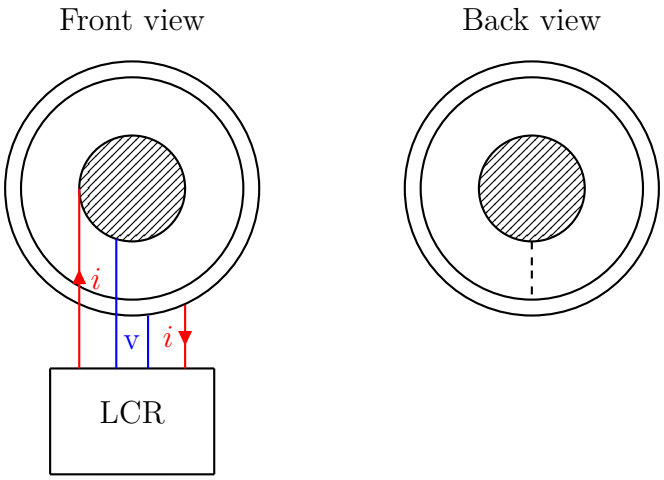

Figure 5.14: Connection of measuring the inductance by connectng conductor and shield.

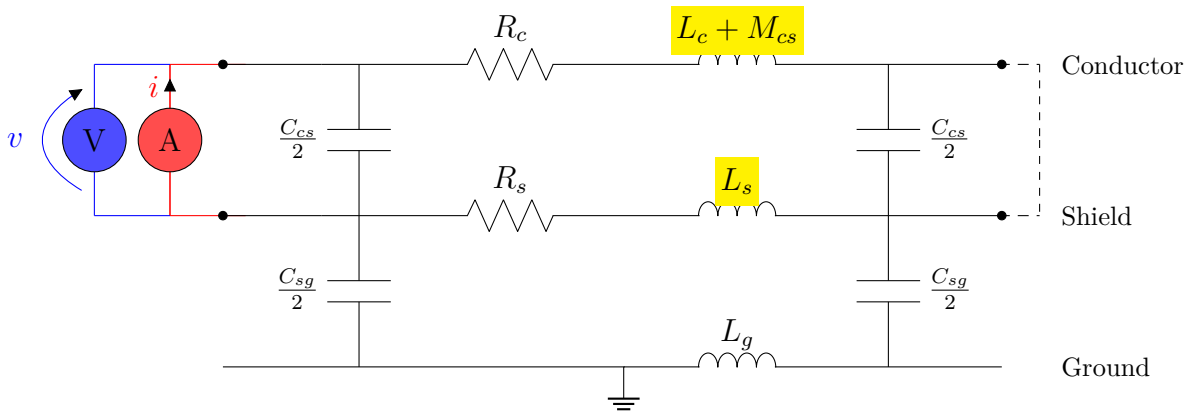

Figure 5.15: Measurement of total inductance in conductor and shield ($L_c + M_{cs} - L_s$) as equivalent pi-model.

To conclude which path the current will choose to flow back will depend on the measured impedance of each measurement. The smaller value of impedance will be the choosing path for the return current. This will be discussed more in Chapter 8.

5.4.2 Measurement of mutual inductance

The value of mutual inductance between the conductor and the shield (M_{cs}) can simply be computed from the differential between the measurements in Figure 5.7 and 5.9. It can be expressed as

$$(L_c + M_{cs}) - L_c = M_{cs} \tag{5.3}$$

in addition, the value of M_{cs} can also be obtained directly from using the LCR instrument without having the total inductance of the conductor ($L_c + M_{cs}$) available as in Figure 5.9, where current probes and voltage probes will be placed at both ends of the shield and conductor, respectively as shown in Figure 5.16. When the current flows through the shield it will create a magnetic field around it where the voltage in the conductor will be induced due to the change of magnetic flux. This will render the value of mutual inductance between the shield and the conductor (M_{sc}).

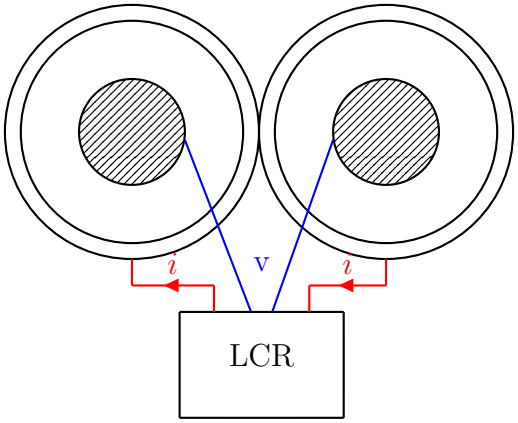

Figure 5.16: Connection of measuring the mutual inductance between conductor and shield.

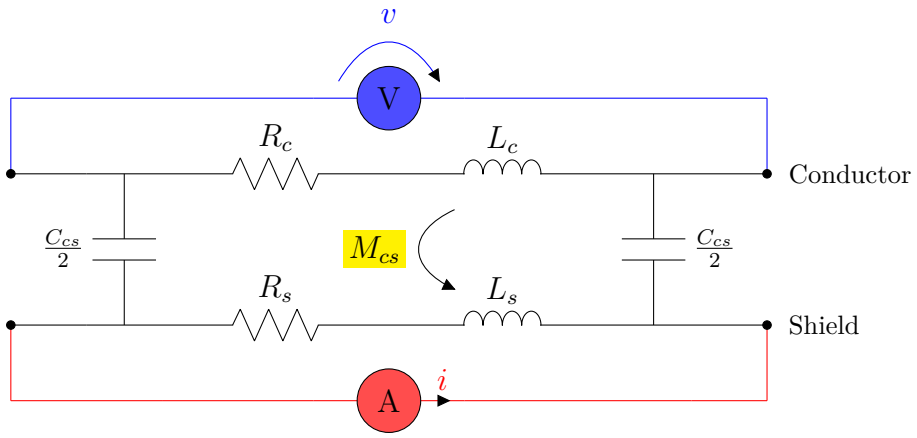

Figure 5.17: Measurement of mutual inductance between shield and conductor (M_{sc}) as equivalent pi-model.

It is also worth to mention that the mutual inductance between conductor and shield (M_{cs}) should give the same result as M_{sc},

$$M_{cs} = M_{sc} \tag{5.4}$$

By verifying this statement, the value can be obtained by using the same measurement method of M_{cs} but also vice versa which can be shown below

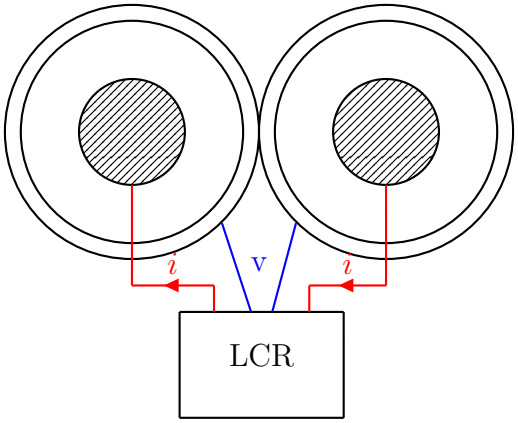

Figure 5.18: Connection of measuring the mutual inductance between conductor and shield.

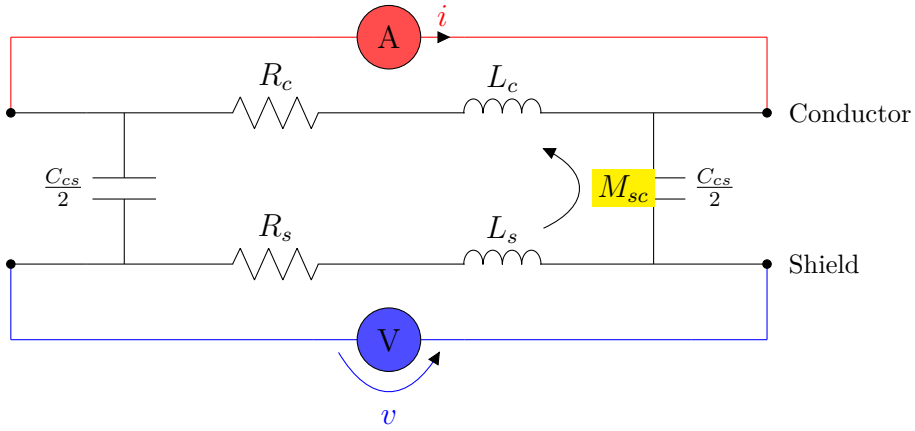

Figure 5.19: Measurement of mutual inductance between conductor and shield (M_{cs}) as equivalent pi-model.

When all the parameters of inductance are measured in a single coaxial cable, the mutual inductance between two coaxial cables placed parallel to each other will also need to be taken into consideration. The mutual inductance in this case will only be between both shields of the two cables which can be presented as in following figure.

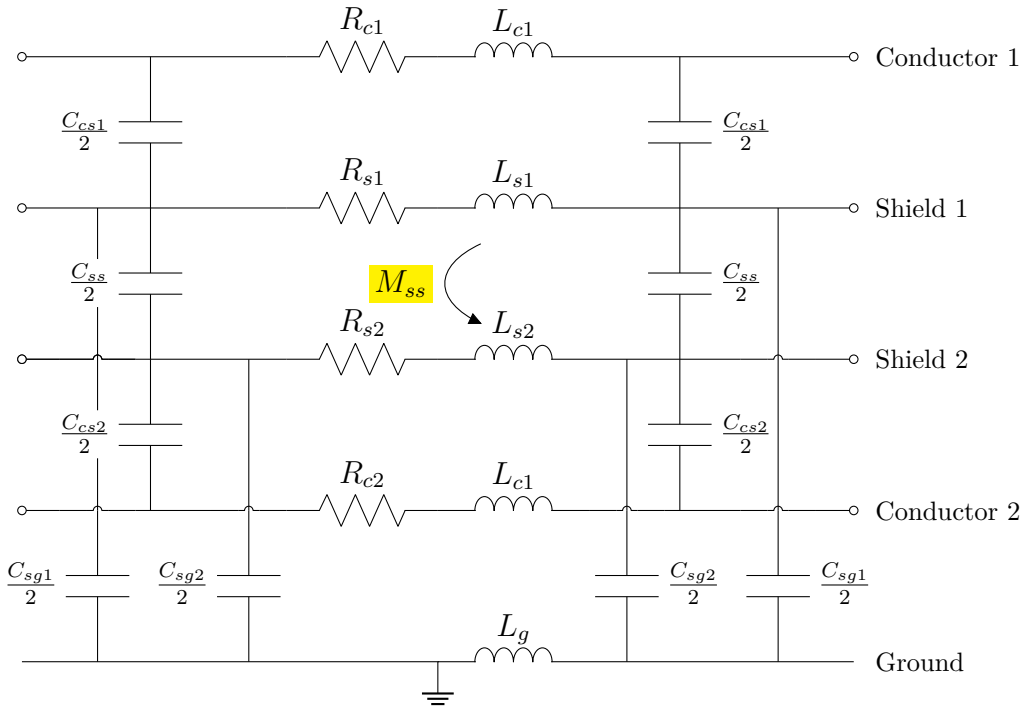

Figure 5.20: Mutual inductance between two shielded coaxial cable placed parallel with each other as equivalent pi-model.

The measurement procedure will remain the same as in the previous method that is used to measure only L_c. The reason is to obtain the change of inductance for different frequencies, the result will later be used to subtract with the self-inductance of the conductor. The difference between these two will then be equal to the mutual inductance between both shields (M_{ss}).

For the case set-up, there will be two test cables used where both are bent as a U-shape and placed close to each other which can be seen in Figure 5.26, this is due to the need of reaching the range of the test probes.

Figure 5.21: Two test cables beside each other.

For the open circuit case, assume that the inner test cable has shield 1 and outer one has conductor 2. The current probes and voltage probes will be placed at both ends of conductor 2 and shield 1 is open-circuited as illustrated below.´

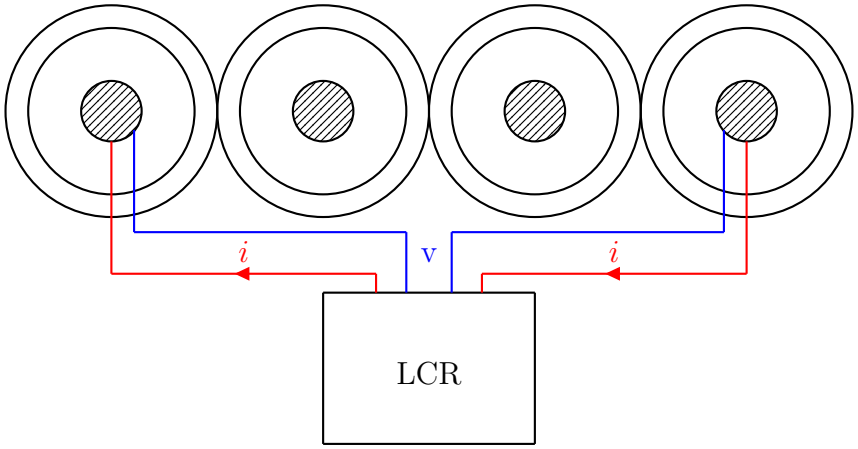

Figure 5.22: Connection of measuring the mutual inductance between shields.

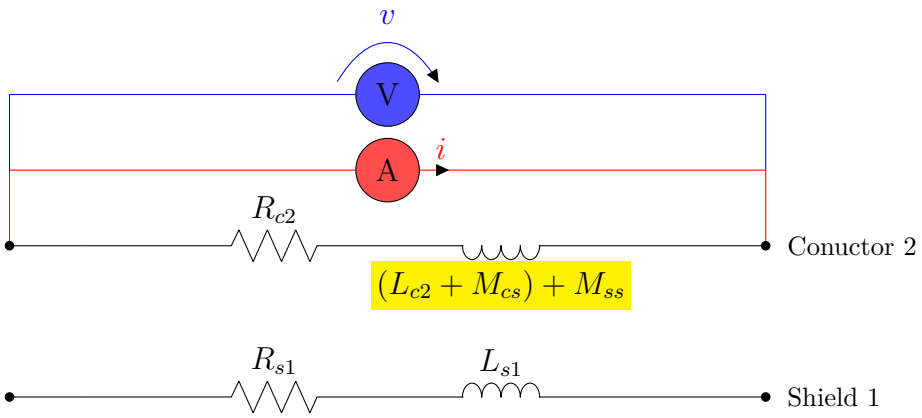

Figure 5.23: Measurement of mutual inductance between shields of two cables (M_{ss}) as equivalent pi-model.

By performing for the short circuit case, the current probes and voltage probes are placed at both ends of conductor 2 while shield 1 is short-circuited as shown below.

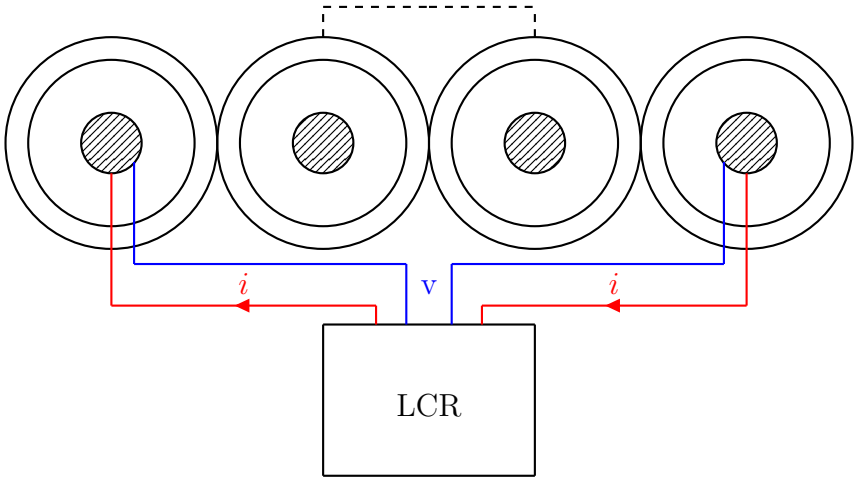

Figure 5.24: Connection of measuring the mutual inductance between shields.

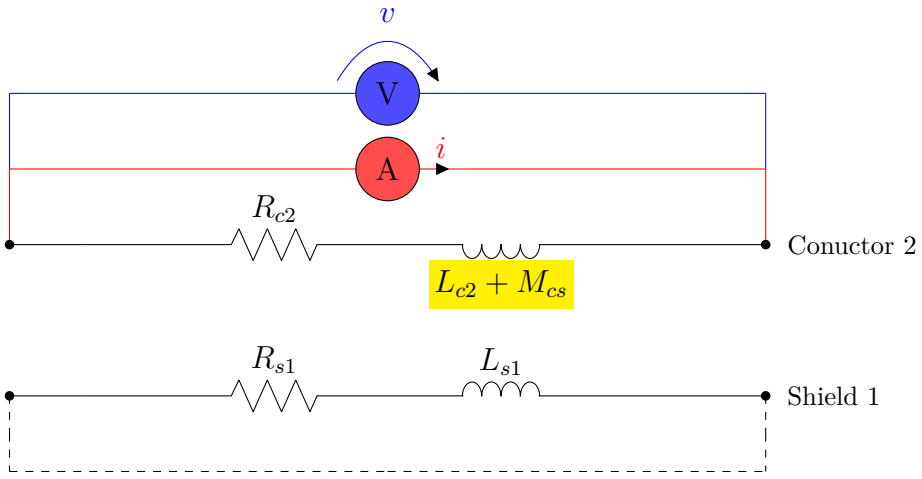

Figure 5.25: Measurement of mutual inductance between shields of two cables (M_{ss}) as equivalent pi-model.

The final expression of calculating the mutual inductance M_{ss} is by taking the result from open circuit case subtracts with the result from short circuit case which is equal to the following equation.

$$[(L_{c2} + M_{cs}) + M_{ss}] - [(L_{c2} + M_{cs})] = M_{ss} \tag{5.5}$$

5.4.3 Measurement of capacitance

To find the values of capacitance in a coaxial cable, a single test cable should be enough to use, since only one end of the cable will be required to perform the measurement.

Figure 5.26: A stretched out test cable.

Firstly, the capacitance between the conductor and the shield (C_{cs}) can be found by sending the current into the cable conductor and receiving it back from the shield. The voltage probes will then be placed between the conductor and shield to measure the potential between these two points. While the other end of the cable will be open-circuited. By obtaining C_{cs} as accurately as possible, the other capacitors in the cable can be short-circuited which is illustrated in Figure 5.27.

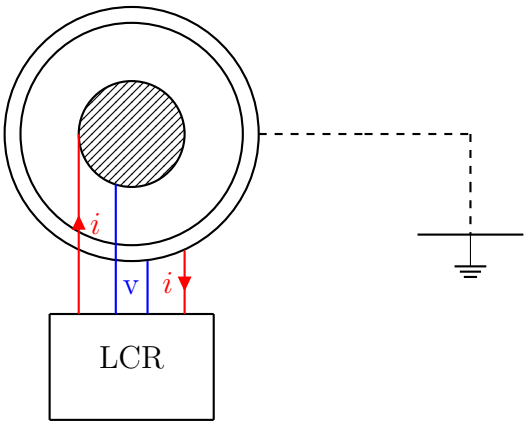

Figure 5.27: Connection of measuring the capacitance between conductor and shield.

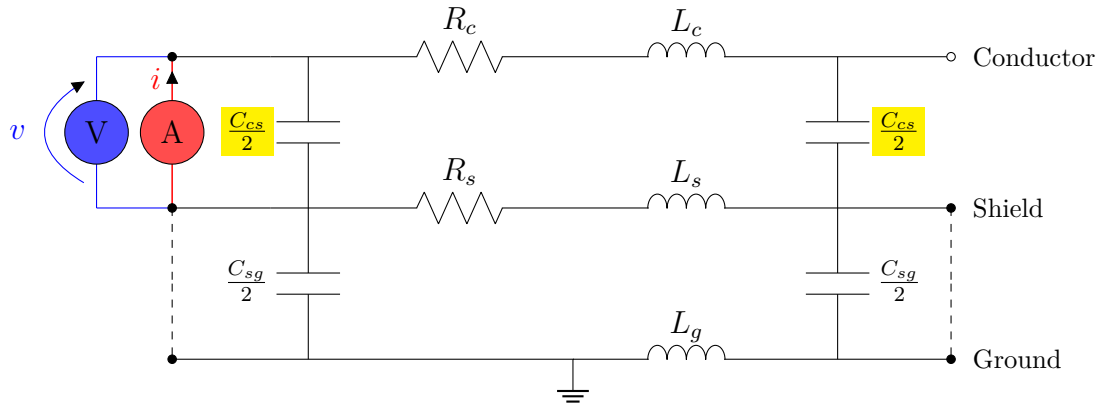

Figure 5.28: Measurement of capacitance between conductor and shield (C_{cs}) as equivalent pi-model.

Secondly, the capacitance between the shield and ground plane (C_{sg}) can be taken into consideration, through letting the current to be sent into the shield and return back from the ground plane. The voltage probes will be clamped between the shield and the ground plane to measure the potential between them. The other end of the cable will be open-circuited. To obtain C_{sg} as precise as possible C_{cs} (between conductor and shield) can be short-circuited so that they are not included in the measured result. The set-up can be shown in Figure 5.29.

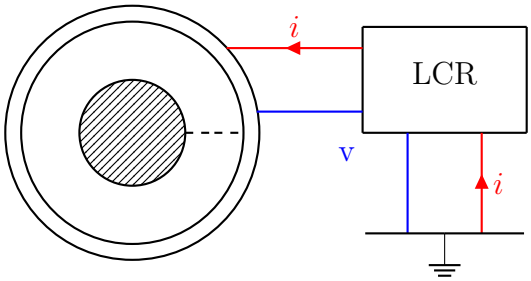

Figure 5.29: Connection of measuring the capacitance between shield and ground plane.

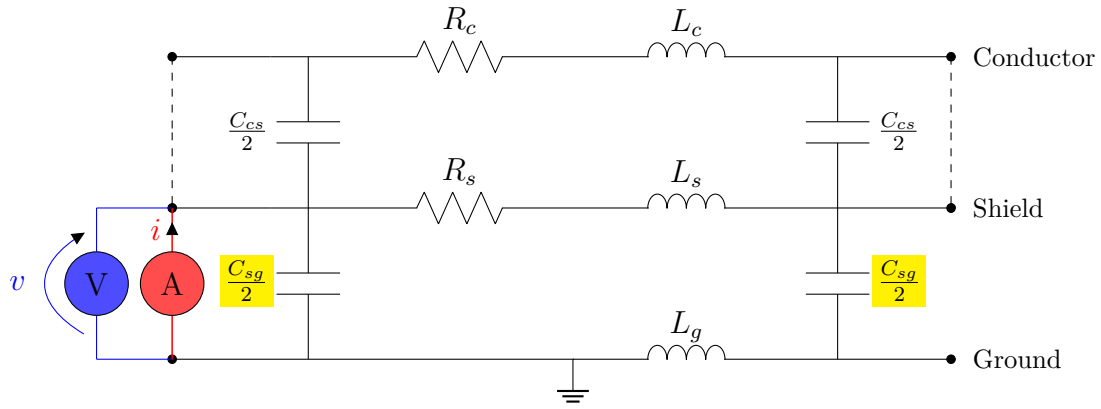

Figure 5.30: Measurement of capacitance between shield and ground (C_{sg}) as equivalent pi-model.

When all the values of capacitance in a single cable are obtained, the capacitance between two cables should also be obtained to be able to design a complete model of a shielded coaxial cable. This capacitance will be the one that is located between two shields (C_{ss}) which can be seen in Figure 5.31.

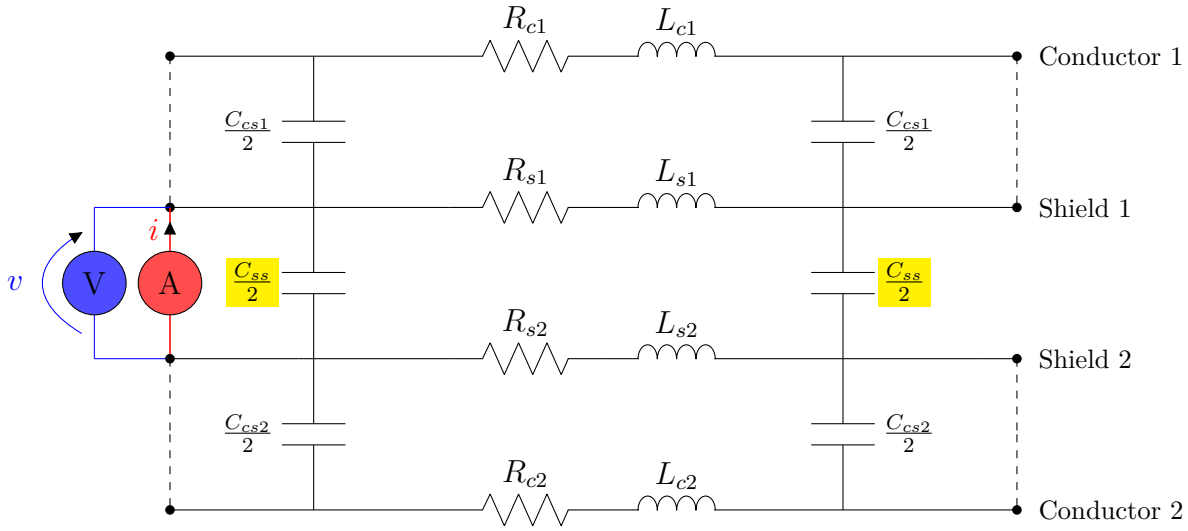

Figure 5.31: Measurement of capacitance between shield 1 and shield 2 (C_{ss}) as equvivalent pi-model.

To find C_{ss}, there will be two strected out test cables placed parallel with each other. Where both shields of the cables at one end are connected to the current and voltage probes while the other ends will be open-circuited as shown below.

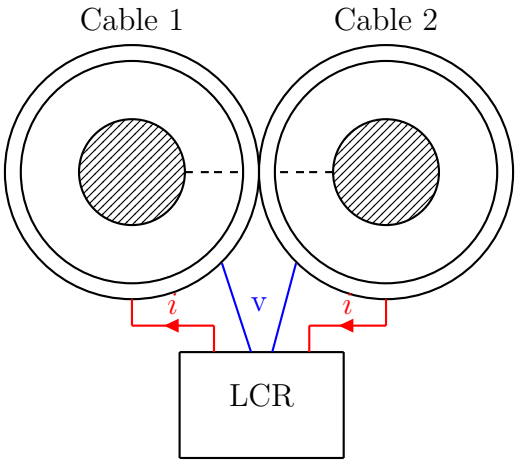

Figure 5.32: Connection of measuring the capacitance between two shielded coaxial cables.

5.5 Impedance measurement of twinaxial cable

This section will describe various measurement methods for obtaining the desired parameters in Figure 2.10. It is important to know that there are several parameters which are equal to each other, such as the self-inductance of both conductors ($L_{c1} = L_{c2}$), coupling capacitance ($C_{cs1} = C_{cs2}$) and mutual inductance ($M_{cs1} = M_{cs2}$) between both conductors and the shield. Since they give the same value, it is possible to just measure one parameter.

5.5.1 Measurement of inductance

Firstly, the self-inductance of the conductor (L_{c1} and L_{c2}) is measured differently from the coaxial cable case since in twin-axial cable there consists two conductors. The test cable that will be used for measuring L_c will be laid as a straight line which can be seen in Figure 5.33 because it is sufficient to measure one end of the cable.

Figure 5.33: Twin-axial cable laid straight.

The self-inductance can be obtained by connecting current probes at each conductor and measuring the voltage between both of them. At the other side of the cable, both conductors are short-circuited with each other to create a current path which can be illustrated in Figure 5.34. Since the current will flow back and forth at both conductors, therefore the total distance of current flow will be duplicate. This means that to obtain the value of inductance for one conductor, the measured result will be divided by two.

$$L_x = L_{c1} + L_{c2} = 2L_{c1} \tag{5.6}$$

where L_x is the measured inductance and L_{c1} and L_{c2} is basically equal to each other since both are from the conductors that have the same dimensions and length. Hence, the self-inductance for one conductor (L_c) is

$$L_c = \frac{L_x}{2} = \frac{2L_{c1}}{2} = L_{c1} \tag{5.7}$$

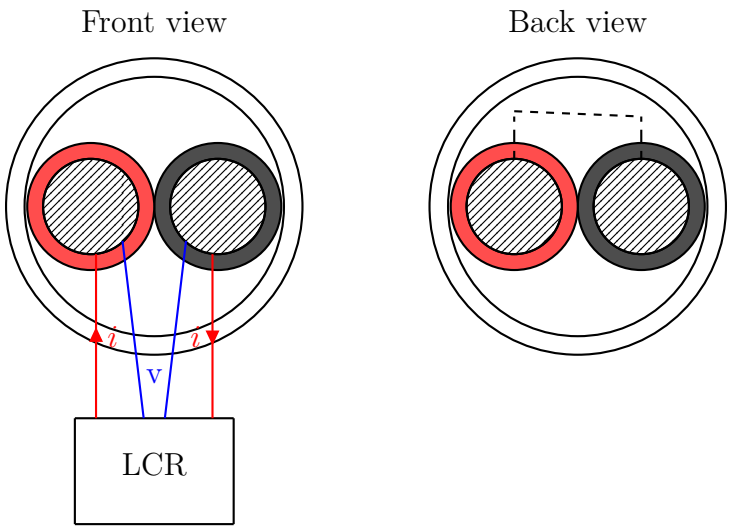

Figure 5.34: Connection of measuring L_{c1} in shielded twin-axial cable.

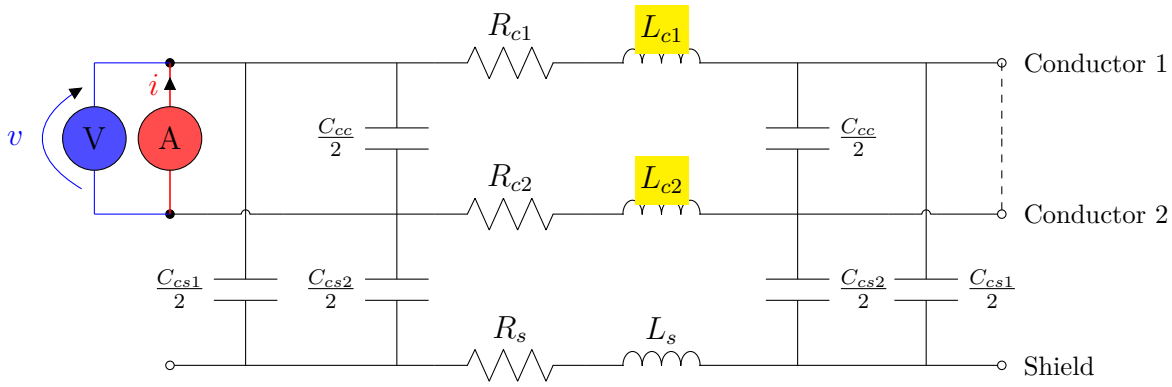

Figure 5.35: Measurement of self-inductance in conductor 1 (L_{c1}) of a shielded twin-axial cable as equivalent pi-model.

The test cable that will be used for measuring the rest of inductance in model will be bent as a U-shape which can be seen in Figure 5.36, with the same reason as for the coaxial cable case. The self-inductance of shield can be simply measured by performing LCR measurement at the shield which can be shown in Figure 5.37.

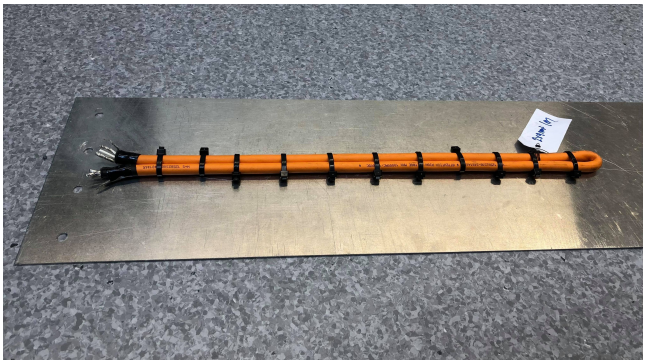

Figure 5.36: Twin-axial cable bend as U-shape.

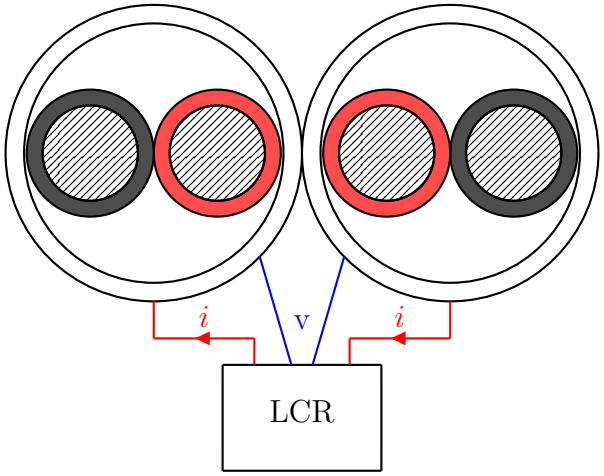

Figure 5.37: Connection of measuring L_s in shielded twin-axial cable.

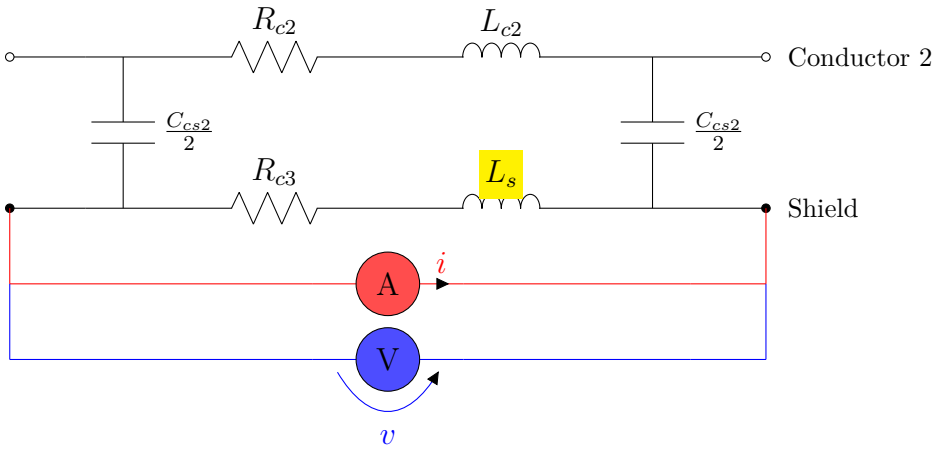

Figure 5.38: Measurement of self-inductance in shield (L_s) of a shielded twin-axial cable as equivalent pi-model.

The mutual inductance between both conductors (M_{cc}) can be measured by connecting current probes and voltage probes at each conductor separately, see Figure 5.39. By placing the current and voltage probes, respectively, at either conductor is inconsequential because both conductors have completely the same dimensions so even if they are connected vice versa the result will still be the same.

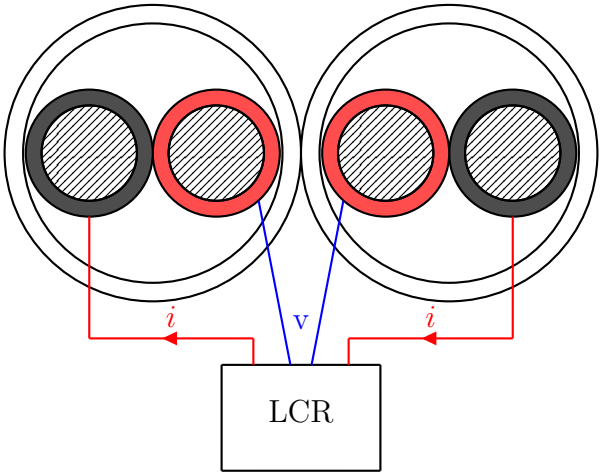

Figure 5.39: Connection of measuring M_{cc} in shielded twin-axial cable.

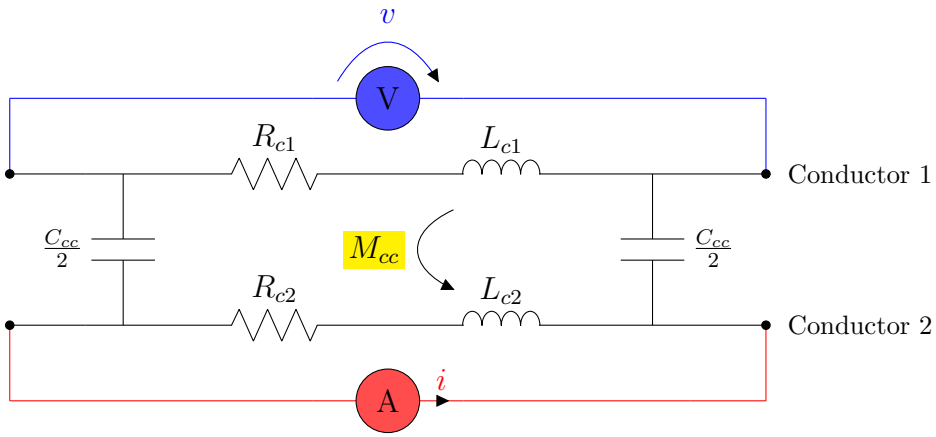

Figure 5.40: Measurement of mutual inductance between conductor 1 and conductor 2 (M_{cc}) of a shielded twin-axial cable as equivalent pi-model.

The mutual inductance between each conductor and shield (M_{cs1} and M_{cs2}) can be measured with the same principle as M_{cc}, where both the current probe and the voltage probe will be placed at conductor 2 (black) and the shield, respectively as in Figure 5.41. Note that the mutual inductance between conductor 1 and shield (M_{cs1}) will be equal to M_{cs2}.

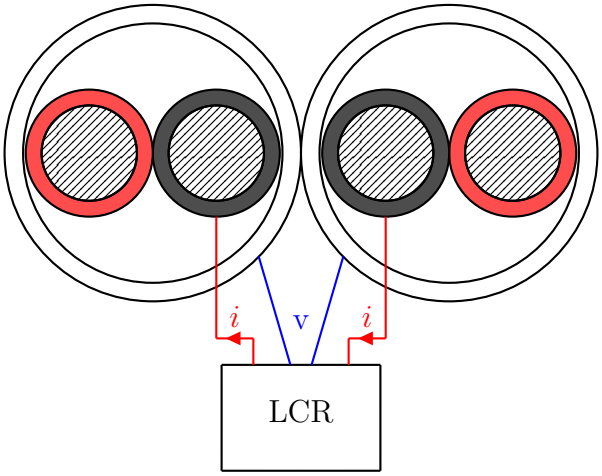

Figure 5.41: Connection of measuring M_{cs2} in shielded twin-axial cable.

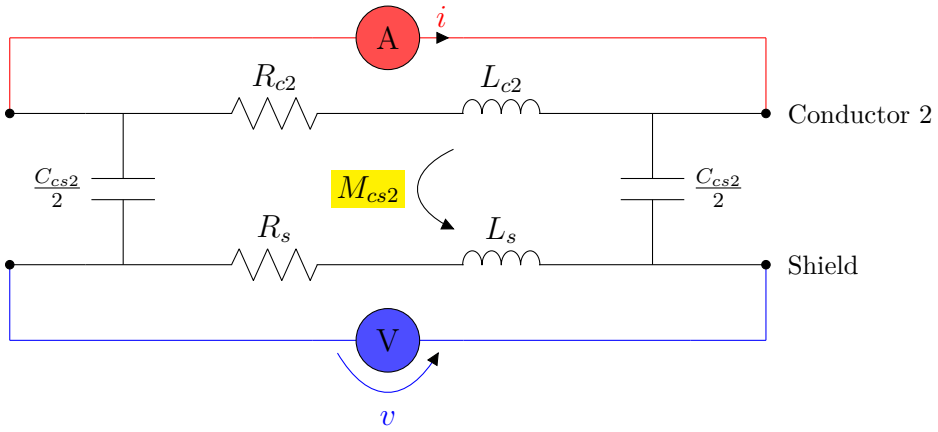

Figure 5.42: Measurement of mutual inductance between conductor 2 and shield (M_{cs2}) of a shielded twin-axial cable as equivalent pi-model.

5.5.2 Measurement of capacitance

In order to obtain the capacitance couplings in a shielded twin-axial cable is more complex compared to the shielded coaxial cable. The measurement methods of performing the LCR measurement for the twin-axial cable will thereby differ from the coaxial cases unlike for the inductance measurements where they have similarities, where the test cable will instead be outstretched as a straight line similar to the capacitance measurement of a coaxial cable. According to the pi-model in Figure 2.10, there will be three different capacitance couplings that will be taken into consideration.

Firstly, the capacitance between the two conductors (C_{cc}). The value of C_{cc} cannot be obtained individually because there will always be parasitic capacitive couplings at different locations of the cable included in the measurement. By preventing the parasitic capacitance as much as possible, the setup can be seen as in Figure 5.43.

Where the current and voltage probes are placed at each conductor respectively, and one of the conductors is short-circuited. Which conductor is short-circuited is insignificant since both conductors have the same dimension regardless. Assume that conductor 2 (black) is short-circuited in this case.

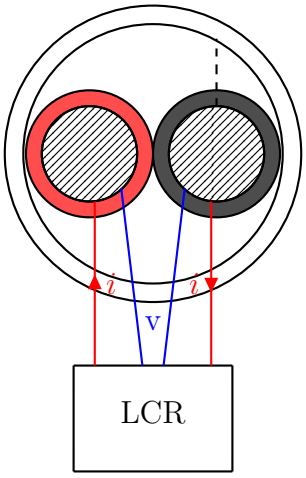

Figure 5.43: Connection of measuring C_{cc} between both conductors of shielded twin-axial cable.

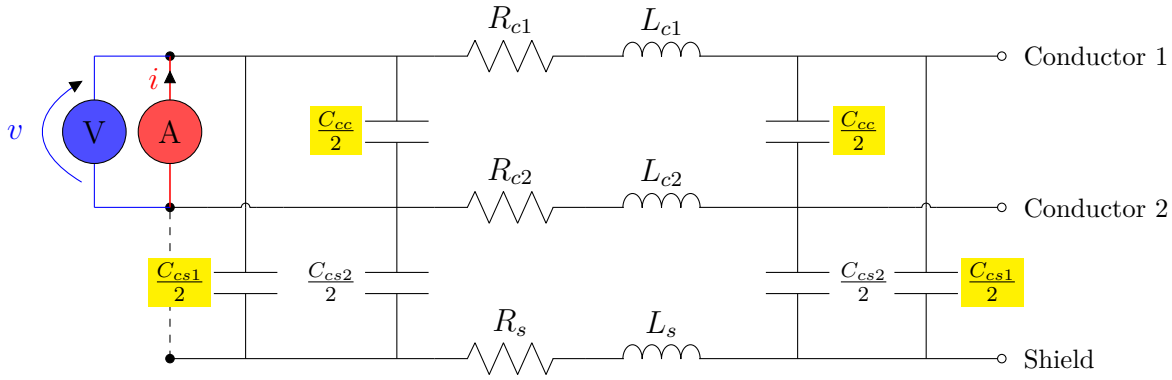

Figure 5.44: Measurement of C_{cc}+C_{cs1} of a shielded twin-axial cable as equivalent pi-model.

In Figure 5.44, it can be clearly seen that the measured capacitance for this case setup results in C_{cc}+C_{cs1}. To calculate C_{cc}, the value of C_{cs1} needs to be known, where C_{cs1} is the capacitance coupling between conductor 1 (red) and the shield. To obtain C_{cs1}, the measurement setup can be seen in Figure 5.43, where the current and voltage probes are clamped between conductor 1 (red) and the shield while both conductors are short-circuited to each other in order to not include the parasitic capacitance C_{cc}.

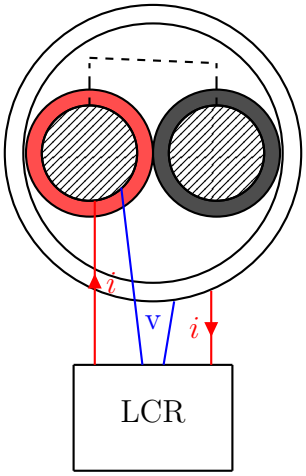

Figure 5.45: Connection of measuring C_{cs} between conductor and shield of shielded twin-axial cable.

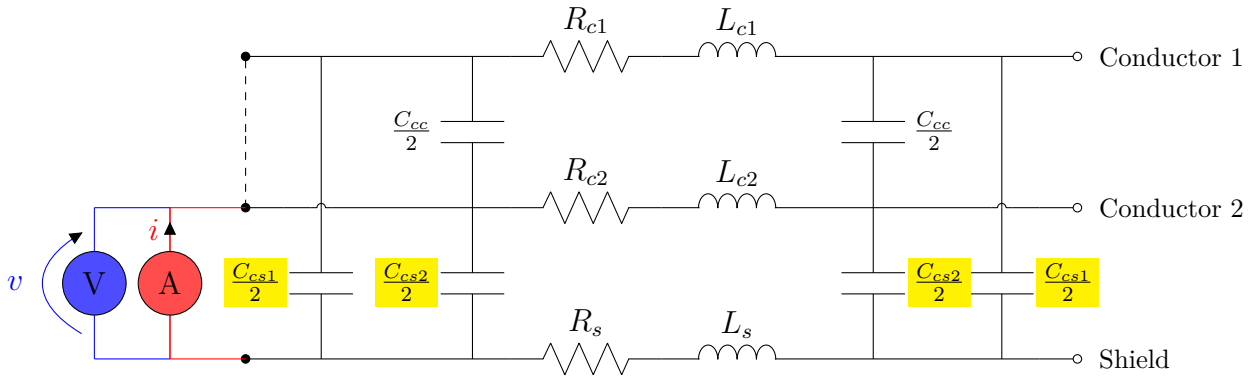

Figure 5.46: Measurement of C_{cs1}+C_{cs2} of a shielded twin-axial cable as equivalent pi-model.

According to the pi-model in Figure 5.46 the measured capacitance is equal to the sum of C_{cs1}+C_{cs2} where it was mentioned above that C_{cs1}=C_{cs2}. Hence, the measured capacitance is consequently equal to

$$C_{cs1} + C_{cs2} = C_{cs1} + C_{cs1} = 2C_{cs1} \tag{5.8}$$

since C_{cs1} is now known, which can be used to calculate C_{cc}. The expression for computing C_{cc} can be written as

$$C_x = C_{cc} + C_{cs1} \tag{5.9}$$

where C_x is the measured capacitance which is obtained from Figure 5.43.

$$C_{cc} = C_x - C_{cs1} \tag{5.10}$$

Lastly, the parameter that will be measured is the capacitive coupling between the shield and ground C_{sg}. The measurement can be conducted by connecting the current and voltage probes between shield and ground plane. However, if the conductors are open circuited the parasitic capacitance couplings such as C_{cc}, C_{cs1} and C_{cs2} can be included in the measured result which is undesired. In order to prevent all these parasitic capacitances, short circuit the connections is the solution. Where both conductors are short-circuit to each other and also each conductor is short-circuit to the shield. The measurement setup can be seen in Figure 5.47.

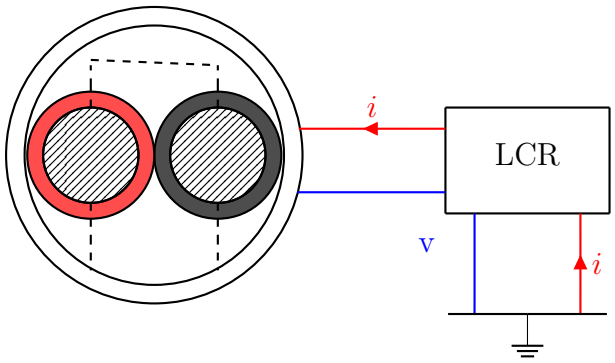

Figure 5.47: Connection of measuring C_{cs} between conductor and shield of shielded twin-axial cable.

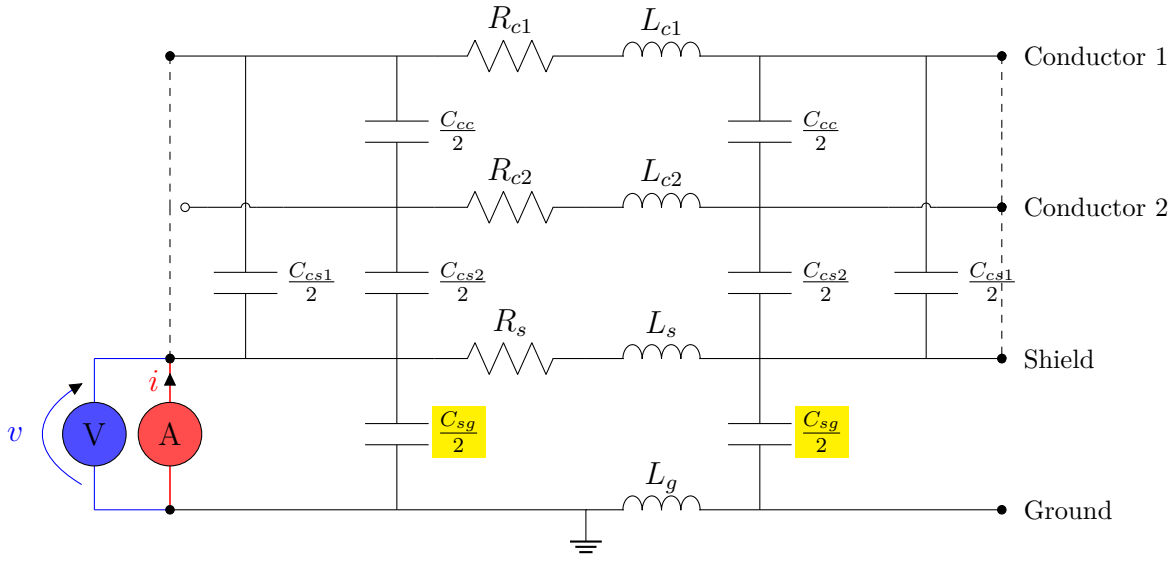

Figure 5.48: Measurement of C_{sg} of a shielded twin-axial cable as equivalent pi-model.

6
Analysis of results

6.1 Measured parameters for one coaxial cable

6.1.1 Inductance $L_c + M_{cs}$

By applying current through the conductor, and measuring the voltage drop in the frequency domain one can obtain the result as in Figure 6.1. The measurement starts at 300Hz, because the Pearson probe is inaccurate below this frequency. That is why the resistive part of the conductor is not shown, but only the inductive part. Figure 6.1 shows the amplitude plots, the phase plots are omitted for simplicity. As expected, the impedance varies with different cable lengths as can be seen in Figure 6.1. In order to obtain the inductance, a value is chosen in the linear region. The black, blue and green graphs are for 1m, 5m and 10m cables respectively.

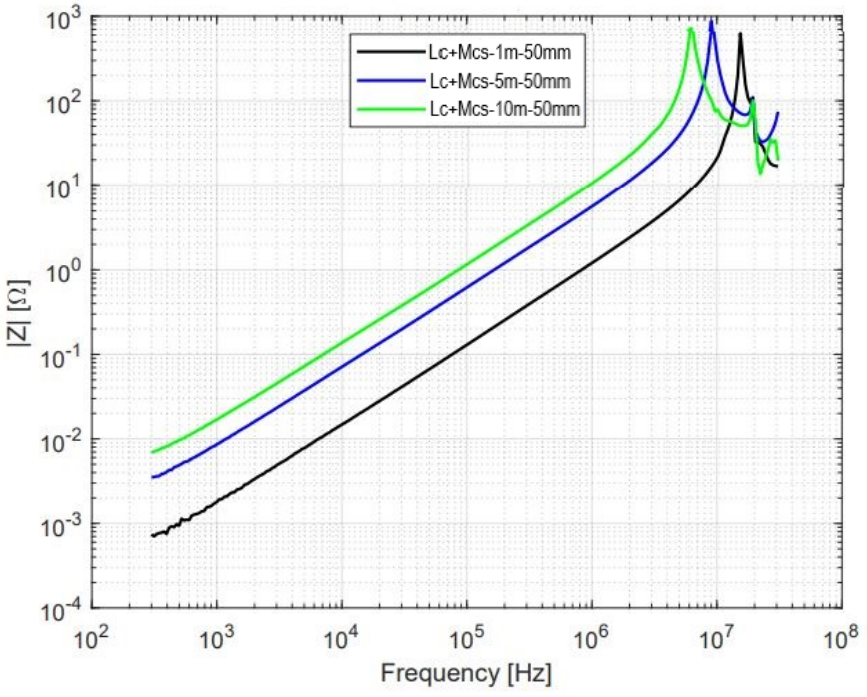

Figure 6.1: Measurement of $L_c + M_{cs}$ of 1m, 5m and 10m for $50mm^2$ cable

The inductance can be found for each cable length in Table 6.1. As can be seen, the inductance is quite scalable, even though it is not 100%.

Table 6.1: Inductance calculated at $f = 97130$ Hz

Length [m]	Inductance [μH]	Ratio compared to 1m
1	0.21	1.00
5	0.99	4.71
10	1.85	8.81

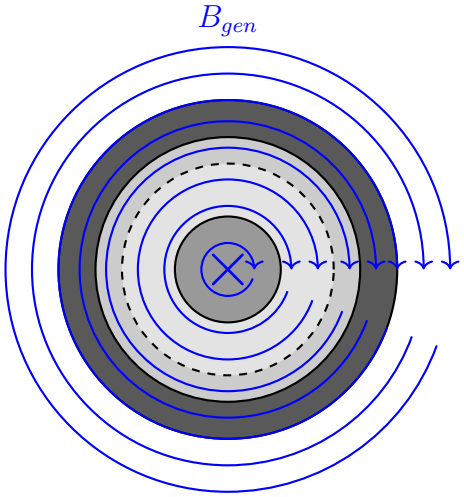

Figure 6.2: Measurement of $L_c + M_{cs}$

Another way of interpreting the results is that Figure 6.1 shows the inductance that is due to the whole magnetic field generated in Figure 6.2. In other words, there is nothing limiting the field lines created by a current in the conductor, as the shield is an open circuit.

As a clarification for Figure 6.1, Figure 6.3 is illustrating each important region when measuring inductive impedance. As can be seen there is a resistive part in very low frequencies, and a growing inductive part for higher frequencies and finally a resonance region. The phase plot can also be shown in the same figure. Worth to notice is that the phase angle is approximately at 90° most of the linear region, however it is changing due to the skin effect.

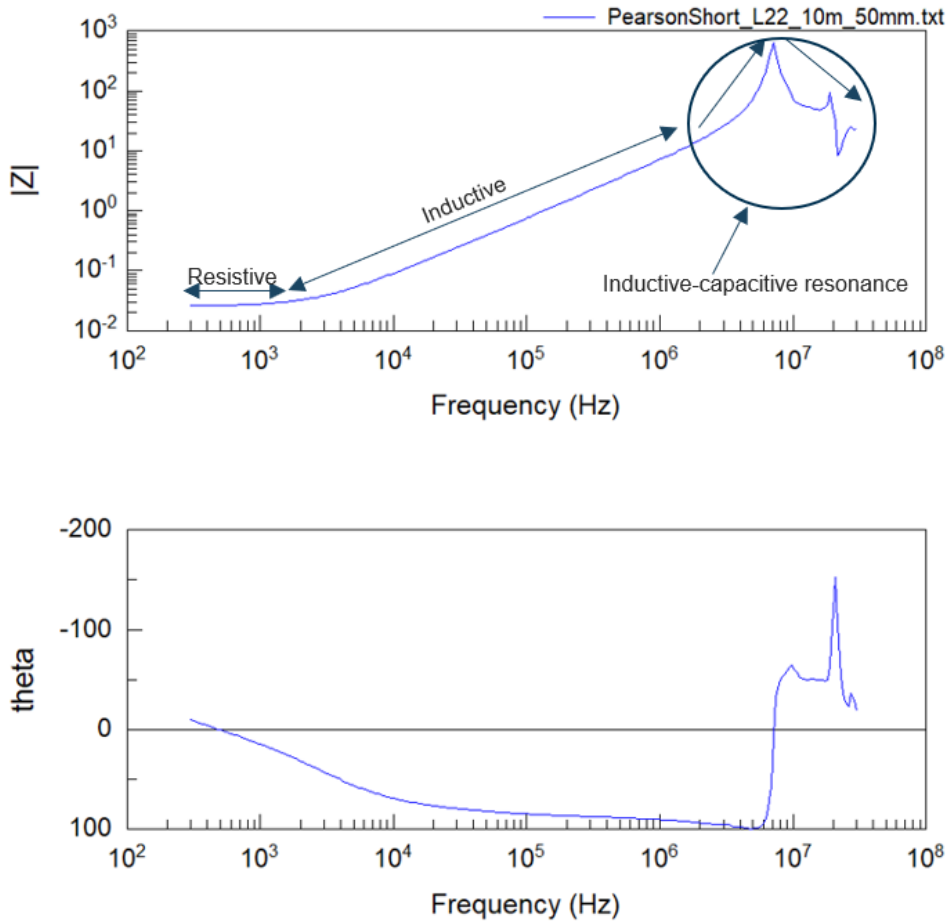

Figure 6.3: Illustration of important R-L-C regions of inductive impedance measurement

6.1.2 Inductance L_s

Doing the same procedure but for the shield, similar results can be obtained in Figure 6.4. However, now a part of the resistive behaviour can be seen which is due to the lower inductance in the shield as well as a higher resistance.

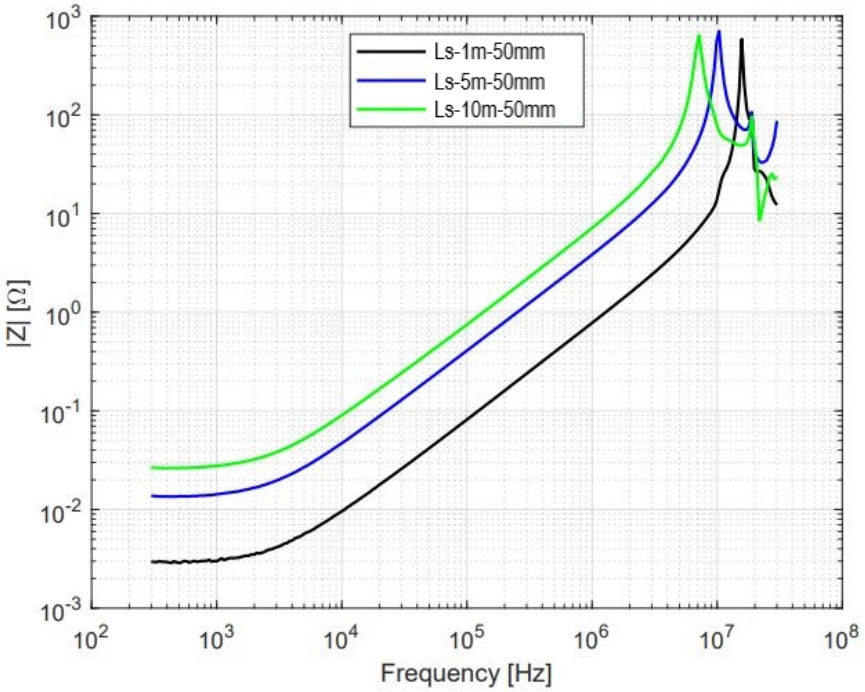

Figure 6.4: Measurement of L_s of 1m, 5m and 10m for $50mm^2$ cable

What can be noticed is that the resonance point also moves to the left as the cable length increases, as the total inductance as well as capacitance increases which is as expected.

Table 6.2: Inductance calculated at $f = 97130$ Hz

Length [m]	Inductance [μH]	Ratio compared to 1m
1	0.13	1.00
5	0.65	5.00
10	1.20	9.23

6.1.3 Inductance M_{cs}

By applying the current to the shield, and measuring the voltage induced in the conductor the plots in Figure 6.5 will be obtained. Worth to mention that here, purely inductive behaviour is seen (apart from the resonance point) which is as expected because the induced voltage will be due to the magnetic field that is varying. And thus the resistive effects will not be shown as in the previous case.

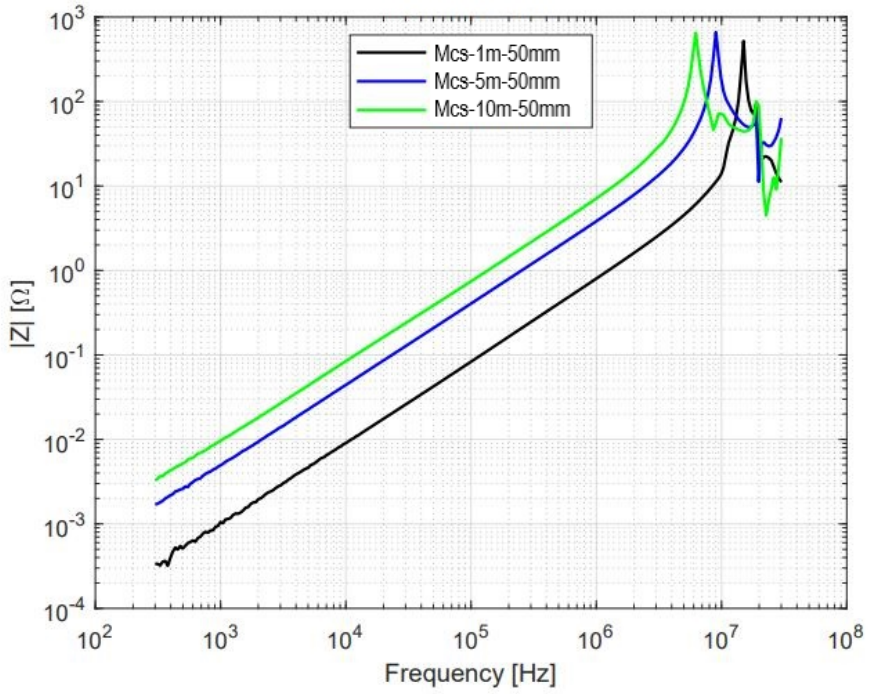

Figure 6.5: Measurement of M_{cs} of 1m, 5m and 10m for $50mm^2$ cable

Table 6.3: Inductance calculated at $f = 97130$ Hz

Length [m]	Inductance [μH]	Ratio compared to 1m
1	0.13	1.00
5	0.65	5.00
10	1.18	9.07

6.1.4 Inductance M_{sc}

By doing the opposite, applying current in the conductor and measuring voltage over the shield, M_{sc} can be obtained, and the result is presented in Figure 6.6.

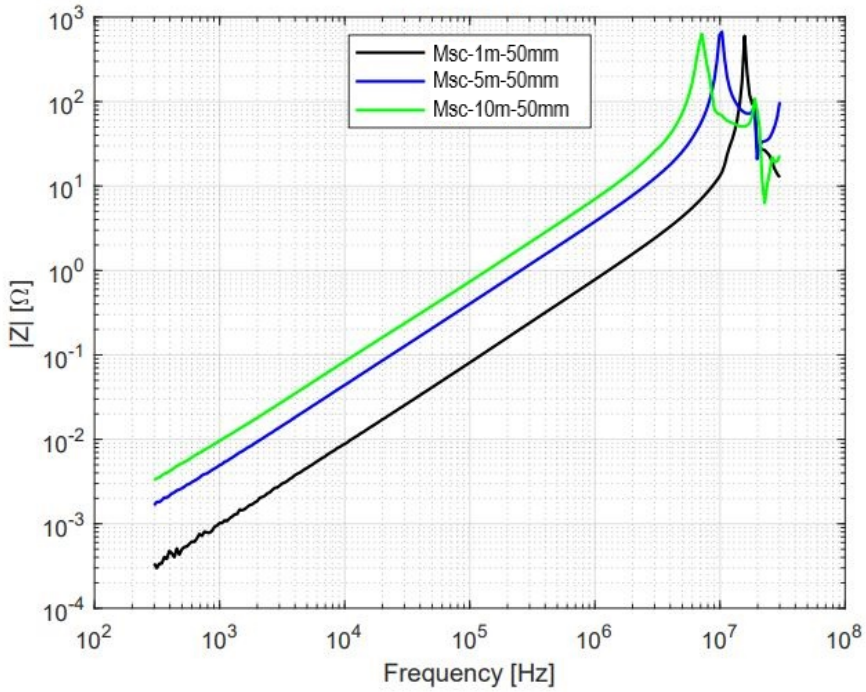

Figure 6.6: Measurement of M_{sc} of 1m, 5m and 10m for $50mm^2$ cable

Table 6.4: Inductance calculated at $f = 97130$ Hz

Length [m]	Inductance [μH]	Ratio compared to 1m
1	0.13	1.00
5	0.64	4.92
10	1.20	9.23

Comparison between L_s, M_{cs} and M_{sc}

As can be seen in Table 6.2, 6.3 and 6.6 the results are very close to each other. It is as expected, M_{cs} is equal, or at least very close to M_{sc}. That is because of the field that is generated is the same in both cases. However, the fact that the shield inductance is the same as the mutual inductance of the shield is something more surprising. The self-inductance of the shield depends on the same magnetic flux as the common flux between conductor and shield(M_{sc} and M_{cs}) that is the reason why the inductance is the same. By recalling from Figure 4.6 in the COMSOL modelling, it was known that the self inductance of the conductor would be dependent on the magnetic flux between conductor and shield. However the flux that is beyond the shield would logically be called the mutual inductance. That is because it is the

same field the shield would experience when applied a current on it (a magnetic flux from the shield to the outside), hence calling it the mutual inductance. One other way of reasoning through this is that because the shield is enclosing the conductor, all the flux lines from the shield will be common to the conductor and hence the observed flux from the conductor itself is equal to the shield inductance. Because what the conductor sees when a current is applied to the shield, is the same field the shield would see [23].

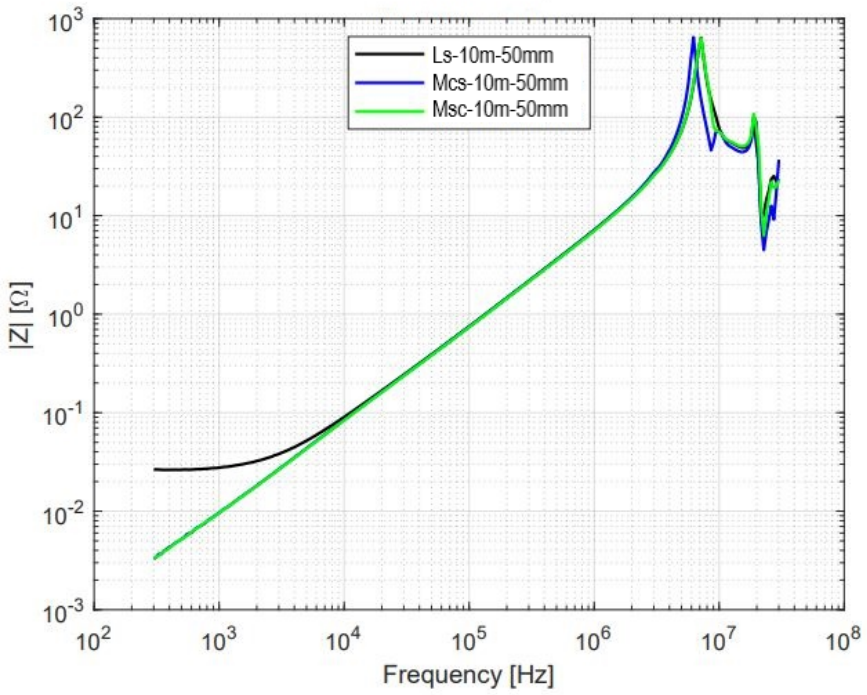

Figure 6.7: Comparison of L_s, M_{cs} and M_{sc} (10m for $50mm^2$ cable)

It is clearly shown that even for higher frequencies than 100kHz, the behaviour is the same for the three parameters L_{22}, M_{12} and M_{21}, as shown in Figure 6.7.

Measurement of $L_c + M_{cs}$ and when the shield is short circuited

Figure 6.8 shows two scenarios. One being a simple measurement of $L_c + M_{cs}$, and the second the same measurement just that the shield is short circuited. For very low frequencies the slope is the same as for both graphs, indicating $L_c + M_{cs}$. For frequencies approximately higher than 1 kHz the blue graph starts to deviate from the black graph. Because the shield is short circuited the inductance will now be lower. When the shield is short circuited, it means that now there is a possibility for a current to flow in the shield. The current will flow because of the induced voltage driving the current through the shield. However, the direction of magnetic flux from the shield is not the same as the magnetic flux created by the conductor when a current is applied to it. Which means that some of the magnetic flux will cancel

each other out, because of the opposite directions. Which is basically why there is less inductance in the blue graph, because of the field cancellation. The parts of the field that cancels each other out must be the parts that both of the conductor and shield is sharing, in other words the mutual inductance. It is the mutual field that cancels out each other. This is a very important relation, because now one can say that the difference in inductance between the black and blue graphs should be the mutual inductance, in other words the "missing part" or the reduction, since the reduction in inductance is due to the induced field in the shield when it is short circuited. To summarize, one can say there is two ways of calculating the mutual inductance. One way is the way of feeding current in one conductor and measuring the voltage in the other conductor but also the way described above when shorting the shield and measuring $L_c + M_{cs}$.

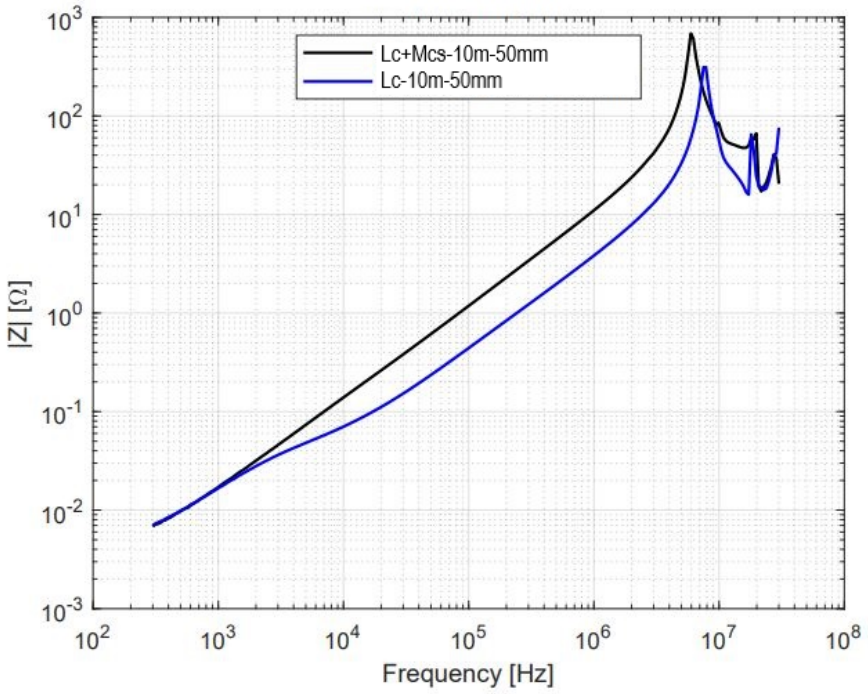

Figure 6.8: Measurement of $L_c + M_{cs}$ and when the shield is short circuited (10m $50mm^2$ cable) using Pearson

As a comparison, Figure 6.9 shows the same measurement as in Figure 6.8 but with a possibility of displaying the behaviour at even lower frequencies, because of using the four-wire kelvin method.

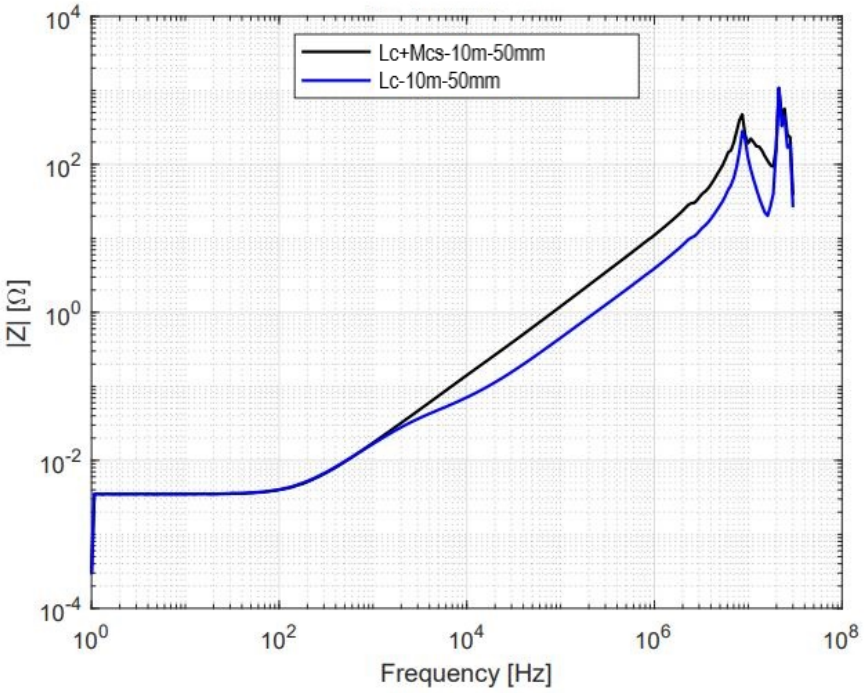

Figure 6.9: Measurement of $L_c + M_{cs}$ and when the shield is short circuited (10m $50mm^2$ cable) using Four-wire kelvin

However what is left as inductance in the blue graph in Figure 6.8, has to be the self-inductance of the conductor, as described in section 3.2.1. That is because now, when the shield is short circuited it allows for a return current to pass through the shield equal in magnitude to the sending current. Which then in turns cancels out the mutual field between the conductor and shield so that what is left is the magnetic flux inside conductor and the flux between conductor and shield. So, to properly obtain the self inductance of the conductor (L_c) the shield needs to be short circuited otherwise the flux lines will expand outside and what is measured is simply $L_c + M_{cs}$, where M is mutual inductance between conductor and shield. It is also recommended to short the shield, because if the sending current that is flowing in the conductor returns through the shield in opposite direction then any field outside the screen will be zero which in turns mean less interference with other objects.

Another way of interpreting this can be done by using Figure 6.10 as well as Figure 6.11. Firstly a current is applied to the conductor and the shield is short circuited in Figure 6.10, which will allow for a current to flow. A voltage is induced in the shield because of the varying magnetic flux from the conductor, which then drives a current through the shield. The current is opposite in direction to the current in the conductor. As the induced current flows through the shield, it will produce its own magnetic field, called B_{ind} marked in red. The field will oppose the generated field, B_{gen}, and will cancel out parts of the generated field.

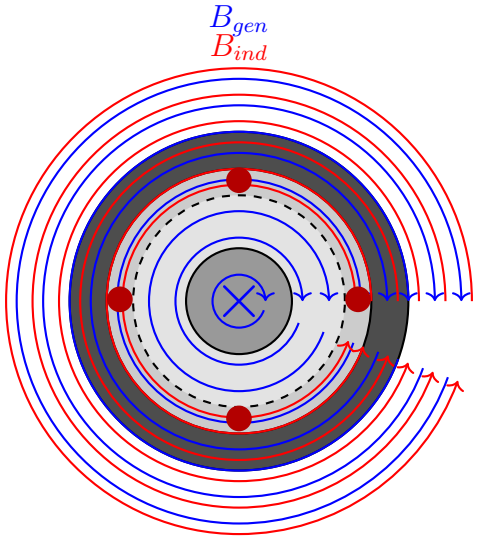

Figure 6.10: Magnetic fields created by conductor and induced in opposite direction by the shield when short circuited

It is parts of the mutual field that will cancel, any other field will remain the same. In other words its safe to say that the mutual inductance is what will cancel out each other out. What is left is the inductance due to the magnetic field inside the conductor and between the conductor and the shield. This is the inductance that is called the self-inductance of the conductor shown in Figure 6.11.

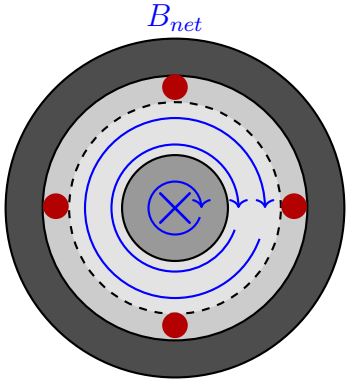

Figure 6.11: Net magnetic flux

Measured example from a truck

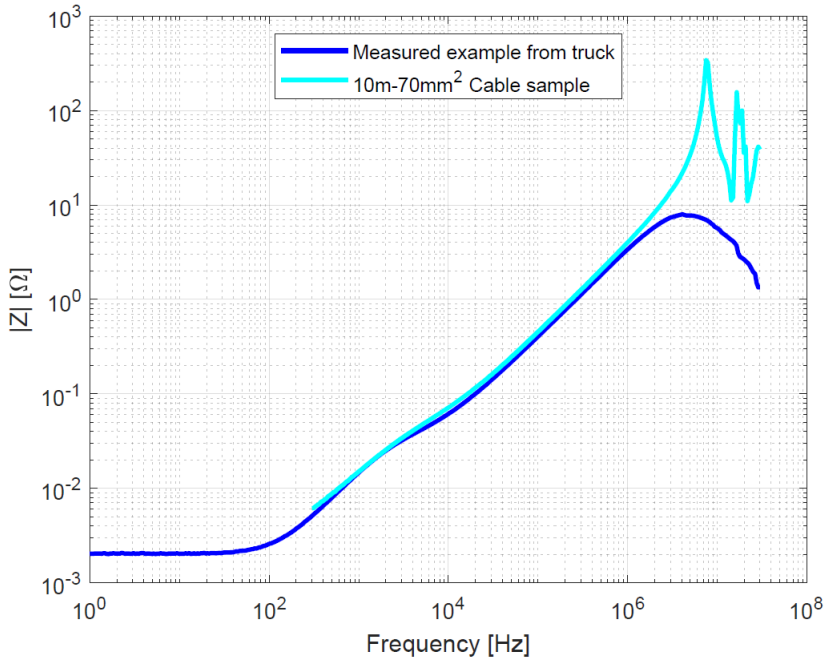

Figure 6.12: Measurement of L_c when the shield is short circuited (8m 70mm^2 cable) - from a truck, in f $\approx$ 100 kHz

In Figure 6.12 an equivalent example of short circuiting the shield and measuring the conductor impedance is shown. What can be noticed, is that even for this measurement same behaviour can be seen. The plateau can also be found in the figure for both measurements. However worth to mention is that the truck measurement is done with 4WK as can be seen, due to the low frequency region being included also. But the cable sample measurement was done with Pearson method. When it comes to value comparison, the truck measured example rendered in $L_c = 0.0794\ \frac{\mu H}{m}$. To compare with the single cable being measured, a 10m 70 mm^2 cable sample is chosen as seen in the figure. The measured value is equal to $L_c = 0.0715\ \frac{\mu H}{m}$. There is difference in the values even though the same cables are used. The reason behind this could possibly be because of the different techniques when short circuiting the shield. In the truck the shield is short circuited with the connectors, but for the single cable test the shield is shorted together forming a closed loop. The difference in inductance could maybe depend on the connectors, and its inductive path when shorting the shield to this connection. However this has not been confirmed yet, but could be a valid discussion for further testing. However, the values are still quite close to each other which shows that the cable testing is still valid.

6.1.5 Capacitance C_{cs}

The capacitive impedance between conductor and shield is obtained and found in Figure 6.13.

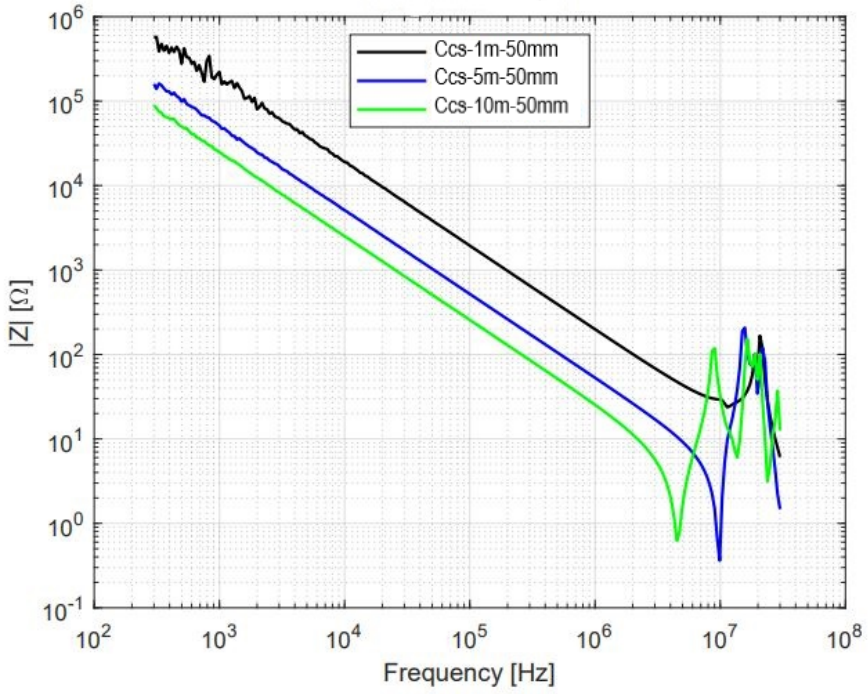

Figure 6.13: Measurement of C_{cs} of 1m, 5m and 10m $50mm^2$ cable

The graphs are decaying at increasing frequency, that is because of the capacitive behaviour, the phase is $-90°$ compared to $+90°$ for the inductive behaviour. More capacitance is found for longer cables, which can be seen in the blue and green lines.

6.1.6 Impedance in shield compared to ground

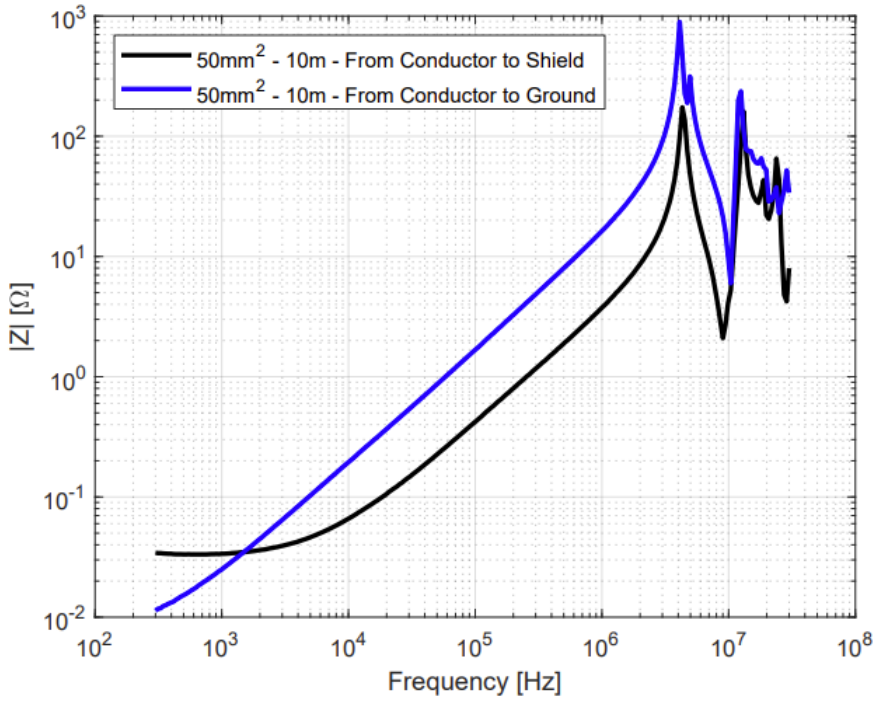

Figure 6.14: Measurement of impedance if the return current flows through the shield or the ground plane

In Figure 6.14 two scenarios are shown. The current is let to flow from the conductor and return back from the shield (black graph). The other scenario is when the current is fed to the conductor and is returning from the ground plane. The purpose of this measurement is to show the difference in impedance if the current is fed back through the ground plane or the shield. And as can be seen the impedance is way higher for the ground case, compared to the shield case. Which means that the current would rather go through the shield than through the ground plane. The ratio between the impedance of the current through ground plane or the shield is approximately equal to 4 times. Which means that at a frequency at about 100kHz the impedance path from conductor through the ground plane is four times higher than when the same current flows back through the shield instead.

The value of inductance in the ground plane for 10m length is calculated to 0.82 μH, and is then equal to 0.082 $\frac{\mu H}{m}$. The way of calculating the ground impedance is done when comparing the impedance when the current only flows in the conductor and when it flows in the ground plane. The difference in impedance between these two measurements is the ground impedance.

6.2 Twin-axial cable measurement results

6.2.1 Measurement of L_c

The measurement of self inductance in the conductor can be done by applying current in both conductors but in opposite direction. As can be seen in Figure 6.15 and 6.16 the current is applied, in opposite directions but separately. Worth to notice is the direction of magnetic field that changes depending on the current direction.

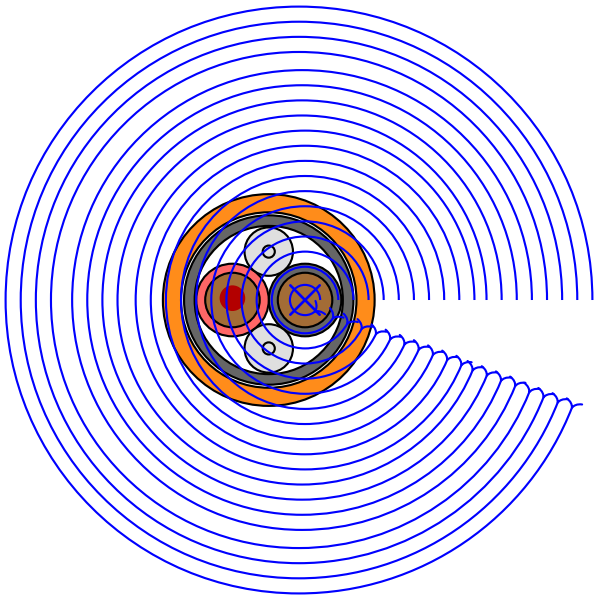

Figure 6.15: Magnetic field due to current in one conductor

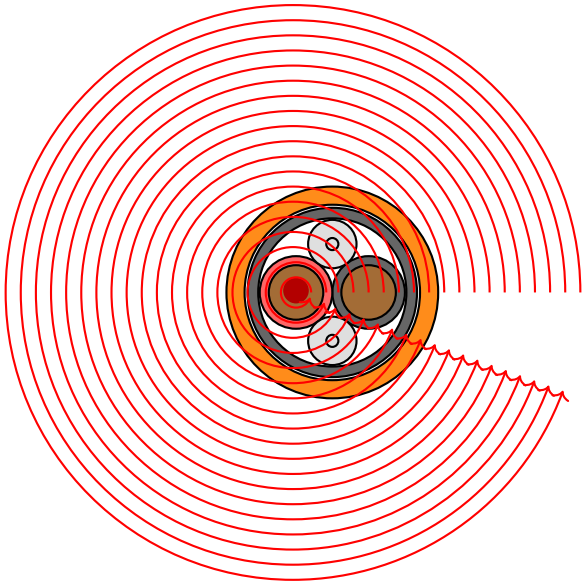

Figure 6.16: Magnetic field due to current in the other conductor

If one would now take a look at the combined magnetic field as current flows in both conductors at the same time one would see the result as Figure 6.17. As the magnetic field grows outside the cable, one can see that the blue and red magnetic field lines start to align with each other more, and the only difference is the direction of the magnetic field (arrow sign). This indicates that outside the cable to the right and to the left of the cable, the magnetic field lines cancel each other out. As defined earlier, the mutual inductance was defined as field lines that are shared between for example two conductors. It means that if a current is applied in one conductor and generates a magnetic field, and then the current is applied on the other conductor that generates a magnetic field. The area where both of the fields are "shared", is the mutual inductance, meaning a field that they both share, it is common to both conductors. This is the case to the field that can be seen in Figure 6.17, the lines align with each other, except for the small offset between the lines that has to do with the placement of the conductors.

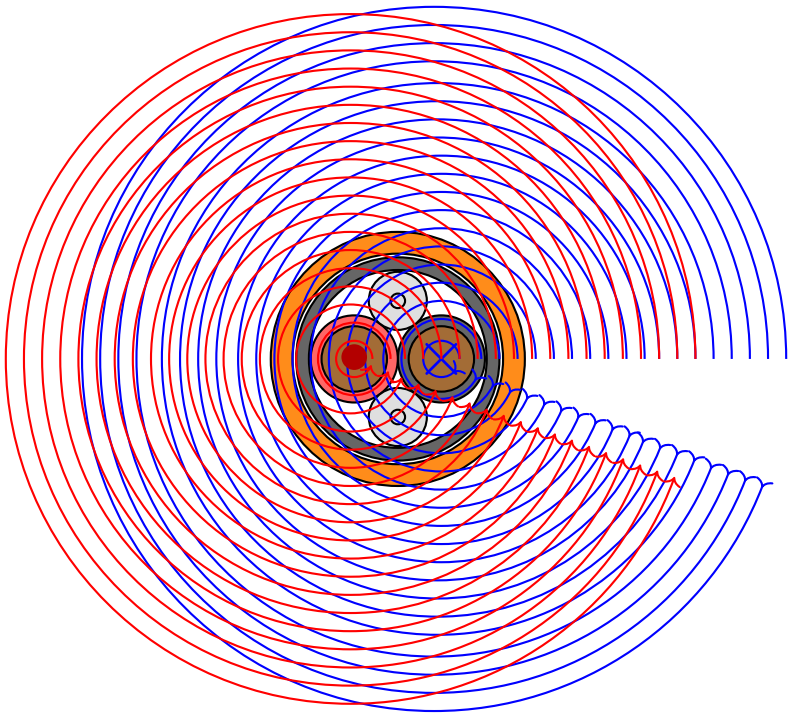

Figure 6.17: Magnetic field lines cancelling out on the outside of cable

If one would remove the field lines that are canceled out, then what is rest would be the field yielding the self inductance of both conductors. The example can be seen in Figure 6.18 (where some of the field lines are shown). Both the blue and red magnetic field lines will meet if the blue arrow is rotated clockwise until it is located side by side with the red arrow. In this scenario both field lines are pointing upwards meaning that they, in this moment, add up with each other. If blue field lines generate self inductance in the blue wire and red field lines generate self inductance in the red wire then if they are summed together the result will yield in $2L_c$.

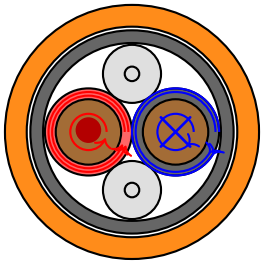

Figure 6.18: Illustration of magnetic field givnig rise to $2L_c$

Measuement results

In Table 6.5 the results for twinaxial cable parameters is found for both LCR measurement and COMSOL simulation.

Table 6.5: Results of 2x4mm^2 cable with 10m cable length (scaled to per meter) obtained from LCR measurement and COMSOL, at frequency $\approx$ 100 kHz.

Parameter	LCR	COMSOL
L_c $[\frac{\mu H}{m}]$	0.17	0.16
L_s $[\frac{\mu H}{m}]$	0.17	0.06
M_{cs} $[\frac{\mu H}{m}]$	0.168	0.101
M_{cc} $[\frac{\mu H}{m}]$	0.181	0.0481
C_{cs} $[\frac{pF}{m}]$	194.73	153.39
C_{cc} $[\frac{pF}{m}]$	59.20	49.67

As a comparison for the self inductance L_c, by using COMSOL simulation 0.5 $\frac{\mu H}{m}$ was obtained, and by using equation (3.15) 0.524 $\frac{\mu H}{m}$ was obtained (in DC). Which then shows that the COMSOL simulation is not far off from the hand calculation of this parameter. However, there is difference in some parameters above, and the reason for this could be of the difficulty of COMSOL modelling sometimes. Specially the shield resistance $R_{s,DC}$ is hard to obtain correctly in COMSOL if the shield is not braided in the COMSOL simulation itself. It could also affect the shield behaviour at higher frequencies differently compared to in real life measurements. That can in fact be seen when the shield inductance is varying at 100 kHz by a lot compared to the LCR value. The same can be observed for the mutual inductance.

However if one compares simply the stationary values for the twinaxial cable, from LCR measurement, comsol and hand calculation then the values are closer to each other as can be seen in Table 6.6.

Table 6.6: Values from 2x4mm^2 obtained from LCR measurement, COMSOL and hand calculation **at stationary**

Parameter	LCR	COMSOL	Hand cal.
$2L_c\ [\frac{\mu H}{m}]$	0.530	0.500	0.524
$L_c\ [\frac{\mu H}{m}]$	0.265	0.250	0.262
$L_s\ [\frac{\mu H}{m}]$	0.234	0.200	0.192
$M_{cs}\ [\frac{\mu H}{m}]$	0.191	0.203	0.192
$M_{cc}\ [\frac{\mu H}{m}]$	0.200	0.220	0.222
$C_{cs}\ [\frac{pF}{m}]$	194.73	153.39	183.36
$C_{cc}\ [\frac{pF}{m}]$	59.22	49.67	79.46

The difference between comsol values and LCR values at higher frequencies could be due to the development of skin effect which is different compared to in the real measurement (LCR). Because at very low frequencies (below approxiomately 100 Hz) the comsol simulation is very close to the LCR measurement and hand calculation. But above 100 Hz and more the inductance for the comsol simulation drops a lot in value. For M_{cc} following plot is obtained in Figure 6.19 during a comsol simulation. As can be seen at around 100 Hz and after the inductance drops a lot in value, however this is not the case in LCR measurement. The drop in LCR measured inductance is there but not as high as during comsol simulation

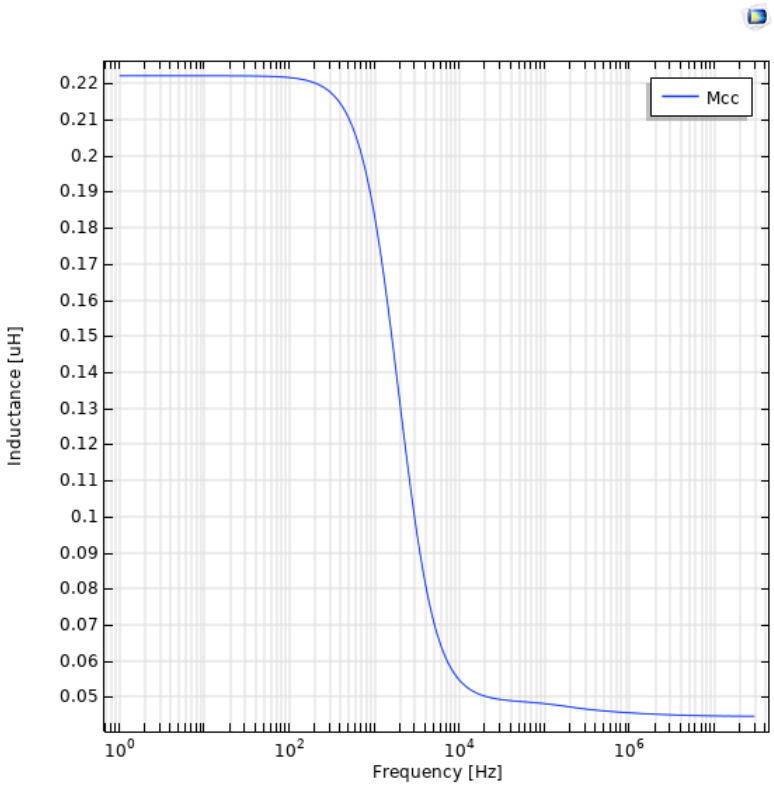

Figure 6.19: M_{cc} inductance drop in frequency domain

6.3 Measurements versus simulation of coaxial cables

In order to simulate same behaviour as the measurements, PLECS Standalone is used for the circuit simulations. It is used because Volvo GTT uses it in its daily work but also because of its simplicity and fast computation times for simpler circuits.

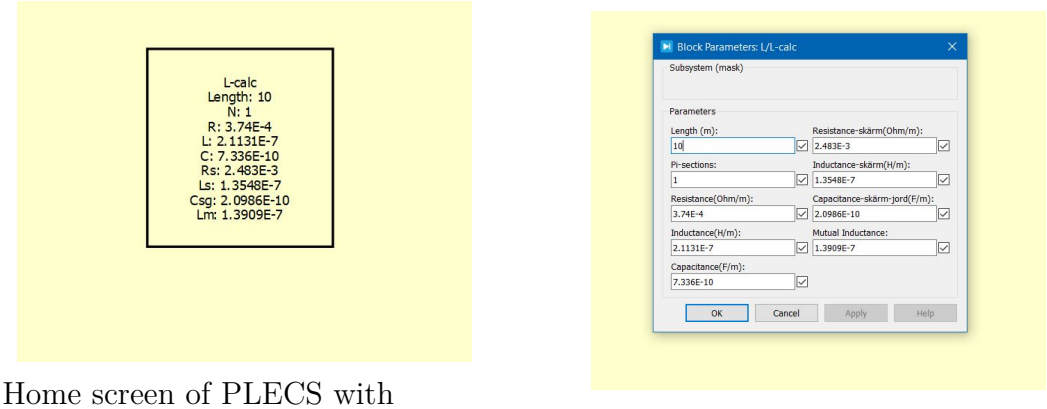

(a) Home screen of PLECS with subsystem

(b) Menu for entering parameters

Figure 6.20: PLECS home screen

In Figure 6.20a the subsystem block can be seen where all components are put into. In Figure 6.20b the parameters can easily be changed and substituted when using 'subsystem(mask)' in PLECS. The values are stored in a variable that is then put into the component value.

In Figure 6.21 the set up that is used for evaluating and running each test is shown. There are four current sources that are joined by four manual breakers. Each manual breaker is set at once for each parameter depending on what one wants to obtain. In this set up the shield inductance is of importance, that's why it is in it's active position and the rest are grounded. Moving on, there is for each current source one corresponding volt-meter that basically senses the voltage when the current runs through a part of the circuit. The current sources are joined by a perturbation block as it is called, and it is basically a signal that controls the current flow. On the other hand, there is a response block for the voltage which serves its purpose in measuring the response for various signals as a result of the signals fed through the current source. As the frequency response of the circuit is of importance, these variables will be changing over a frequency range. Basically a frequency sweep is done, in AC sweep under Simulation in PLECS.

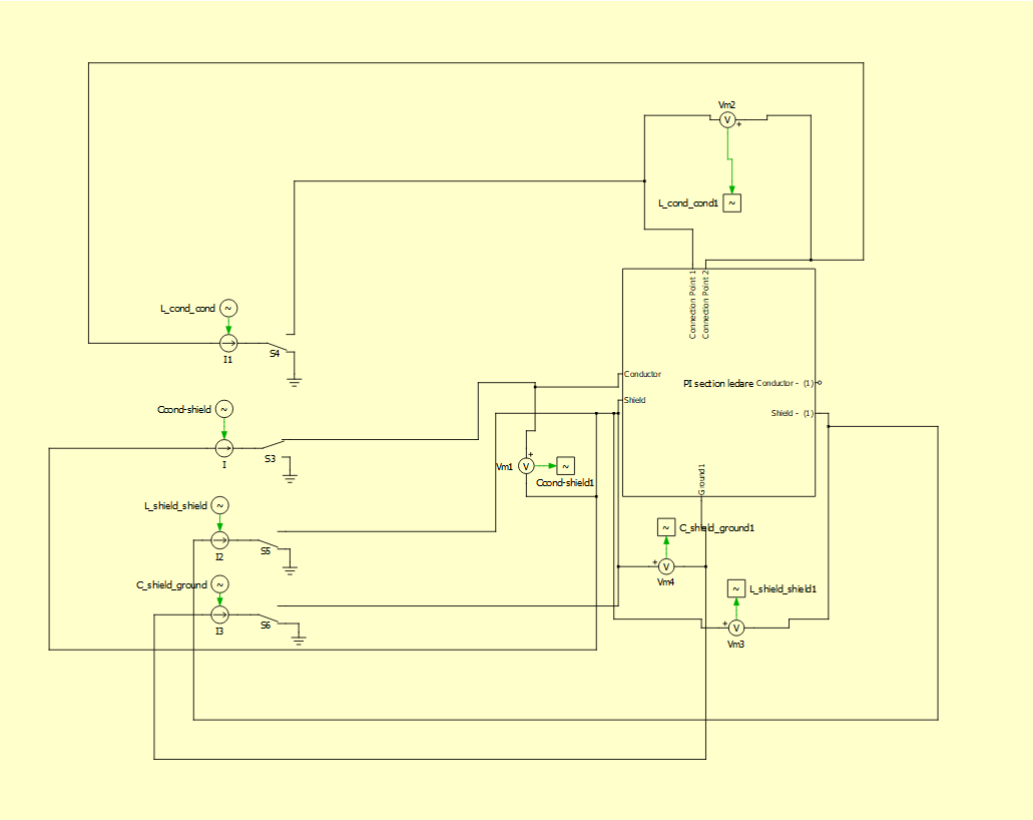

Figure 6.21: Whole set-up for computing all parameters of a pi section of a single coaxial cable

Moving on further into the circuit the pi section can be found in Figure 6.22, it is the subsystem block that was also shown in Figure 6.21, called "*PI section ledare*".

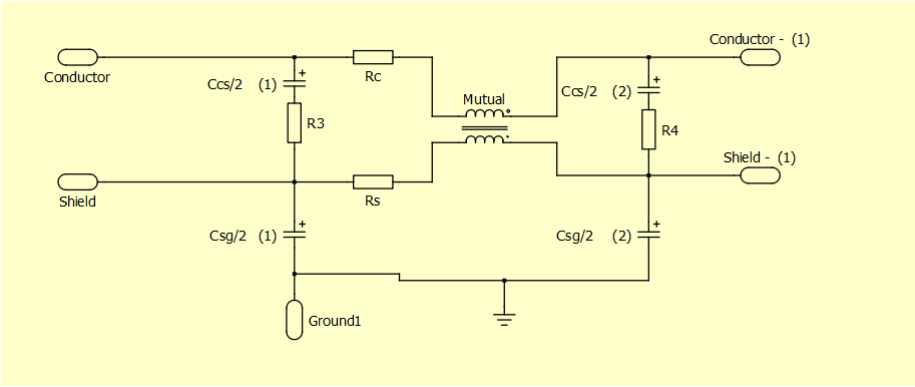

Figure 6.22: Pi section in PLECS for a single coaxial cable over ground

The resistors R3 and R4 are used as dummy resistors and are not in fact a part of the model itself but they serve as a help in running the tests. That is because PLECS tend to give errors when a current source is applied to a capacitor, due to the big step in voltage. To overcome this simulation error, R3 and R4 are put just to be able to run the simulation, their value are insignificant. The mutual inductor "Mutual", includes all inductances in the circuit. The block includes 4 elements, a

2x2 matrix where the diagonal elements are the mutual inductances and the cross-diagonal elements are $L_c + M_{cs}$ and L_s. C_{cs} is the conductor to shield capacitance and C_{sg} is the shield to ground capacitance , half the value on both sides. R_c and R_s serve as the resistance of conductor, and shield separately. The mutual inductor named "*Mutual*" in Figure 6.22 looks like follows

$$\begin{bmatrix} \mathrm{L}_c + M_{cs} & \mathrm{M}_{cs} \\ \mathrm{M}_{sc} & \mathrm{L}_s \end{bmatrix} \tag{6.1}$$

worth to mention is that the results in this section will only show the $50mm^2$ cable, for simplicity reasons 70 and 95 mm^2 cables results will be put in Appendix.

6.3.1 Measured and simulated $L_c + M_{cs}$

By applying the current in the conductor and measuring the voltage drop one can obtain the value of $L_c + M_{cs}$.

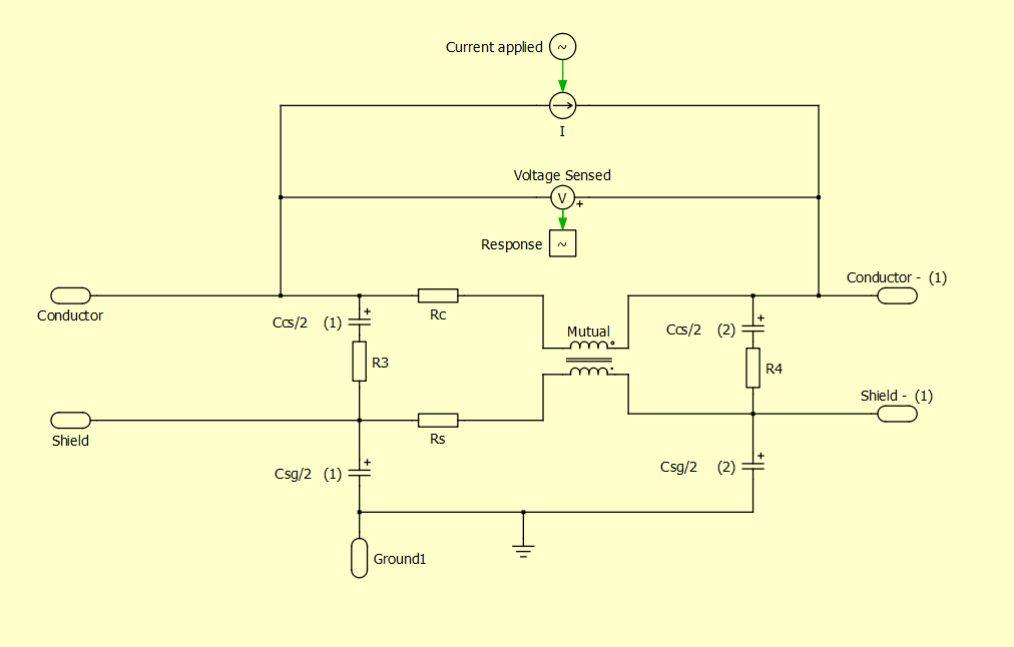

Figure 6.23: Simulation set-up for obtaining $L_c + M_{cs}$

The result can be seen in Figure 6.24, where at low frequencies the resistive behaviour is dominant. With increasing frequency the ωL term starts to grow and becomes dominant, this is the linear region. After some time, and at very high frequencies a L-C resonance circuit appears between mainly the inductance in the conductor and the capacitance between conductor and shield. However due to stray capacitances in the measurements and measurement errors, it is very hard to try to match the resonance point of measurement and simulation together. Even though the simulation parameters are extracted from the COMSOL simulation, the values seem to be very close as the graph shows. However, there are points where the simulation does not match with the measurement. This is mainly due to the skin effect

in the conductor, during higher frequencies the current gets "pushed" outwards of the conductor leaving little to no current left in the conductor which means that the magnetic fields inside the conductor goes to zero and the inductance for higher frequencies will then be lowered. It will be evident later on, that the inductance at higher frequencies is lower than the inductance for lower frequencies. Because the inductance is frequency dependent in the measurements, it means that it will be very hard to match it with the simulation. However, the shape of the graph is completely correct, but the problematic of only being able to put one value for the conductor inductance in the simulation model makes it very hard to match the measurements at all frequencies. For that reason, the value for the inductance is chosen around 100 kHz in COMSOL. Another reason why 100kHz is chosen is because the CM currents flow in the system from approximately 100kHz-10MHz. Thus it is important to be able to account for the CM current as well by using values in 100kHz range.

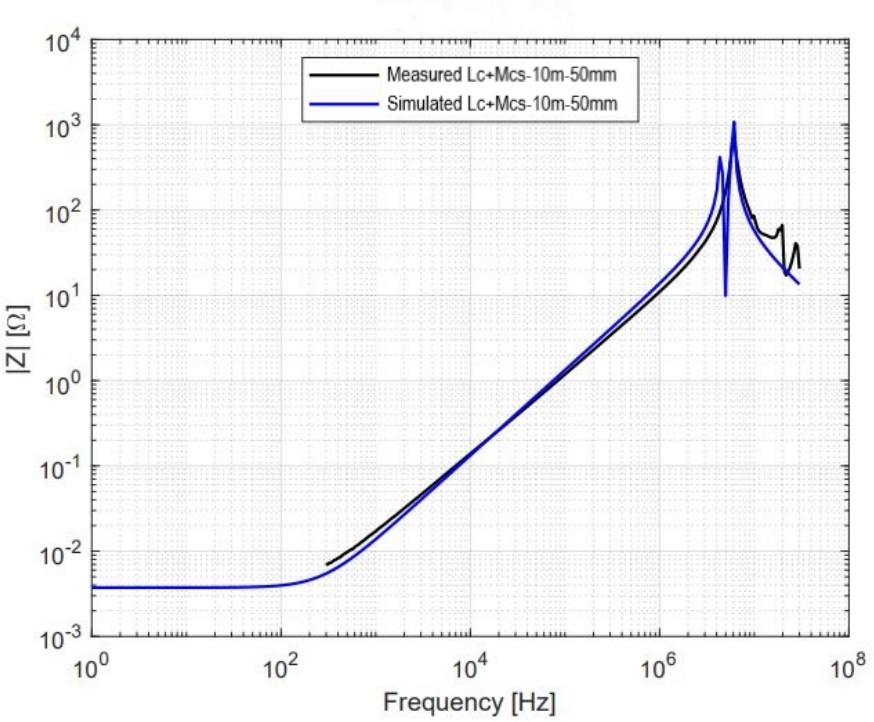

Figure 6.24: Simulation and measurement results for $L_c + M_{cs}$ (Pearson)

It is clearly shown that around 20 kHz the slope matches, below this frequency the inductance and thus the slope is higher for the measurements. For frequencies higher than 20 kHz the inductance is less than the simulation.

Table 6.7: Inductance at various frequencies, COMSOL compared to measurements

Frequency [kHz]	$L_c + M_{cs}$ $[\frac{\mu H}{m}]$ (COMSOL)	$L_c + M_{cs}$ $[\frac{\mu H}{m}]$ (Measurements)
10	0.21	0.21
100	0.18	0.18
1000	0.17	0.17

To show the behaviour at lower frequencies the four-wire kelvin method is used and the result can be seen in Figure 6.25.

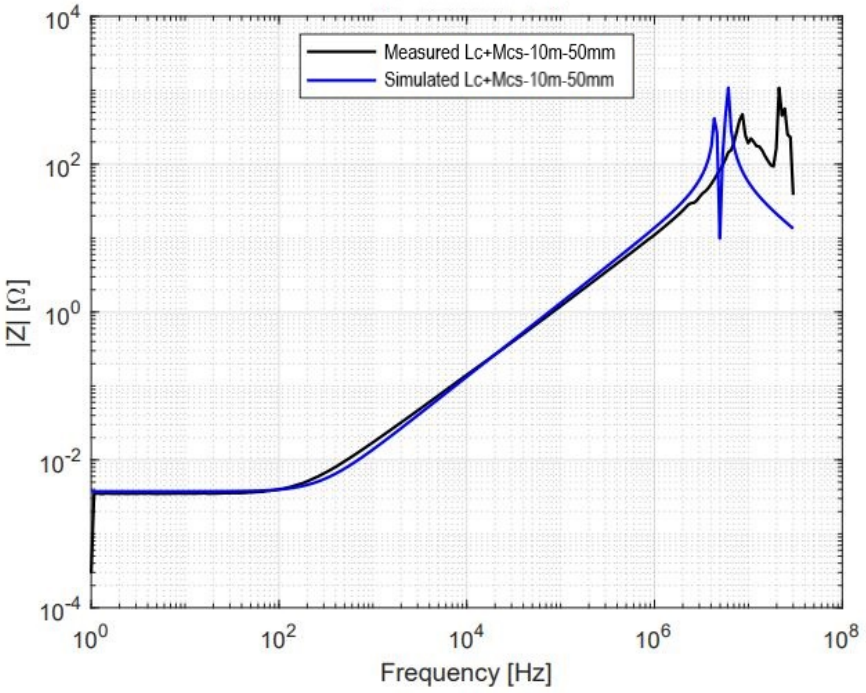

Figure 6.25: Simulation and measurement results for $L_c + M_{cs}$ (4WK)

6.3.2 Measured and simulated L_s

As for the shield inductance it can be simulated in a similar way just that now the current and voltage probes are set at the shield.

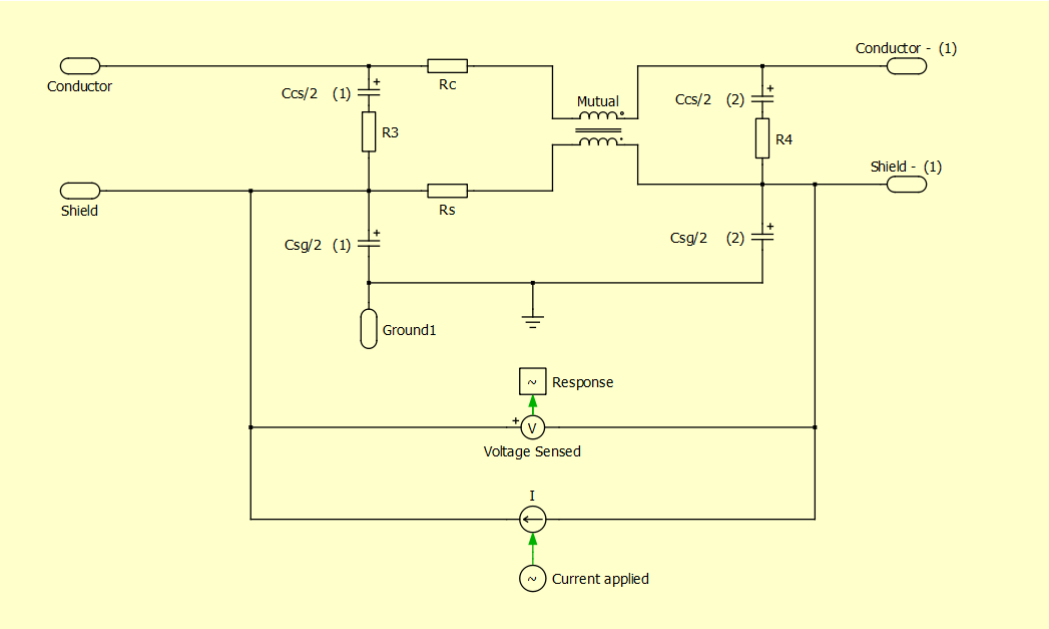

Figure 6.26: Simulation set-up for obtaining L_s

The result is obtained in Figure 6.27 as a comparison to L_s for 10m cable in the measurements.

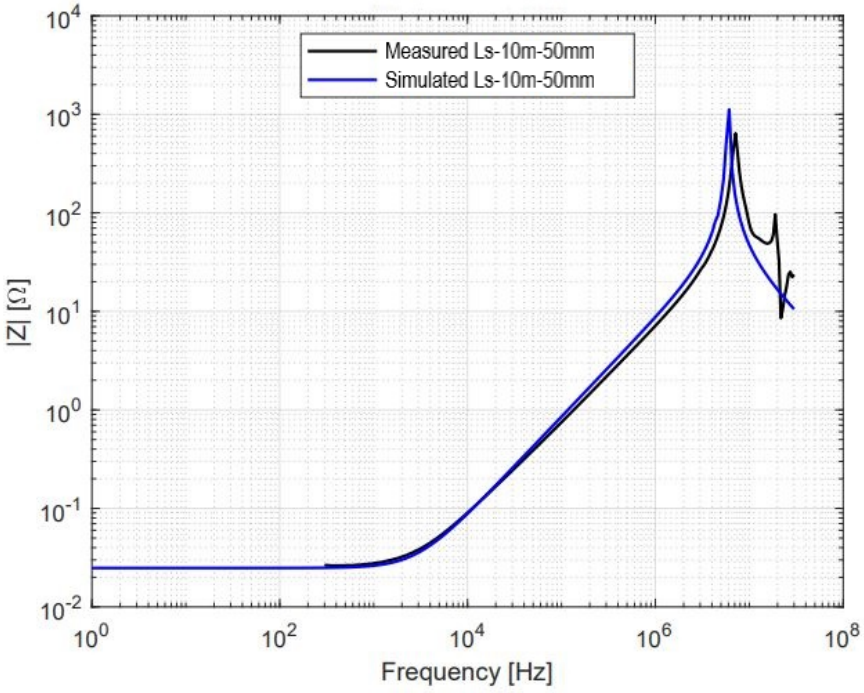

Figure 6.27: Simulation and measurement results for L_s

Table 6.8: Inductance at various frequencies, COMSOL compared to measurements

Frequency [kHz]	L_s $[\frac{\mu H}{m}]$ (COMSOL)	L_s $[\frac{\mu H}{m}]$ (Measurements)
100	0.13	0.12
500	0.12	0.11
1000	0.12	0.11

The simulation and measurements match pretty well up to approximately 40 kHz from Figure 6.27, the inaccuracy at higher frequencies is then because of the skin effect as discussed about earlier. Same observation is made here, the inductance is decreasing for higher frequencies, even though the decrease is not as high as for the conductor. The reason could be because of the higher internal inductance and magnetic energy stored in the conductor because of its circular shape than the shield because it is braided, and thinner.

6.3.3 Measured and simulated M_{cs}

Here the shield is fed with current and voltage is sensed through the conductor, and the results of simulation and measurement is shown in Figure 6.29, and the setup in Figure 6.28.

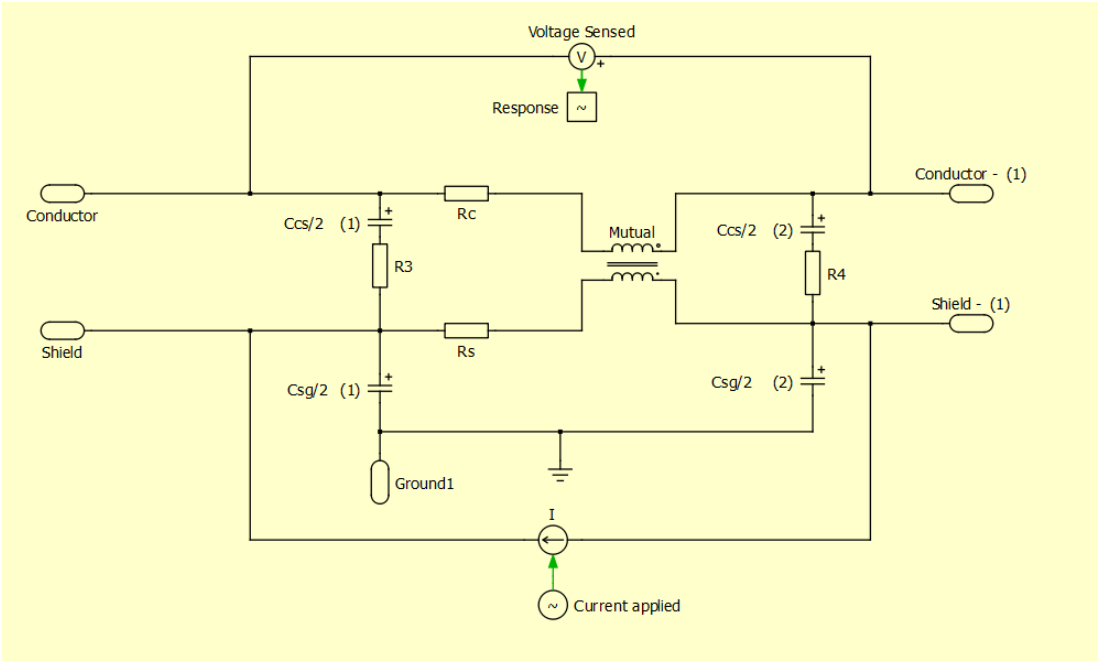

Figure 6.28: Simulation set-up for obtaining M_{cs}

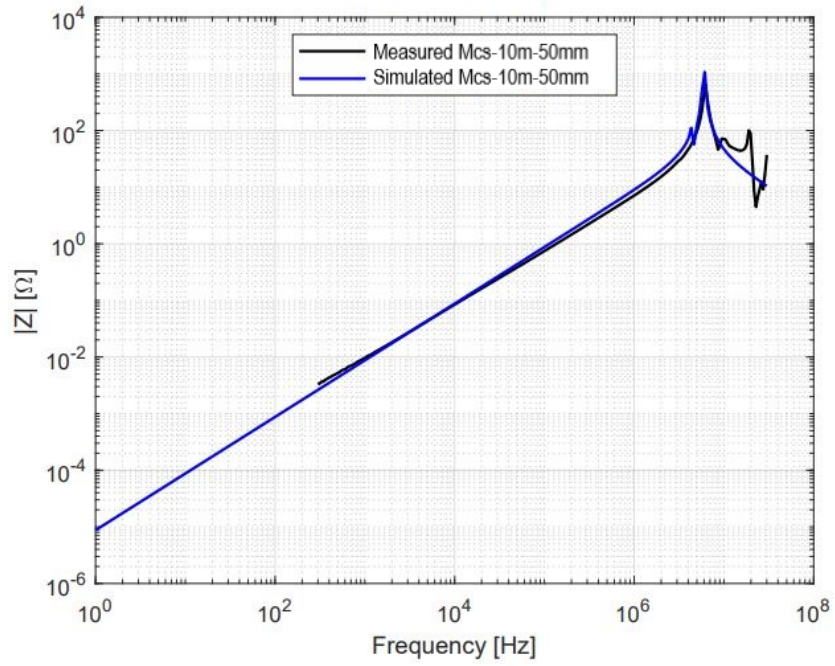

Figure 6.29: Simulation and measurement results for M_{cs}

The shape of the graph is similar and the simulation model seems to be correct. The slope matches at around 10 kHz or a bit lower than that, however same observation of skin effect is evident even for the mutual inductance, which is interesting. However, it is also evident by looking at Table 6.9 that the change in inductance for higher frequencies is very small. The change in inductance from lower->higher frequencies is quite high, but the change from high->higher frequencies is a lot lower. For example, the change in inductance in 10 kHz to 100 kHz is higher than the change from 100 kHz to 1 MHz, as shown in Table 6.9. This could be because the skin effect is very effective in for lower to higher frequencies, but at very high frequencies (for instance >1 MHz) the skin effect is already established so that the reduction in inductance is far less.

Table 6.9: Inductance at various frequencies, COMSOL compared to measurements

Frequency [kHz]	M_{cs} $[\frac{\mu H}{m}]$ (COMSOL)	M_{cs} $[\frac{\mu H}{m}]$ (Measurements)
10	0.14	0.13
100	0.13	0.12
1000	0.12	0.11

6.3.4 Measured and simulated M_{sc}

Same procedure is done, just that now the current and voltage probes have changed sides to measure the mutual inductance sensed on the shield.

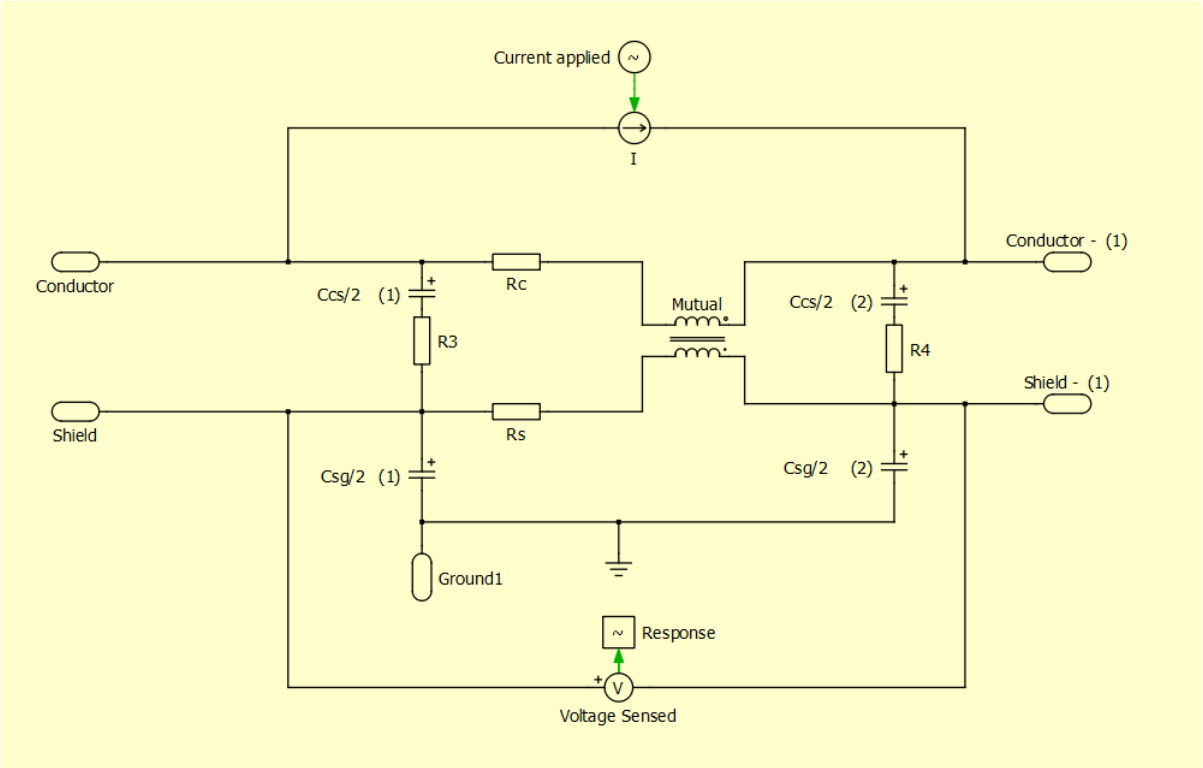

Figure 6.30: Simulation set-up for obtaining M_{sc}

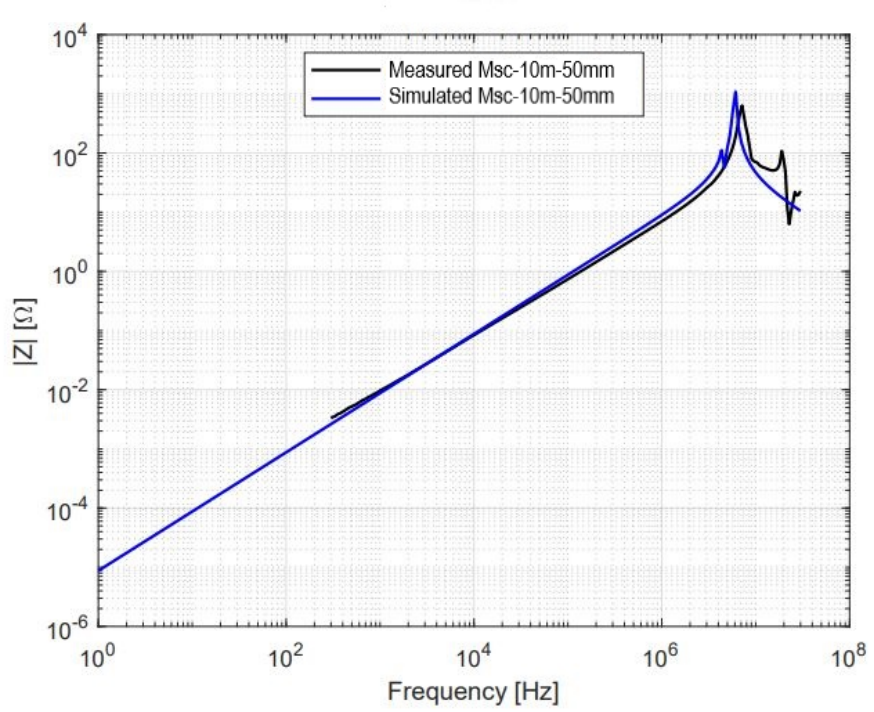

Figure 6.31: Simulation and measurement results for M_{sc}

Very similar behaviour in the graphs can be found by comparing Figures 6.31 and 6.29, which is as expected. The values in Tables 6.10 and 6.9 are also very similar.

Table 6.10: Inductance at various frequencies, COMSOL compared to measurements

Frequency [kHz]	M_{sc} $[\frac{\mu H}{m}]$ (COMSOL)	M_{sc} $[\frac{\mu H}{m}]$ (Measurements)
10	0.14	0.13
100	0.13	0.12
1000	0.12	0.12

Measuring $L_c + M_{cs}$ and short circuiting the shield

The way of measuring this parameter can be seen in Figure 6.32 and the results can be seen in Figure 6.33 as well as 6.34.

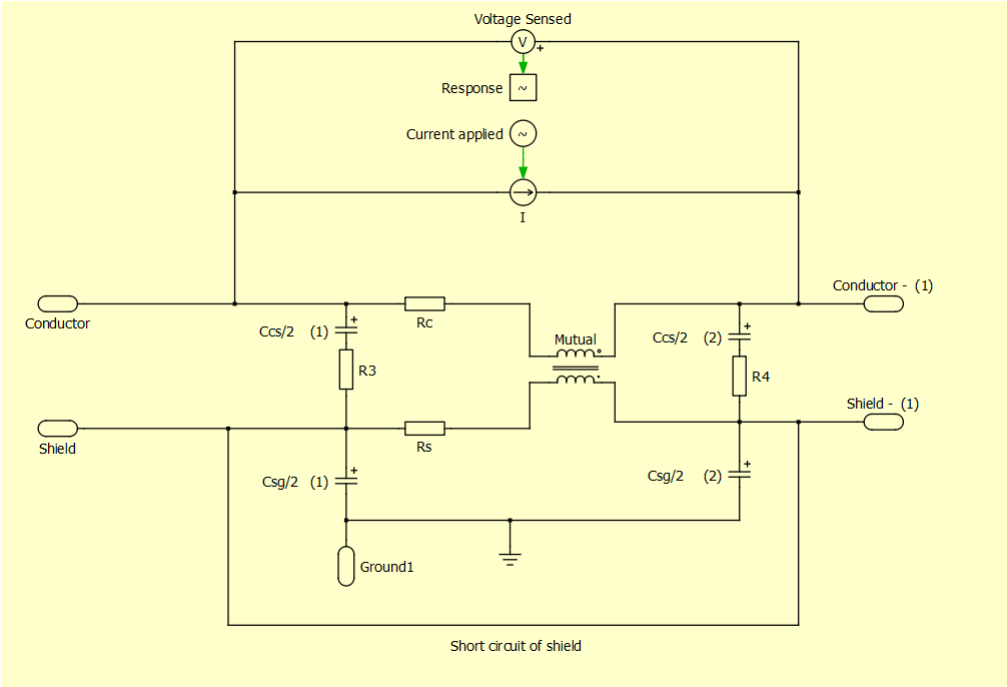

Figure 6.32: Simulation set-up for obtaining L_c

Here the purpose of shorting the shield is to limit the magnetic field lines from the conductor only to the shield inner boundary, in order to obtain the self-inductance of the conductor. As said before, if the shield was not shorted, one would obtain $L_c + M_{cs}$ where M is the mutual inductance and L_c the self inductance of the conductor.

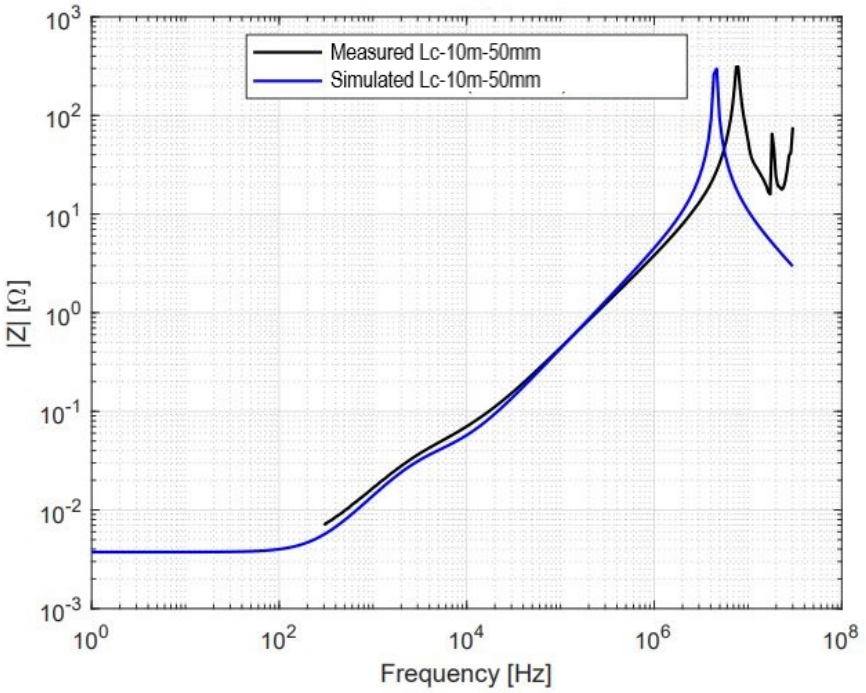

Figure 6.33: Simulation and measurement results for $L_c + M_{cs}$ with short circuited shield (Pearson method)

The very important behaviour of both the simulation and measurement results in Figures 6.33 and 6.34 is the "plateau" that occurs around 3 kHz approximately and ends at around 20 kHz. The plateau is because of the magnetic field cancellation between conductor's generated field and shield's induced field. Perhaps this can be better realized in Figure 6.34, as the low frequency behaviour is shown. The inductance before the plateau is $L_c + M_{cs}$ and after the plateau it is simply L_c.

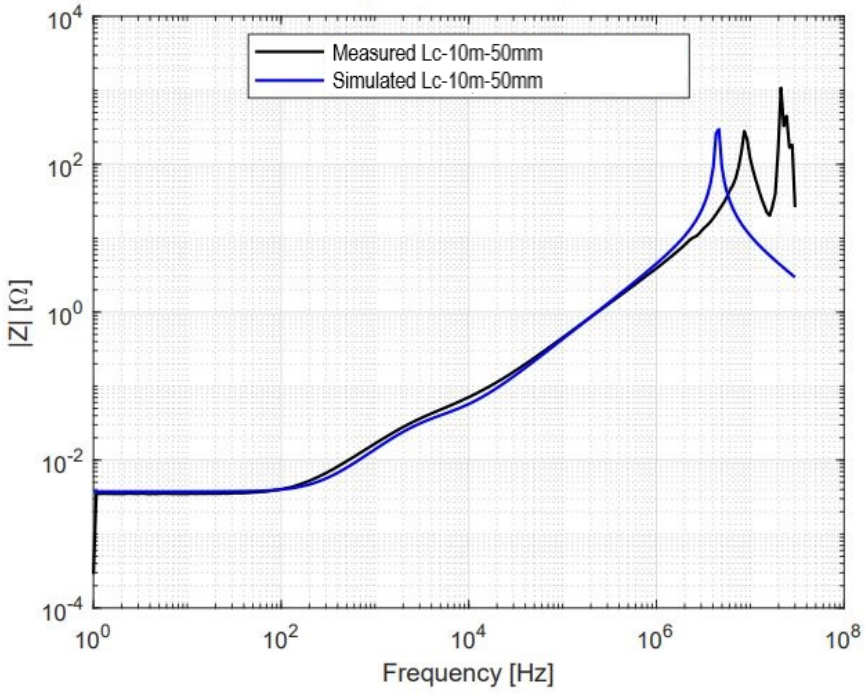

Figure 6.34: Simulation and measurement results for $L_c + M_{cs}$ with short circuited shield (4WK method)

Table 6.11: Inductance at various frequencies, COMSOL compared to measurements

Frequency [kHz]	L_c $[\frac{\mu H}{m}]$ (COMSOL)	L_c $[\frac{\mu H}{m}]$ (Measurements)
10	0.06	0.09
100	0.05	0.07
1000	0.04	0.06

The inductance at the beginning of the COMSOL simulation, expresses L_c, which means that at higher frequencies the internal inductance of the conductor will decrease, and this is what can be observed in Table 6.11. What is left of inductance at 1 MHz is almost only due to the flux linkage between conductor and shield, i.e. almost nothing in the conductor itself.

6.3.5 Measured and simulated C_{cs}

By applying the current through the conductor and back from the shield, and measuring the voltage drop one can obtain the capacitance between conductor and shield. The set-up and result are illustrated in Figures 6.35 and 6.36.

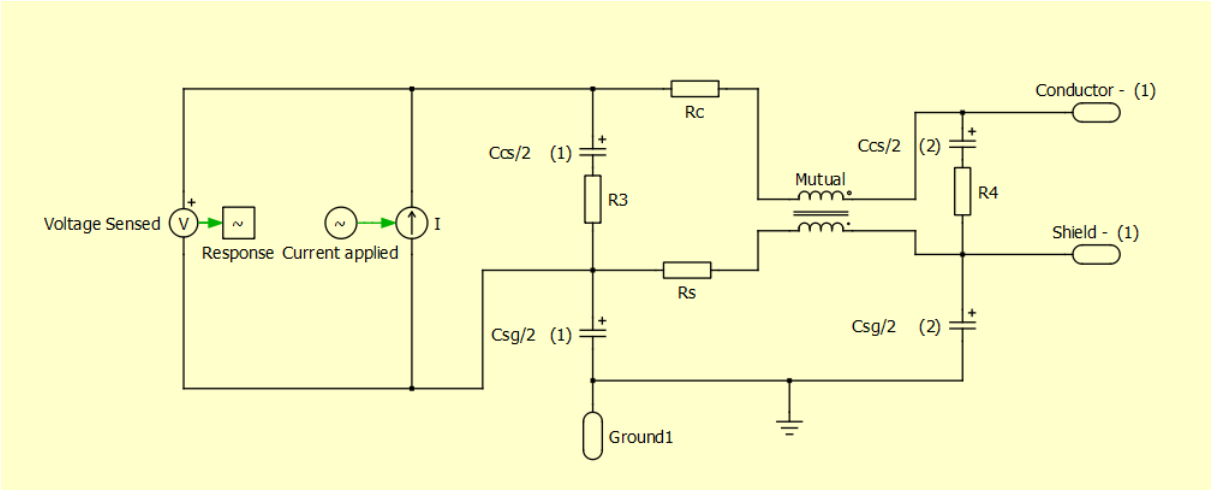

Figure 6.35: Simulation set-up for obtaining C_{cs}

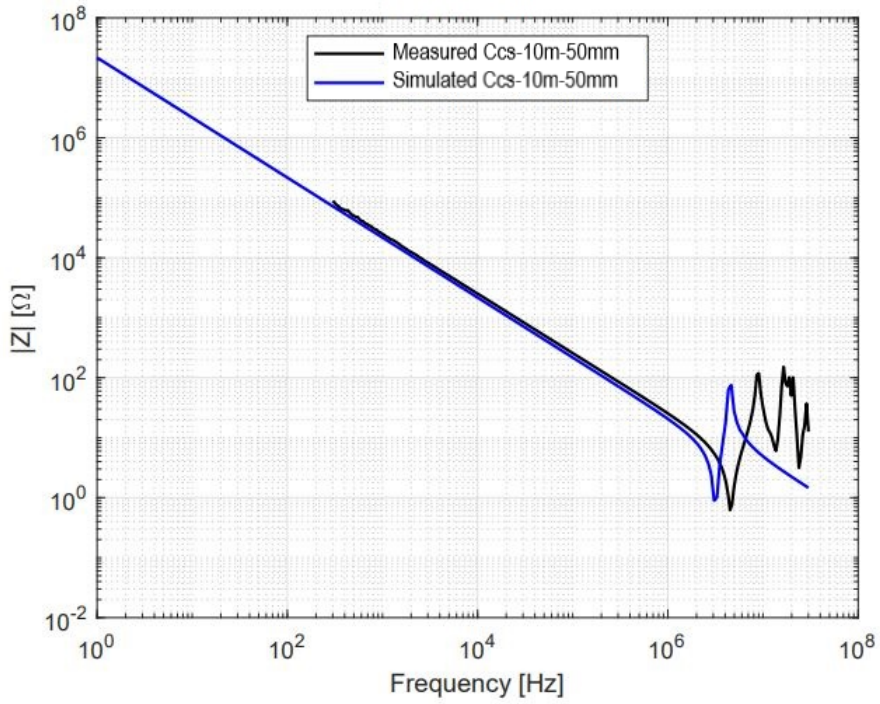

Figure 6.36: Simulation and measurement results for C_{cs}

However, the table for the comparison with different frequencies will not be done for the capacitance. Since, the capacitance variation is not as frequency dependent as the inductance or the resistance. The COMSOL simulations did not show any change over a frequency sweep, neither did the measurements give any noticeable difference.
Table 6.12 shows a final comparison of the important parameters in COMSOL simulation and measurements.

Table 6.12: Comparison results of 1x50mm^2 cable with 10m cable (scaled to per meter) obtained from LCR measurement and COMSOL, at frequency $\approx$ 100 kHz.

Parameter	LCR	COMSOL
$L_c + M_{cs}$ $[\frac{\mu H}{m}]$	0.19	0.18
L_s $[\frac{\mu H}{m}]$	0.12	0.12
M_{cs} $[\frac{\mu H}{m}]$	0.12	0.12
M_{sc} $[\frac{\mu H}{m}]$	0.12	0.12
L_c $[\frac{\mu H}{m}]$	0.07	0.05
M_{ss} $[\frac{\mu H}{m}]$	0.02	0.003
C_{cs} $[\frac{pF}{m}]$	620.78	733.62
R_c $[\frac{m\Omega}{m}]$ - at stationary	0.37	0.25
R_s $[\frac{m\Omega}{m}]$ - at stationary	2.48	0.78

C_{ss} and C_{sg} are not shown, because of the difficulty in obtaining correct results. More about this will be discussed in the section Discussion.

7
Discussion

7.1 Skin effect

The problem of skin effect is both seen in the measurements and also the simulations. Perhaps the problem in simulation is more problematic. With that being said, it is very tough to make a model that will fit in all frequencies, when the inductance is decreasing for higher frequencies. However, this is probably not impossible to make. One just needs to account for the skin effect in the model by using some other parameters. Or perhaps it is easier, in our case, to have one model working for lower frequencies up to maybe 100kHz and another model working from 100kHz and above for higher frequencies. That is because, the drop in inductance is not as much as for higher frequencies compared to the drop in the low-mid frequency range. However, this would make the computation of a whole system simulation a lot trickier and more time exhausting, by simulating two separate models. The resistance, which has not been mentioned too much in this report, is in fact increasing in frequency which also makes it trickier. In the model a simple value for resistance and inductance is put, but however as seen they are frequency dependent.

7.2 Resonance point

In this project the importance of the resonance point has not be investigated much. There are reasons behind this statement. In simulations the main goal was to get fairly good results in the linear region of the graph, while the resonance point was not thought about too much. The reason behind this comes down to a couple of factors. The resonance point for high frequencies, >1MHz, is very hard to match in a simulation software (even if the exact same values are chosen as the measurements that are obtained). The reason for this are stray parameters introduced in the measurement. By for example placing the test probes a little bit further out compared to further in on the shield for example, will give changes in the measured results. It is because when one introduces a little piece of wire that is unwanted in the measurement then it will affect the results, sometimes the change is remarkable.

As an example, Figure 7.1 shows two scenarios of measuring a $0.01\mu F$ capacitor. One being, placing the test probes as close as possible to the capacitor, and the other by placing the test probes furthest away as possible from the capacitor. By placing the probes further out, one will introduce the little piece of wire seen in the figure. This little piece of wire will introduce more inductance into the circuit.

Having a look at the result in Figure 7.2, one can see that there is a difference in the resonance point. The capacitance (the linear region) is the same for both of the scenarios. However what is changing is the increment of inductance in one of the circuits (blue graph) which then shifts the resonance point to the left in the graph. Even though the difference may seem very small, the resonant frequency is changing a lot. Have in mind, that the values are in MHz in the region of resonance point, so the difference is quite big.

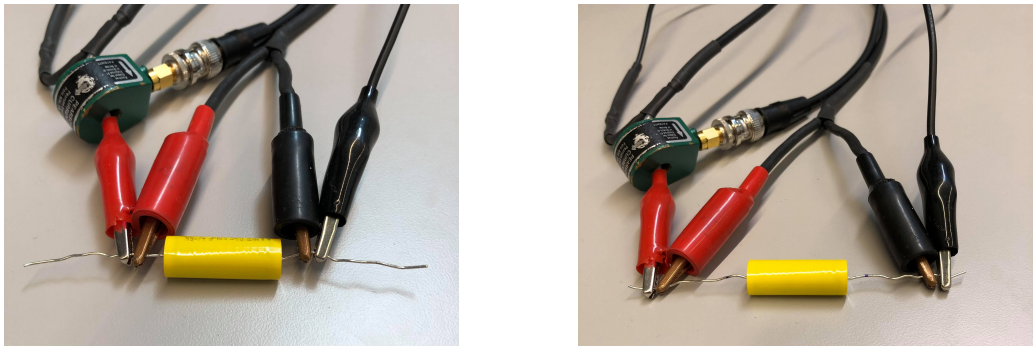

(a) Placing test probes **further in** the capacitor of $0.01\mu H$

(b) Placing test probes **further out** the capacitor of $0.01\mu H$

Figure 7.1: Different scenarios of placing test probes at a $0.01\mu H$ capacitor.

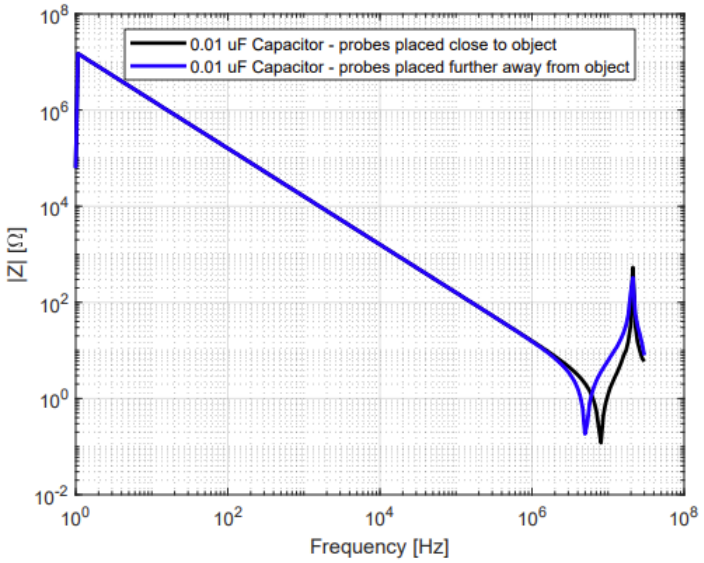

Figure 7.2: Measurement of a 0.01 μF capacitor, when test probes are placed close to the capacitor and further away.

The resonance point is because of the mentioned reasons above, not investigated as much in this report. There is always inaccuracies in measurements, even if one tries very hard to achieve the best results possible. A big error that is introduced is the placement of measuring probes. Generally one would like to place the test probes

as close as possible to avoid these stray effects. In this report many measurements has been conducted, re-occurring measurements, during many days. What has been noticed is that sometimes for the same measurements but on different days the measured values are different, even if one tries to lay the test probes as good as possible with as little error introduced as possible. It is of course very hard to place the test probes exactly on the same place of the cable each time, which will also introduce differences. But during our work, we have been thinking if the LCR meter may also introduce errors. Is it important to keep it on for some time before measuring the cables, how long is this time, or does it not matter? Does the LCR meter need to be "warm" before measuring, to get the most correct values? For now it is very tough to make any conclusions regarding this, even though one can have a thought about it. These are things that will hopefully be touched more about (alongside other topics) in future works.

7.3 Importance of parameters

There are some values which are of certain importance. For example the self inductance of each conductor and shield as well as the mutual inductance between conductor and shield. These are very important, because the current mainly flows through these regions during operation, and it is thus important to get them right. However the capacitances between shield-ground or shield-shield are in some cases important, but they were not able to be obtained correctly unfortunately. For a future work, it would be advised to study the coupling between shield-shield and shield-ground. Even though the mutual inductance between the cables is determined, it goes to show that this value is very small compared to other inductances in the circuit. It would make sense in some applications perhaps to neglect this parameter, because of its minimal value. It is also important, as mentioned, to get the conductor-shield mutual inductance correct as it affects the behaviour of the impedance a lot, recall the example of when the shield is shorted and measuring $L_c + M_{cs}$ for example.

7.4 Comsol simulation

The COMSOL simulation has got issues, even though the simulation works fairly good and the results are close to the measurements. The reason behind this statement is because of the problem of creating a model that will be exact as in real life. For example the conductor in a real cable, is usually made out of very thin copper wires instead of one bulk single conductor as in the simulation made. This can play its role on the current distribution and also the skin effect when comparing COMSOL with reality. Another issue of the simulation model is the shield. It is modelled very simply as a metal surrounding the insulation of the cable, however as seen in practice this is not the case. The shield is in practice braided, which if put into the COMSOL model could definitely change the outcome of the results. The models made, are simply done in 2D and expecting to give per unit length parameters of a cable. Which in fact works kind of well. However, it showed that the real cable

that is for example 10m is not as linear as in the COMSOL modelling. It is not as easy to multiply the values with 10, and obtaining 10m values, especially regarding the capacitance. The capacitance in the measurement, after a lot of testing and cancelling possible errors, gave same result regardless. It had a pretty poor value to ratio comparison, which makes us to think that the insulation material is perhaps nonlinear. However this has to be further investigated to completely confirm this.

Even though all parameters are extracted, it does not mean they will work perfectly together and perhaps there are parts in our model that are missing. The COMSOL modelling is done one by one, each parameter at once without taking other sources into account. For example some values maybe needs to be corrected to when they actually are put into use. That is, for example, when the cables are in full operation. Are we really seeing L_c in the conductor at that time? Or is the other machinery affecting its result, so that what is seen is not 100% L_c. COMSOL is used, when a current is flowing in the conductor, when a current is flowing in the shield. It means each case is done separately. It would be more interesting to see a whole dynamic simulation to see how the parameters may change. That would probably be more realistic.

7.5 Environmental aspects

This report is in many aspects very technological. However, there are some aspects that are worth of being mentioned. The environmental aspect is a part of this work even though it is not very apparent sometimes. The whole idea of this work is to model and simulate cable models as a part of the ongoing electrification of electric vehicles. Electric vehicles are good in many aspects, and if its energy is used from renewable energy sources then it is a good match. Many of the cars today are however not electrical which has its impact on the environment. By creating cable models, and making them properly functional and representative of the reality one can definitely impact the electrification as well as the environmental aspect. The electric vehicle, as talked about earlier, consists of many parts. In order to make a functional electric vehicle, it is very crucial to get the cable model correct, and the cable model is of particular importance as it connects and joins important parts together. It would be very bad for the electrification of vehicles if the understanding as well as calculation of electrical parameters were done poorly. Hence, we can say that the cable modelling definitely plays its role environmentally, but also ethically, as a part of improving the electrification of vehicles.

8

Conclusion and recommendations

To finally conclude this work, one can say that the cable modelling is far from an easy task, even though it is sometimes taught as a single series R-L circuit. It has been shown that the part of getting the modelling equal or at least very close to the simulations is not as easy as it was first thought. The goal of achieving 5% or less in deviation from the measured values, is not achieved in all cases even though some values are very close to each other and fulfill this criteria. To conclude, it can be said that four successful models has been obtained. A single coaxial cable model, two parallel coaxial cables model, three phase coaxial cable model, and a twinaxial model. In addition to that the simulation models have same behavior as the measured models, which indicate their validity.

However as in any work there are things which did not work as good. There are parameters, like C_{ss} and C_{sg} that were tricky to obtain as a correct value. After trying a lot of times, the same outcome was given, which was not satisfying. It is worth to mention that the COMSOL modelling for the coaxial cable worked fairly good. However, for the twinaxial case it did not work as expected. For future works, it is highly encouraged to keep on working on the shield-shield couplings, as well as the shield-ground couplings, and the twin-axial case. It would be interesting to try to measure on a real electric vehicle to see if there are differences in measured values compared to the single cable testings. Even though some comparison is made in the report, it would be better to include more examples but also investigate why there could be differences. To also work more on the cable modelling in COMSOL is also advised, to further improve the twin-axial model is advised as well.

This project has been very demanding but also very giving in the technical aspect, and perhaps this project can bring further more ideas in the future, and even better works!

Bibliography

[1] Automotive products RADOX® cables and system solutions, Pfäffikon, Switzerland: HUBER+SUHNER AG, 2020.

[2] TMC, "The importance of shielded cables," 2017. [Online]. Available: https://www.tmccables.com/techresources/cables/shielded-cables/ Accessed on: 2020-08-06.

[3] AlphaWire, "Understanding Shielded Cable," Elizabeth, USA, 2009. [Online]. Available: https://www.mouser.com/pdfdocs/alphawire-Understanding-Shielded-Cable.pdf, Accessed on: 2020-08-06.

[4] All about circuit, "Ground and Other Reference Points," 2015. [Online]. Available: https://www.allaboutcircuits.com/video-lectures/ground-reference-points/, Accessed on: 2020-08-09.

[5] P. Wilson, "The ground plane," in The Circuit Designer's Companion, 3rd ed., Oxford, England: Newnes, 2012, ch. 2, pp. 61-62.

[6] K. Feldhues, M. Diebig, S. Frei, "Analysis of the Low Frequency Shielding Behavior of High Voltage Cables in Electric Vehicles," in Proceedings of the 2014 International Symposium on Electromagnetic Compatibility (EMC Europe 2014), Gothenburg, Sweden, 2014, pp. 408-413. [Online]. Available: https://ieeexplore.ieee.org/document/6930941, Accessed on: 2020-08-06.

[7] A. Consoli, G. Oriti, A. Testa, A.L. Julian, "Induction motor modeling for common mode and differential mode emission evaluation," in Proceedings of IAS '96. Conference Record of the 1996 IEEE Industry Applications Conference Thirty-First IAS Annual Meeting, San Diego, CA, USA, 1996, pp. 1-4. [Online]. Available: https://ieeexplore.ieee.org/document/557097, Accessed on: 2020-08-06.

[8] M. Moon, H. Kim, J. Song, Y. Kwack, D. Kim, B. Kim, E. Kim, J. Kim, "Modeling and Analysis of Return Paths of Common Mode EMI Noise Currents From Motor Drive System in Hybrid Electric Vehicle," in Proceedings of the 2015 Asia-Pacific Symposium on Electromagnetic Compatibility (APEMC), Taipei, Taiwan, 2015, pp. 82-85. [Online]. Available: https://ieeexplore.ieee.org/document/7175395, Accessed on: 2020-08-06.

[9] Circuit Globe, "Nominal Pi model of a Medium Transmission line," [Online]. Available: https://circuitglobe.com/nominal-pi-model-of-a-medium-transmission-line.html, Accessed on: 2020-08-06.

[10] H. Saada, Power System Analysis, USA: The McGraw-Hill companies, Inc., 1999.

[11] D. Fahlgren, D. Heinerås, "Analysis of Optimization of High Power Cables Design for both DC and AC in Electric Vehicles," Lic. the-

sis, Department of Electric Power Engineering, Chalmers University of Technology, Gothenburg, Sweden, 2017. [Online]. Available: https://odr.chalmers.se/handle/20.500.12380/253220

[12] N. Ida, "Gauss's Law and the Electric Potential", in Engineering Electromagnetics, 3th ed., Akron, OH, USA:Springer, 2015, ch.4, sec.7, pp.186-187

[13] N. Ida, "Magnetic materials and properties", in Engineering Electromagnetics, 3th ed., Akron, OH, USA:Springer, 2015, ch.9, sec.4, pp.453-454

[14] B. Adamczyk, "Magnetically coupled circuits", in Foundations of Electromagnetic Compatibility, 1th ed., New Jersey, USA:John Wiley and Sons, 2017, ch.10, sec.1, pp.243-245

[15] L. Bengtsson, B. Karlström, Transformer och filter. Malmö, Sweden: Holmbergs i Malmö, 2017.

[16] David K. Cheng, "Static electric fields", in Field and wave electromagnetics, 2th ed., Edinburgh Gate, UK:Pearson, 2014, ch.3, sec.10, pp.124-125

[17] J. James, "Analysis of stranded multi-conductor cable in multilayered dielectric media," 2011. [Online]. Available: https://www.slideshare.net/jimmijamesarrow/analysis-of-stranded-multiconductor-cable-in-multilayered-dielectric-media, Accessed on: 2020-08-06.

[18] David K. Cheng, "Inductances and inductors", in Field and wave electromagnetics, 2th ed., Edinburgh Gate, UK:Pearson, 2014, ch.6, sec.11, pp.237-238

[19] Clayton R. Paul, "The per-unit length parameters for two-conductor lines", in Analysis of multiconductor transmission lines, 2d ed., New Jersey, USA:John Wiley and Sons, 2008, ch.4, sec.2, pp.127

[20] K. Feldhues, M. Diebig and S. Frei, "Analysis of the low frequency shielding behavior of high voltage cables in electric vehicles," 2014 International Symposium on Electromagnetic Compatibility, 2014, pp. 408-413, doi: 10.1109/EMCEurope.2014.6930941.

[21] H. Saada, Power System Analysis, USA: The McGraw-Hill companies, Inc., 1999.

[22] Newtons4th Inc., "IAI2 Impedance Analyzer," [Online]. Available: https://www.newtons4th.com/products/impedance-analysis-interface-2/, Accessed on: 2020-08-06.

[23] StudyLib, "Estimates of mutual inductance," [Online]. Available: https://studylib.net/doc/18617471/estimates-of-mutual-inductance, Accessed on: 2020-08-06.

[24] PIC Wire & Cable, "Grounding Wires & Cables," [Online]. Available: https://www.picwire.com/resources/technical-articles/grounding-wire-cable/, Accessed on: 2020-08-06.

A

Appendix

Table A.1: Values obtained from using COMSOL **at stationary**

Parameter	1x50mm^2	1x70mm^2	1x95mm^2	Description
$L_{c1} + M_{cs1}$ $[\frac{\mu H}{m}]$	0.272	0.259	0.258	Total inductance of Cable 1
$L_{c2} + M_{cs2}$ $[\frac{\mu H}{m}]$	0.272	0.259	0.258	Total inductance of Cable 2
L_{c1} $[\frac{\mu H}{m}]$	0.092	0.085	0.088	Self-inductance in C1
L_{c2} $[\frac{\mu H}{m}]$	0.092	0.085	0.088	Self-inductance in C2
L_{s1} $[\frac{\mu H}{m}]$	0.177	0.172	0.168	Self-inductance in S1
L_{s2} $[\frac{\mu H}{m}]$	0.177	0.172	0.168	Self-inductance in S2
M_{cs} $[\frac{\mu H}{m}]$	0.180	0.174	0.171	Between S1 and C1
M_{sc} $[\frac{\mu H}{m}]$	0.180	0.174	0.171	Between C1 and S1
M_{ss} $[\frac{\mu H}{m}]$	0.068	0.068	0.067	Between S2 and S1
C_{cs1} $[\frac{pF}{m}]$	733.62	889.87	820.90	Between C1 and S1
C_{sg1} $[\frac{pF}{m}]$	216.23	225.63	238.30	Between S1 and G
C_{ss} $[\frac{pF}{m}]$	93.23	98.09	104.70	Between S1 and S2
C_{sg2} $[\frac{pF}{m}]$	216.23	225.63	238.30	Between S2 and G
C_{cs2} $[\frac{pF}{m}]$	733.62	889.87	820.90	Between S2 and C2
R_{c1} $[\frac{m\Omega}{m}]$	0.24	0.16	0.12	Self-resistance in C1
R_{s1} $[\frac{m\Omega}{m}]$	0.78	0.81	0.53	Self-resistance in S1
R_{s2} $[\frac{m\Omega}{m}]$	0.78	0.81	0.53	Self-resistance in S2
R_{c2} $[\frac{m\Omega}{m}]$	0.24	0.16	0.12	Self-resistance in C2

Table A.2: Values obtained from hand calculation **at stationary**

Parameter	1x50mm^2	1x70mm^2	1x95mm^2	Description
$L_{c1} + M_{cs1}$ $[\frac{\mu H}{m}]$	0.269	0.255	0.253	Total inductance of Cable 1
$L_{c2} + M_{cs2}$ $[\frac{\mu H}{m}]$	0.269	0.255	0.253	Total inductance of Cable 2
L_{c1} $[\frac{\mu H}{m}]$	0.092	0.085	0.088	Self-inductance in C1
L_{c2} $[\frac{\mu H}{m}]$	0.092	0.085	0.088	Self-inductance in C2
L_{s1} $[\frac{\mu H}{m}]$	0.177	0.170	0.165	Self-inductance in S1
L_{s2} $[\frac{\mu H}{m}]$	0.177	0.170	0.165	Self-inductance in S2
M_{cs} $[\frac{\mu H}{m}]$	0.177	0.170	0.165	Between S1 and C1
M_{sc} $[\frac{\mu H}{m}]$	0.177	0.170	0.165	Between C1 and S1
M_{ss} $[\frac{\mu H}{m}]$	0.069	0.069	0.069	Between S2 and S1
C_{cs1} $[\frac{pF}{m}]$	733.60	889.85	820.88	Between C1 and S1
C_{sg1} $[\frac{pF}{m}]$	177.63	178.76	181.79	Between S1 and G
C_{ss} $[\frac{pF}{m}]$	88.81	89.37	90.89	Between S1 and S2
C_{sg2} $[\frac{pF}{m}]$	177.63	178.76	181.79	Between S2 and G
C_{cs2} $[\frac{pF}{m}]$	733.60	889.85	820.88	Between S2 and C2
R_{c1} $[\frac{m\Omega}{m}]$	0.25	0.16	0.12	Self-resistance in C1
R_{s1} $[\frac{m\Omega}{m}]$	—	—	—	Self-resistance in S1
R_{s2} $[\frac{m\Omega}{m}]$	—	—	—	Self-resistance in S2
R_{c2} $[\frac{m\Omega}{m}]$	0.25	0.16	0.12	Self-resistance in C2

Table A.3: Values obtained from LCR measurement **in frequency $\approx$ 100kHz**

Parameter	1x50mm^2	1x70mm^2	1x95mm^2	Description
$L_{c1} + M_{cs1}$ $[\frac{\mu H}{m}]$	0.190	0.164	0.159	Total inductance of Cable 1
$L_{c2} + M_{cs2}$ $[\frac{\mu H}{m}]$	0.190	0.164	0.159	Total inductance of Cable 2
L_{c1} $[\frac{\mu H}{m}]$	0.070	0.060	0.065	Self-inductance in C1
L_{c2} $[\frac{\mu H}{m}]$	0.070	0.060	0.065	Self-inductance in C2
L_{s1} $[\frac{\mu H}{m}]$	0.120	0.106	0.095	Self-inductance in S1
L_{s2} $[\frac{\mu H}{m}]$	0.120	0.106	0.095	Self-inductance in S2
M_{cs} $[\frac{\mu H}{m}]$	0.120	0.104	0.094	Between S1 and C1
M_{sc} $[\frac{\mu H}{m}]$	0.120	0.104	0.095	Between C1 and S1
M_{ss} $[\frac{\mu H}{m}]$	0.020	0.017	0.014	Between S2 and S1
C_{cs1} $[\frac{pF}{m}]$	620.78	681.58	645.06	Between C1 and S1
C_{sg1} $[\frac{pF}{m}]$	—	—	—	Between S1 and G
C_{ss} $[\frac{pF}{m}]$	—	—	—	Between S1 and S2
C_{sg2} $[\frac{pF}{m}]$	—	—	—	Between S2 and G
C_{cs2} $[\frac{pF}{m}]$	620.78	681.58	645.06	Between S2 and C2

Table A.4: Values from 2x4mm^2 obtained from LCR measurement, COMSOL and hand calculation **at stationary**

Parameter	LCR	COMSOL	Hand cal.	Description
$2L_c$ $[\frac{\mu H}{m}]$	0.530	0.500	0.524	Self-inductance of two conductors
L_c1 $[\frac{\mu H}{m}]$	0.265	0.250	0.262	Self-inductance in C1
L_c2 $[\frac{\mu H}{m}]$	0.265	0.250	0.262	Self-inductance in C2
L_s $[\frac{\mu H}{m}]$	0.234	0.200	0.192	Self-inductance in S
M_{cs} $[\frac{\mu H}{m}]$	0.191	0.203	0.192	Between S and C
M_{cc} $[\frac{\mu H}{m}]$	0.200	0.220	0.222	Between C1 and C2
C_{cs} $[\frac{pF}{m}]$	194.73	153.39	183.36	Between C and S
C_{cc} $[\frac{pF}{m}]$	59.22	49.67	79.46	Between C1 and C2

Table A.5: Values of cable conductor resistance (R_c) for 50mm^2 obtained from DC measurement

Length [m]	Current applied [A]	Voltage drop [mV]	R_c [$m\Omega$]	R_c per meter [$m\Omega$/m]
5	10	15.8	1.88	0.38
5	20	37.6	1.88	0.38
5	50	94.2	1.88	0.38
10	10	37.4	3.74	0.37
10	20	74.7	3.73	0.37
10	50	186.4	3.73	0.37

Table A.6: Values of cable conductor resistance (R_c) for 70mm^2 obtained from DC measurement

Length [m]	Current applied [A]	Voltage drop [mV]	R_c [$m\Omega$]	R_c per meter [$m\Omega$/m]
10	10	25.9	2.59	0.26
10	20	51.5	2.57	0.26
10	50	128.6	2.57	0.26

Table A.7: Values of cable conductor resistance (R_c) for 95mm^2 obtained from DC measurement

Length [m]	Current applied [A]	Voltage drop [mV]	R_c [$m\Omega$]	R_c per meter [$m\Omega$/m]
10	10	19.4	1.94	0.19
10	20	38.7	1.93	0.19
10	50	96.5	1.93	0.19

Table A.8: Values of cable conductor resistance (R_c) for 2x4mm^2 obtained from DC measurement

Length [m]	Current applied [A]	Voltage drop [mV]	R_c [$m\Omega$]	R_c per meter [$m\Omega$/m]
10	10	480.9	48.09	4.81
10	20	969.0	48.45	4.84

Table A.9: Values of cable shield resistance (R_s) for 50mm^2 obtained from DC measurement

Length [m]	Current applied [A]	Voltage drop [mV]	R_s [$m\Omega$]	R_s per meter [$m\Omega$/m]
5	10	127.7	12.77	2.55
5	20	256.2	12.81	2.56
5	50	644.0	12.88	2.57
10	10	248.3	24.83	2.48
10	20	497.0	24.85	2.48
10	50	1246.0	24.92	2.49

Table A.10: Values of cable shield resistance (R_s) for 70mm^2 obtained from DC measurement

Length [m]	Current applied [A]	Voltage drop [mV]	R_s [$m\Omega$]	R_s per meter [$m\Omega$/m]
10	10	252.6	25.26	2.53
10	20	505.3	25.26	2.53
10	50	1246.0	25.28	2.53

Table A.11: Values of cable shield resistance (R_s) for 95mm^2 obtained from DC measurement

Length [m]	Current applied [A]	Voltage drop [mV]	R_s [$m\Omega$]	R_s per meter [$m\Omega$/m]
10	10	174.4	17.44	1.74
10	20	349.5	17.47	1.75
10	50	874.0	17.48	1.75

Table A.12: Values of cable shield resistance (R_s) for 2x4mm^2 obtained from DC measurement

Length [m]	Current applied [A]	Voltage drop [mV]	R_s [$m\Omega$]	R_s per meter [$m\Omega$/m]
10	10	0.67	67.00	6.70
10	20	1.34	66.70	6.67

Table A.13: Values of cable connector resistance for $70mm^2$ obtained from DC measurement by measuring via **conductor resistance**

N_{cable}	I_{DC} [A]	V_{DC} [mV]	$R_{c,tot}$ [$m\Omega$]	$R_{c,x}$ [$m\Omega$]	$R_{con,c}$ [$m\Omega$]
1	20	2.95	0.15	0.04	0.11
1	50	7.70	0.15	0.04	0.11
1	100	15.10	0.15	0.04	0.11
2	20	6.10	0.30	0.08	0.22
2	50	15.10	0.30	0.08	0.22
2	100	31.20	0.31	0.08	0.23

Table A.14: Parameter description for **Table A.13**

Parameter	Description
N_{Cable}	Number of the cables are measured
I_{DC}	Applied current from the EA-ELR 10080-1000 DC electronic load
V_{DC}	Measured voltage drop by Fluke multimeter
$R_{tot,c}$	Sum resistance of the cable conductor/s and the attached connector/s
$R_{c,x}$	Conductor resistance for 15.8cm cable
$R_{con,c}$	Connector resistance measured via cable conductor ($R_{con,c}$=$R_{tot,c}$-$R_{c,x}$)

Table A.15: Values of cable connector resistance for $70mm^2$ obtained from DC measurement by measuring via **shield resistance**

N_{cable}	I_{DC} [A]	V_{DC} [mV]	$R_{s,tot}$ [$m\Omega$]	$R_{s,x}$ [$m\Omega$]	$R_{con,s}$ [$m\Omega$]
1	10	15.50	1.55	0.40	1.15
1	20	31.00	1.55	0.40	1.15
1	50	78.00	1.56	0.40	1.16
1	100	140.00	1.40	0.40	1.00
2	10	26.20	2.62	0.80	1.82
2	20	52.10	2.60	0.80	1.80
2	50	130.00	2.60	0.80	1.80
2	100	242.00	2.42	0.80	1.62

Table A.16: Parameter description for **Table A.15**

Parameter	Description
N_{Cable}	Number of the cables are measured
I_{DC}	Applied current from the EA-ELR 10080-1000 DC electronic load
V_{DC}	Measured voltage drop by Fluke multimeter
$R_{tot,s}$	Sum resistance of the cable shield/s and the attached connector/s
$R_{s,x}$	Shield resistance for 15.8cm cable
$R_{con,s}$	Connector resistance measured via shield conductor ($R_{con,s}$=$R_{tot,s}$-$R_{s,x}$)

DEPARTMENT OF SOME SUBJECT OR TECHNOLOGY
CHALMERS UNIVERSITY OF TECHNOLOGY
Gothenburg, Sweden
www.chalmers.se

CHALMERS
UNIVERSITY OF TECHNOLOGY